Functional and structural characterization of the *Drosophila* gene *smallish* during epithelial morphogenesis

I n a u g u r a l - D i s s e r t a t i o n

zur

Erlangung des Doktorgrades

der Mathematisch-Naturwissenschaftlichen

Fakultät der Universität zu Köln

vorgelegt von

Irina Peek

aus Büren

Hundt Druck GmbH, Köln

2019

Berichterstatter:	Prof. Dr. Andreas Wodarz
	Prof. Dr. Siegfried Roth
Tag der mündlichen Prüfung:	22.02.2019

Table of contents

Table of contents I

List of figures V

List of tables VII

1 Introduction 1

1.1 Establishment of epithelial cell polarity and cell adhesion 1

1.2 Actomyosin networks and cell adhesion in morphogenesis 5

1.3 Planar cell polarity 7

1.3.1 Planar polarity of the contractile actin-myosin network 9

1.4 Smallish (Smash) 12

1.5 LIM-domain only 7 15

1.6 Src kinases 18

1.6.1 Src42A - A *Drosophila* orthologue of Src 20

1.7 Scope of this thesis 22

2 Materials and Methods 24

2.1 Materials 24

2.1.1 Chemicals, enzymes and kits 24

2.1.2 Fly stocks 24

2.1.3 Antibodies 27

2.1.3.1 Primary Antibodies 27

2.1.3.2 Secondary Antibodies 28

2.1.4 Bacterial strains and Cell Culture Lines 29

2.1.5 Plasmids 29

2.1.6 Vectors 30

2.1.7 Oligonucleotides 30

2.1.8 Microscopes/ Imaging Systems 31

2.1.9 Technical devices 31

2.1.10 Software 32
2.2 Methods 33
2.2.1 Fly work and genetic methods 33
2.2.1.1 Fly breeding 33
2.2.1.2 Gal4-UAS System 34
2.2.1.3 Bacterial Artificial Chromosome 34
2.2.1.4 Injection 35
2.2.1.5 Rescue experiments 35
2.2.1.6 Generation of germline clones 36
2.2.2 Molecular Biology Methods 37
2.2.2.1 Polymerase Chain Reaction 37
2.2.2.2 Gel electrophoresis 37
2.2.2.3 DNA extraction from Agarose gels 38
2.2.2.4 Gateway cloning 38
2.2.2.5 Transformation in *Escherichia coli* 39
2.2.2.6 Plasmid purification 39
2.2.3 Biochemical Methods 40
2.2.3.1 Embryonic protein extraction 40
2.2.3.2 Protein lysate from S2 cells 41
2.2.3.3 Determination of Protein concentration 41
2.2.3.4 Co-Immunoiprecipitation 41
2.2.3.5 SDS PAGE 42
2.2.3.6 Western Blot 44
2.2.4 Histology 45
2.2.4.1 Formaldehyde fixation of embryos 45
2.2.4.2 Heat Fixation of embryos 46
2.2.4.3 Immunostaining 47
2.2.4.4 Analysis of planar cell polarity 47
2.2.5 Cell Culture 47

2.2.5.1 Cultivation of S2 cells 47
2.2.5.2 Transfection of S2 cells 48
2.2.6 Imaging 48
2.2.6.1 Electron Microscopy 48
2.2.6.2 Laser Ablation 48
2.2.7 Statistical analysis 49
3 Results 50
3.1 Loss of maternal and zygotic *smash* leads to severe morphogenetic defects 50
3.2 Rescue of semilethality of *smash* mutant animals 53
3.2.1 GFP-Smash PI deletion constructs show various subcellular localizations 56
3.3 Cortical tension is reduced in *smash* mutant epidermis 58
3.4 Subcellular localization of Smash within the actomyosin network 61
3.4.1 Planar cell polarity is reduced or lost in *smash* mutant embryos 65
3.5 Smash associates with multiple actomyosin components at the ZA 70
3.5.1 Smash is lost upon the loss of Baz 71
3.5.2 Loss of *canoe* leads to defects in Smash localization 71
3.5.3 Phosphorylation of Myosin II is affected in *smash* mutant embryos 73
3.5.4 Smash binds to Rok, Shrm and Moe *in vitro* 75
3.6 Interaction of Smash and Src42A 77
3.6.1 Phosphorylation of Smash by Src42A is independent of its interaction as binding partners 77
3.6.2 Smash contains several binding sites for Src42A 79
3.6.2.1 Phosphorylation by Src42A is not exclusively determined by the LIM-PBM module 82
3.6.3 Subcellular dependency of Smash and Src42A 83
4 Discussion 85
4.1 *smash* regulates morphogenesis and cell bond tension 85
4.1.1 Structure-function analysis 86
4.1.2 Smash as regulator of the actomyosin network 88

4.1.2.1 Interaction of Smash and Src42A 91
4.1.2.2 Smash acts as a scaffold protein 92
4.2 Subcellular localization of Smash is determined by multiple proteins at the ZA 94
4.2.1 Smash regulates planar cell polarity 96
5 Conclusion and Perspectives 99
Abstract 100
Zusammenfassung 101
References 102
List of abbreviations 113
Appendix 116
Acknowledgements/Danksagung 118
Erklärung 119

List of figures

Figure 1: Epithelial cell organization of invertebrates and vertebrates 2

Figure 2: Establishment of polarity in the *Drosophila* epithelium. 4

Figure 3: Apical constriction 5

Figure 4: The Myosin II subclass. 6

Figure 5: Planar cell polarity components 9

Figure 6: Neighbor change events and junction remodeling during germband extension. 11

Figure 7: Smash isoforms. 13

Figure 8: Overexpression of GFP-Smash PM induces apical constriction of follicular epithelial cells. 14

Figure 9: Isoforms of LMO7. 16

Figure 10: LMO7 localizes at AJs together with Afadin and ZO-1 in rat gallbladder. 17

Figure 11: Structure of Src family kinases. 19

Figure 12: Src42A is involved in the formation of basolateral protrusions during germband extension. 21

Figure 13: Scanning EM of *smash*$^{35m/z}$ and wild type embryos at stage 13. 50

Figure 14A: Embryos lacking maternal and zygotic *smash* show severe defects in morphogenesis. 51

Figure 14B: Embryos lacking maternal and zygotic *smash* show severe defects in morphogenesis 52

Figure 15: Bacterial artificial chromosome CH321-21P3 rescues semilethality of *smash*^{35} mutants. 54

Figure 16: Overexpression of Smash PM and Smash PI rescues semilethality of *smash*^{35} mutant animals 56

Figure 17: GFP-Smash PI deletion constructs show different subcellular localizations. 57

Figure 18: Junctions show serpentine shaped phenotype upon the loss of *smash*. 58

Figure 19: Cell bond tension is reduced upon loss of *smash* function. 60

Figure 20: Smash is enriched at myotendinous junctions. 61

Figure 21: Smash is planar polarized in embryonic epidermis. 64

Figure 22: Planar cell polarity is abolished in *smash*$^{35m/z}$ mutant embryos. 70

Figure 23: Smash is abolished in *baz* zygotic mutant embryos. 71

Figure 24: Smash localization is effected upon loss of Cno 73

Figure 25: Phosphorylation of Myosin II is downregulated in *smash*$^{35m/z}$ mutant embryos. 74

Figure 26: Smash binds to Rok, Shrm and Moe *in vitro*. 76

Figure 27: Src42A binds all isoforms of Smash. 79

Figure 28: Src42A binds to all deletion constructs of Smash PI 81

Figure 29: Only GFP-Smash PI C-term is not phosphorylated by Src42A. 82

Figure 30: Src42A localization is not affected upon the loss of *smash*. 84

Figure 31: Scheme of how Smash may act in a multi protein complex. 91

Figure S 1: Smash may bind to Sqh. 117

List of tables

Table 1-1: Src family kinases..... 18

Table 2-1: Fly stocks..... 24

Table 2-2: Primary Antibodies..... 27

Table 2-3: Secondary Antibodies..... 28

Table 2-4: Bacterial strains and cell lines used in this work..... 29

Table 2-5: Plasmids used in this work..... 29

Table 2-6: Vectors used in this work..... 30

Table 2-7: Primer used in this work..... 30

Table 2-8: cDNA clones used in this work..... 38

Table 3-1: Expected band sizes of transfected Smash and Src42A constructs based on their molecular weight. 80

Table 4-1: Overview of Smash binding partners and their molecular function. 93

1 Introduction

1.1 Establishment of epithelial cell polarity and cell adhesion

The formation of cell polarity is fundamental for coordinated shape changes during the development of a complex organism. Polarity is characterized by asymmetric shape, distribution of organelles or polarized localization of proteins and lipids. The latter is essential in processes like asymmetric cell division, in which determinants are inherited unequally among daughter cells (Hartenstein & Wodarz 2013).

Epithelial cells show polarization in two axes, along the apical-basal axis of the cell and in a second axis within the plane of the epithelium, known as planar cell polarity. Both are determined by a group of conserved regulatory molecules that are crucial to provide the basis for these cells to function as physiological and mechanical barriers (Guillot & Lecuit 2013; Harris & Peifer 2005; Suzuki & Ohno 2006). The apical basal polarity is defined by a separation of the plasma membrane in an apical domain, facing the environment or a lumen, and a basolateral domain, facing the interior or adjacent cells. These domains are segregated by the so called zonula adherens (ZA), a cell-cell adhesion complex consisting of adherens junctions (AJs) (Kaplan et al. 2009). AJs are multiprotein belt-like structures encircling the apical side of epithelial cells to ensure dynamic cell- cell contacts and adhesion (Figure 1B). A key element of the AJs is the transmembrane protein E-cadherin. The intracellular portion of E-cadherin is associated with cytoplasmic proteins, like β-catenin, which binds directly to E-cadherin (Ranscht 1994; Harris & Tepass 2010) . Others, like α-Catenin, Vinculin, α-Actinin or the *Drosophila* Afadin homologue Canoe, link the Cadherin/ β-catenin complex to Actin filaments (Knust & Leptin 1996; Sawyer et al. 2009). This dynamic link to the actomyosin network allows epithelial cells to interact with each other in a dynamic fashion as they display morphogenetic processes like rearrangement, movement and cell shape changes, particularly during embryogenesis (Takeichi 2014). In *Drosophila*, the so called subapical region (SAR) is located slightly above the ZA. The SAR contains protein complexes essential for the formation of the ZA and maintenance of cell polarity (Knust & Bossinger 2002). In vertebrates tight junctions (TJ), also known as zonu-

la occludens, are located apical to the ZA. TJs form a primary barrier between individual cells and function as a fence for lateral diffusion between the apical and the basolateral plasma membrane domains (Tsukita et al. 2001). TJs are absent in invertebrates. Instead they feature structurally different junctions called septate junctions (SJ) at the lateral membrane to provide barrier function (Willott et al. 1993). Figure 1A illustrates the different regions of vertebrate epithelial cells in contrast to the composition of the *Drosophila* epithelium.

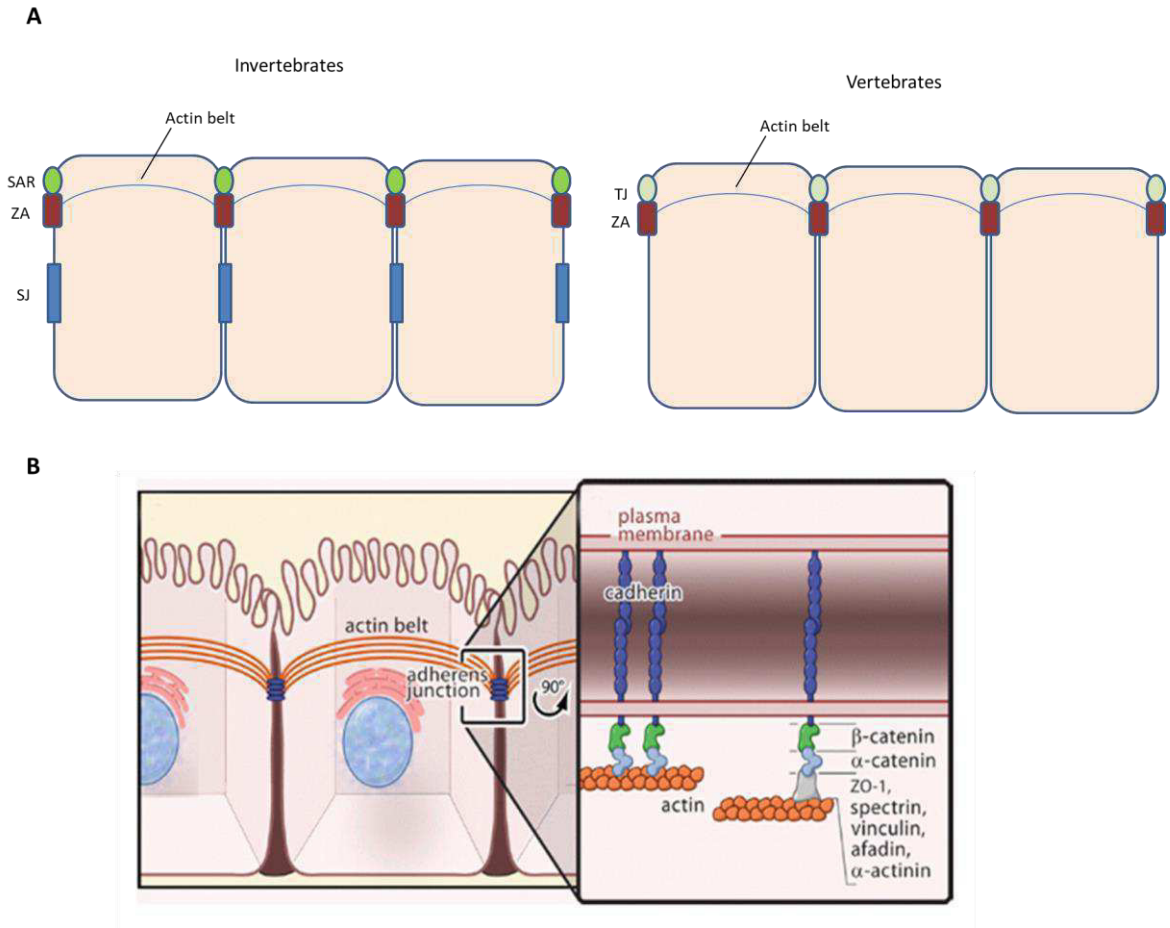

Figure 1: Epithelial cell organization of invertebrates and vertebrates. (A) Different regions of invertebrate cells vs. vertebrate cells. Both are separated in an apical domain facing the lumen and a basolateral domain facing the basement membrane or adjacent cells. These domains are segregated in the region of the zonula adherens (ZA), via adherens junctions (AJs). In invertebrates the subapical region (SAR) is located apical to the ZA. In vertebrates, this domain harbors tight junctions (TJs), which are absent in invertebrates. Instead of TJs invertebrates contain septate junctions (SJs) at the lateral membrane, which function as barriers. (B) Schematic drawing of adherens junctions. AJs form belt like structures encircling the cells. Cadherins form dimers and associate with β-catenin. Other linker proteins like α-catenin, Canoe/Afadin or Vinculin provide a connection to the dynamic actin network ((B) adapted from (Gates & Peifer 2005).

In *Drosophila* embryonic development, the first epithelial tissue is established during cellularization. After 13 nuclear divisions of the fertilized egg, around 6000 nuclei form a monolayer beneath the egg membrane (Mazumdar & Mazumdar 2002). At this stage the plasma membrane already shows polarization, as it is segregated in an apical domain and a basolateral domain surrounding the nucleus (Lye & Sanson 2011). Subsequently the egg membrane invaginates and surrounds each nucleus in a process similar to cytokinesis in order to form the cellularized blastoderm. This cellularization is initiated by the formation of the furrow canal that remains at the leading edge of the invaginating membrane (Tepass et al. 2001). Here, the first so called basal junctions are formed along the emerging lateral membrane (Hunter & Wieschaus 2000), which resolve after cellularization is completed. Analogue to cytokinesis, the contractile actomyosin ring associates with Septins and Anillin in order to provide the force to pull the membrane down (Field & Alberts 1995; Adam et al. 2000). In the end of cellularization the actomyosin ring contracts enclosing the cells. In between this process of cellularization shortly after stage 5, adherens junctions (AJs) arise at the membrane in a spotted pattern (sAJs), which later form the ZA during gastrulation (Simpson & Wieschaus 1990; Tepass & Tanentzapf 2001). At this stage, cells already show a distinct polarization as they exhibit an apical part facing the outside of the embryo and a basolateral membrane, though the mature ZA has not formed yet (Lye & Sanson 2011).

The further establishment of this polarized subcellular organization is mainly controlled by three major protein complexes. One is localized to the SAR of the cells, apical to the ZA, and is composed of the transmembrane protein Crumbs and its intracellular adaptor protein Stardust, known as Crb/Sdt complex (Tepass et al. 1990; Tepass & Knust 1993). This complex acts in a functional hierarchy with another group of polarity proteins, the Bazooka (Baz)–PAR-6 (partitioning defective 6)–atypical protein kinase C (aPKC) complex (Ohno 2001). Baz serves as scaffold protein for aPKC and its activator Par-6 and localizes to the ZA (Wodarz et al. 2000). It recruits Sdt to the plasma membrane by direct interaction between the Postsynaptic density 95/Discs large/Zonula occludens 1 (PDZ) domain of Sdt, which is also a binding site for the C- terminus of Crb (Krahn et al. 2010). Baz also contains a phosphorylation site for aPKC. By the phosphorylation of Baz the connection of the Baz–Sdt complex weakens and after dissociation the PDZ domain of Sdt is available to

form the Crb/Sdt complex (Kaplan et al. 2009; Krahn et al. 2010; Morais-de-Sá et al. 2010). The third protein complex consisting of Lethal giant larvae (Lgl), Discs large (Dlg) and Scribble (Scrib) acts as an antagonist to the Crb/Sdt complex and determines the basolateral membrane domain (Tanentzapf & Tepass 2003; Johnson & Wodarz 2003). This group is also required for the formation of septate junctions (SJ), which function is similar to that of mammalian tight junctions (TJ), for example to control paracellular transport (Su et al. 2013). The tumor suppressors Dlg and Scrib are restricted to the SJ, while Lgl localizes to the entire lateral membrane (Yamanaka & Ohno 2008). Lgl and the kinase Par-1 are also phosphorylation targets of aPKC, which restricts these proteins to the basolateral site (Betschinger et al. 2003; Hurov et al. 2004). Par-1 in turn blocks Baz oligomerization by phosphorylation and inhibits the ectopic formation of the Bazooka/PAR-6/aPKC complex (Benton & St Johnston 2003). This dynamic antagonistic network is of fundamental importance for establishment and maintenance of epithelial cell polarity and integrity. Figure 2 shows an outline of the establishment of the *Drosophila* epithelial polarity including a mature ZA.

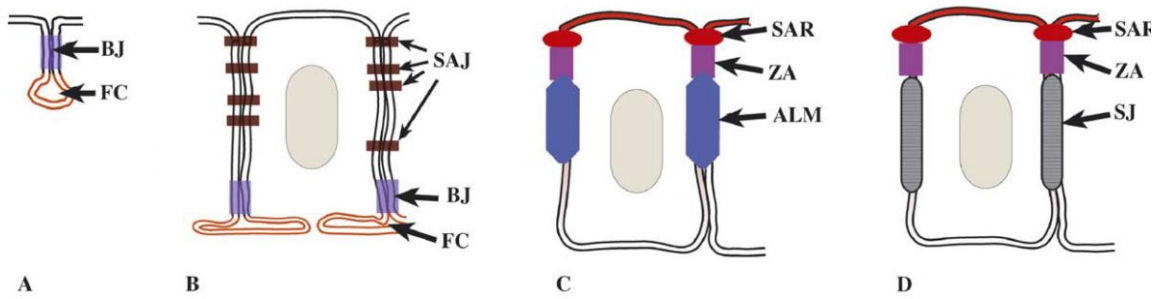

Figure 2: Establishment of polarity in the *Drosophila* epithelium. (A) At the beginning of cellularization the membrane forms furrow canals (FCs) and invaginates by means of the actomyosin network. First basal adherens junctions (BJs) are formed, which resolve after cellularization. (B) Afterwards first AJs in a spotted pattern (SAJs) arise. (C) During gastrulation a subapical region (SAR) and an apical margin of the lateral domain (ALM) are formed. The SAR and the ALM are providing spatial information to position the ZA and control the formation of the continuous mature ZA. (D) At late embryogenesis (after germ band retraction of the embryo), the generation of septate junctions (SJ) occur and the epithelial junctional complex is fully differentiated. Adapted from Müller & Bossinger (2003).

1.2 Actomyosin networks and cell adhesion in morphogenesis

During development, epithelial tissues undergo various morphogenetic processes. At the basis of these movements are the coordinated shape changes of individual cells within the whole area. An important feature is the contraction of the apical region of the cells, known as apical constriction, which for example allows membrane invagination during gastrulation (Figure 3).

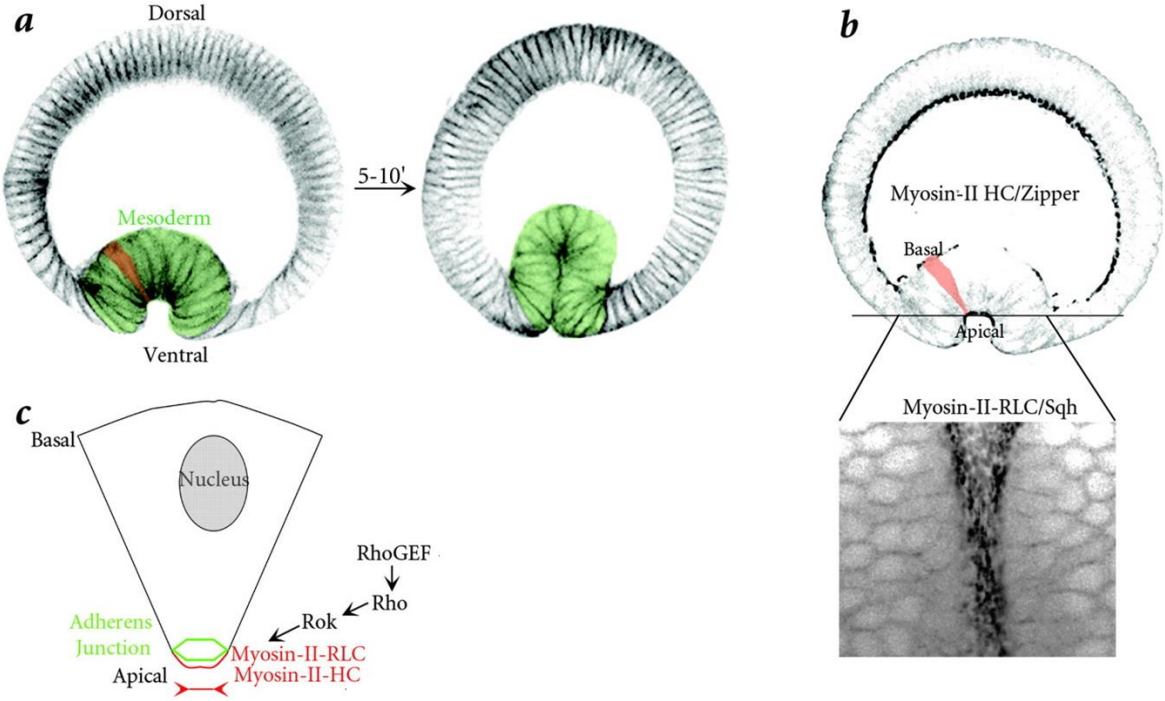

Figure 3: Apical constriction. Invagination movements require the constriction of the apical domain of cells to allow the formation of furrows (adapted and modified from Pilot & Lecuit (2005).

These cellular deformations are driven by a contractile network in the cortex of the cells composed of active cytoskeleton elements like actin filaments, actin crosslinkers and myosin motors (Munjal & Lecuit 2014). Dynamic myosin proteins move along actin filaments under ATP-hydrolysis and thus prevent rigidity of the plasma membrane caused through actin filaments alone (Toyoshima et al. 1987; Howard 1997). Members of the myosin superfamily contain a conserved head region and a divergent tail domain. The head domain carries the conserved actin-binding and ATP-hydrolysis sites. Members of the sub-class

myosin II are characterized by their hexameric composition of two heavy chains, two essential light chains (ELC) and two regulatory light chains (MLRC) (Hartman & Spudich 2012) (Figure 4).

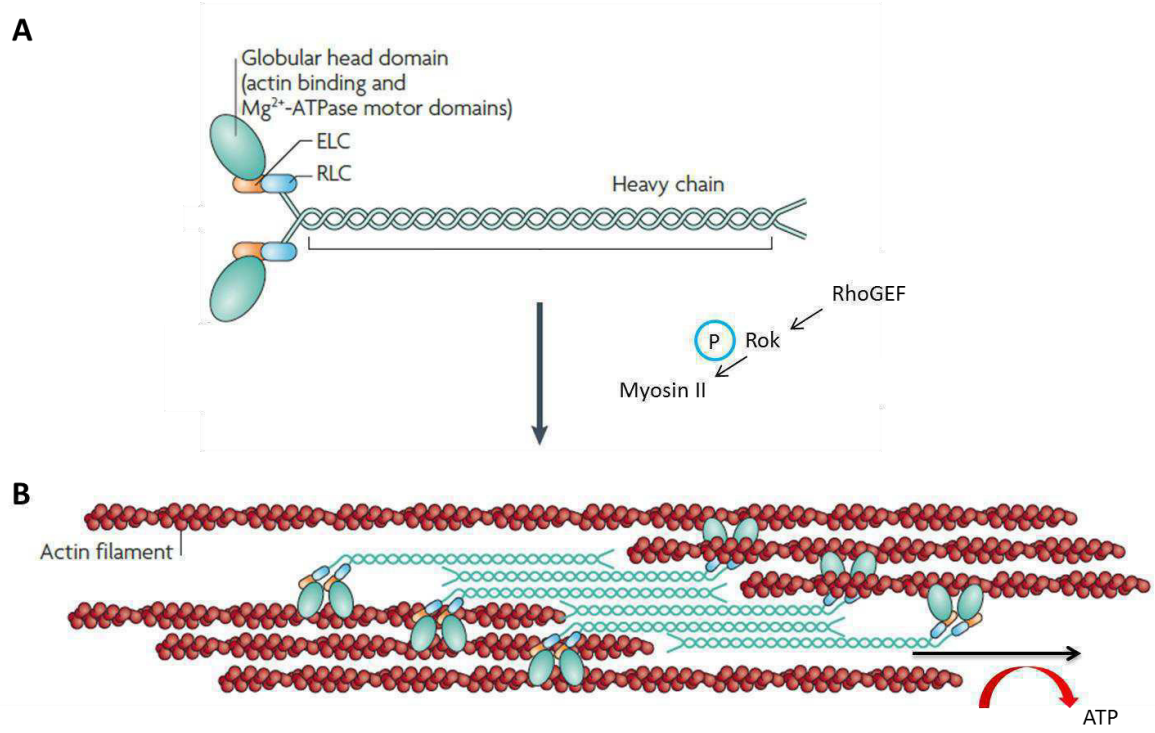

Figure 4: The Myosin II subclass. (A)The dynamic motor proteins consist of two heavy chains, two essential and two regulatory light chains. (A´)Myosin II moves along actin filaments under ATP- hydrolysis via the conserved ATP-hydrolysis domain in the head region to allow contraction and release of the cytoskeleton. Adapted and modified from Vicente-Manzanares et al. (2009).

In *Drosophila* the heavy chain is encode by the gene *zipper* (Young et al. 1993), while MLRC is encoded by the gene spaghetti-squash (sqh) (Karess et al. 1991; Hartman & Spudich 2012; Munjal & Lecuit 2014). In non-muscle cells, like epithelial cells, Myosin II is essential for regulating cytokinesis or generating cortical tension to allow the cells to undergo shape changes in developmental processes (Karess et al. 1991; Martin & Goldstein 2014). The accumulation and activity of Myosin II filaments is regulated by direct phosphorylation of conserved residues (Thr18 and Ser19 in mammals, Thr20 and Ser21 in *Drosophila*) (Amano et al. 1996; Getz et al. 2010). Among various kinases, the Rho-associated coiled coil-containing kinase ROCK, or Rok in *Drosophila*, is a key factor for phosphorylation and thus activation of myosin II (Amano et al. 1996; Mizuno et al. 1999). ROCK in

turn is a downstream effector target of the activated Rho GTPase whose activity is regulated by Guanine nucleotide exchange factors (GEFs) and GTPase-activating proteins (GAPs) (Barrett et al. 1997; Verdier et al. 2006; Watanabe & Hosoya 2007).

1.3 Planar cell polarity

Besides the apical-basal polarity, *Drosophila* epithelial cells also exhibit a polarization within a plane of an epithelial tissue, known as planar cell polarity (PCP) (Figure 5A). PCP is found in various tissues and refers to the alignment of cell polarity across the whole tissue plane, in cells that are spatially separated. The establishment of this alignment is achieved by the asymmetric partitioning of cortical PCP proteins and the intracellular communication between neighboring cells through protein transfer, gradients or endocytosis (Zallen 2007; Devenport 2014). The polarized orientation of PCP components is essential in many developmental processes, like the right orientation of mammalian hair follicles and inner ear hairs, formation of the neural tube or the development of heart and kidney in vertebrates (Wang 2006; Wang & Nathans 2007; Vladar et al. 2009; Mlodzik et al. 2010).

PCP was first investigated in *Drosophila*. Two molecular mechanisms control PCP composition, the “core” and the “Fat–Dachsous (Ft–Ds)” PCP pathways.

The first discovered “core” pathway, shown in Figure 5A, includes the core transmembrane proteins Frizzled (Fz), Van Gogh (Vang, also known as Strabismus/Stbm) and Flamingo (Fmi; also known as Starry night/Stan), and the cytosolic components Dishevelled (Dsh), Prickle (Pk) and Diego (Dgo). These proteins are present at only one side of the cell interface, except for the atypical Cadherin Fmi, which is found bilaterally on both sides and forms homodimers between neighboring cells (Usui et al. 1999; Chen et al. 2008). Vang and Prickle thereby localize to the proximal/anterior side of the cell (Tree et al. 2002; Bastock 2003), while Fz, Dsh and Diego are restricted to the distal/posterior part (Axelrod 2001; Strutt 2001; Feiguin et al. 2001). This unilateral distribution ensures the collective alignment across the tissue, like in its simplest form, in the *Drosophila* adult wing. Here, each cell produces a single actin-rich trichome or hair, all pointing to the distal side of the cell. Mutations in one of the core components lead to randomization of the planar polarity and thus to irregularly growing wing hairs (Wong & Adler 1993).

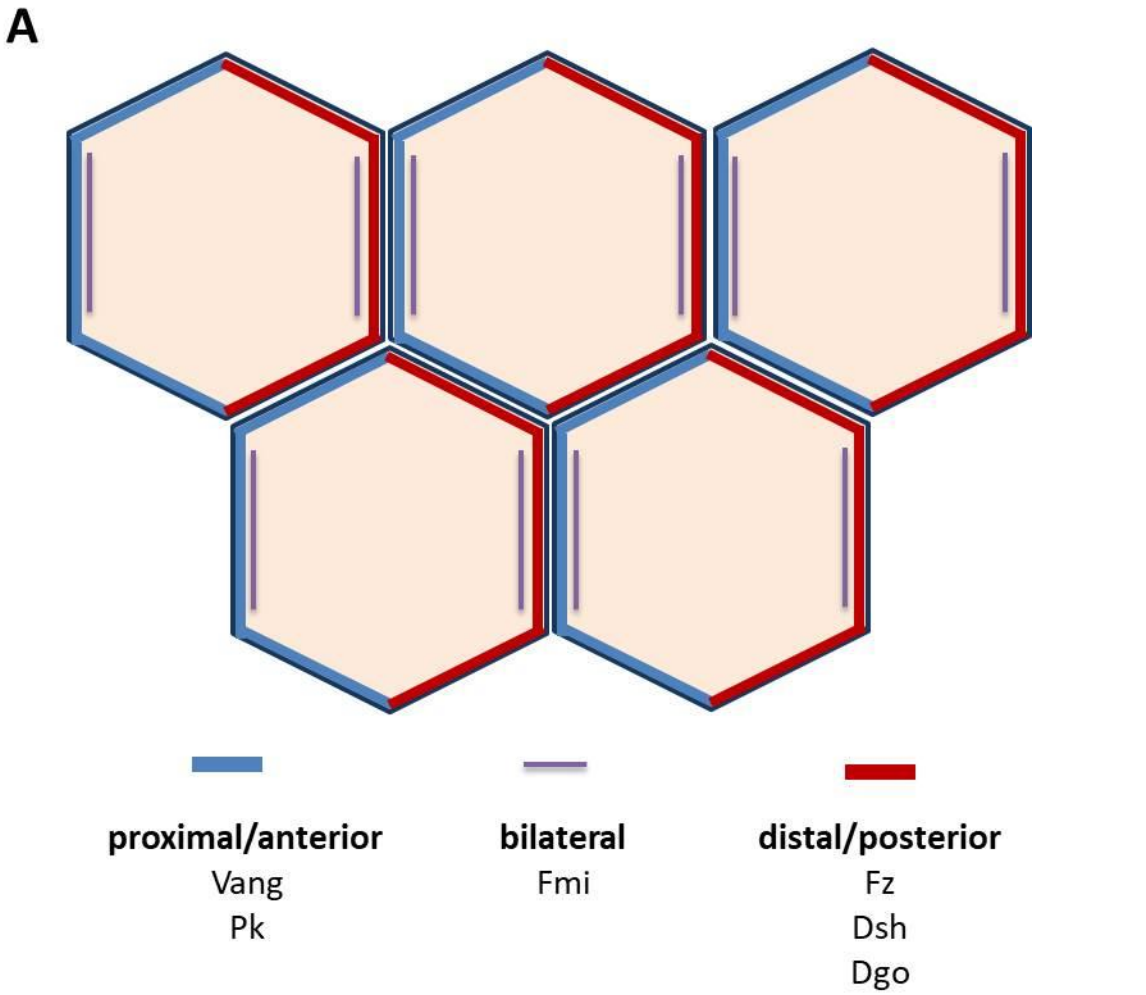
A
proximal/anterior
Vang
Pk
bilateral
Fmi
distal/posterior
Fz
Dsh
Dgo

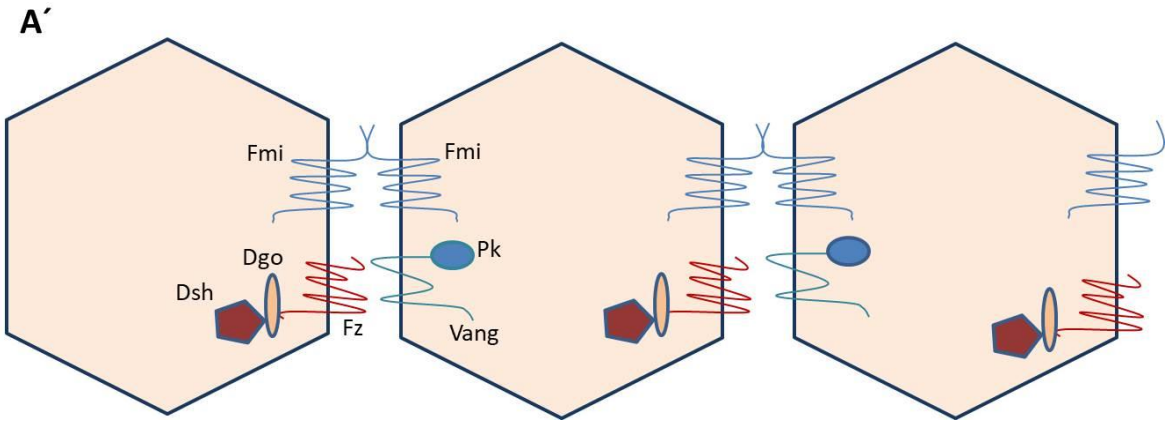
A´
Fmi
Fmi
Pk
Dgo
Dsh
Fz
Vang

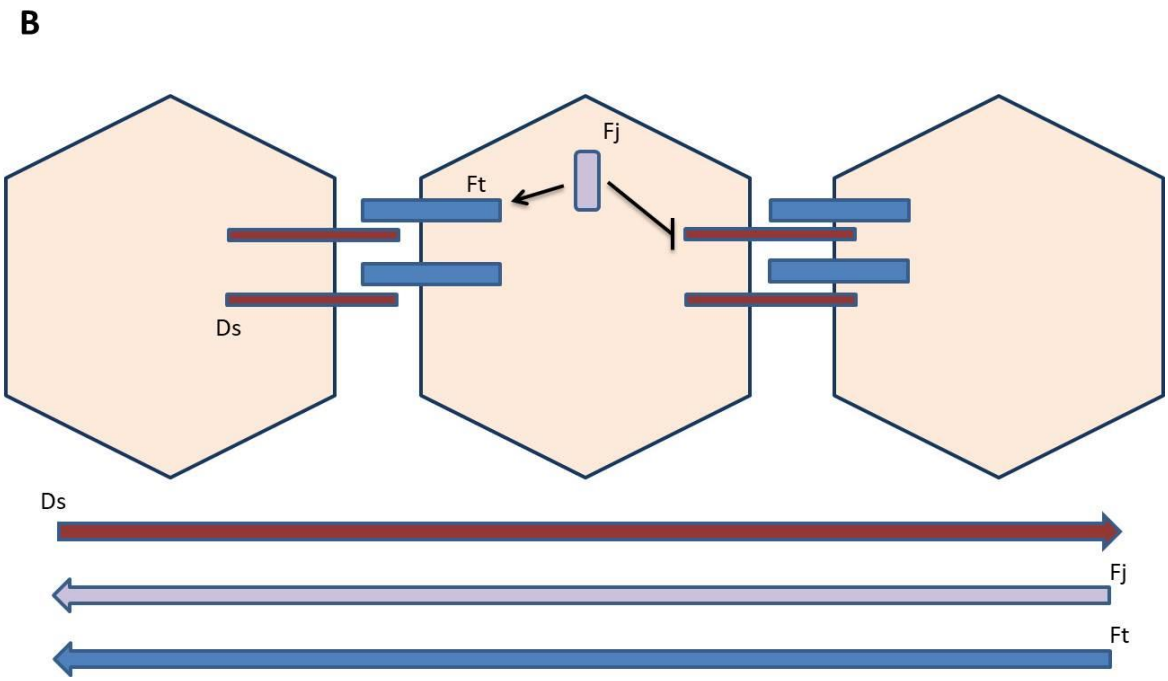

Figure 5: Planar cell polarity components. (A & A´) The core PCP proteins Vang and Pk localize to the proximal/anterior side, while Fz, Dsh, and Dgo localize to the distal/posterior edge. Fmi localizes to both sides, where it forms homodimers between neighboring cells. (B) Asymmetric localization of Ds and Ft, which form heterodimers between adjacent cells. Fj is a positive regulator of Ft and expressed in a gradient across the wing tissue (purple arrow), leading to a graded activity of Ft (blue arrow). Ds is expressed in an opposing gradient (red arrow).

The second, so called "Fat–Dachsous (Ft–Ds)" pathway regulating PCP involves the atypical cadherins Fat (Ft) and Dachsous (Ds) and the Golgi resident transmembrane ectokinase Four-jointed (Fj) (Figure 5B). Ft and its ligand Ds localize at opposite cell contact sides, where they mediate heterophilic cell adhesion by stabilizing each other on the cell surface (Clark et al. 1995; Matakatsu 2004). In contrast to the core PCP proteins, Fj and Ds are distributed in an opposing gradient across the developing wing tissue (Brodsky & Steller 1996; Yang et al. 2002). Fj is a positive regulator of Ft. In consequence, a gradient of Ft activity is present, complementary to that of Fj. This graded expression contributes to the asymmetric distribution of Ft and Ds (Matakatsu 2004; Simon et al. 2010; Devenport 2014).

1.3.1 Planar polarity of the contractile actin-myosin network

Planar polarity is also influenced by proteins which contribute to actomyosin contractility and regulation of actomyosin based cell movements such as the Par proteins Par-3/Baz

and their binding partners aPKC and Par-6 (Harris & Peifer 2007; Lang & Munro 2017). The regulation of the proper localization of components of the actomyosin network is essential for cell rearrangements in *Drosophila* embryogenesis, particularly during germband extension. In this process, the epithelial sheet elongates along the anterior-posterior axis without cell division, but through oriented neighbor change events. Two different types of these so called cell intercalations drive convergent extension: T1-T2-T3 transitions, which involve four cells and rosette formation, involving 5-12 cells. In both processes the apical junctions shrink along the dorsal/ventral (D/V) axis and thus two cells meet at the vertex (T1 transition) or rosettes form with neighboring cells. Subsequently new apical junctions form perpendicular to the lost ones and expand along the AP axis, thus pulling cells further and contribute to the elongation of the germband (Figure 6) (Bertet et al. 2004; Lecuit 2005; Blankenship et al. 2006; Zallen & Blankenship 2008 ; Tada & Heisenberg 2012; Umetsu & Kuranaga 2017).

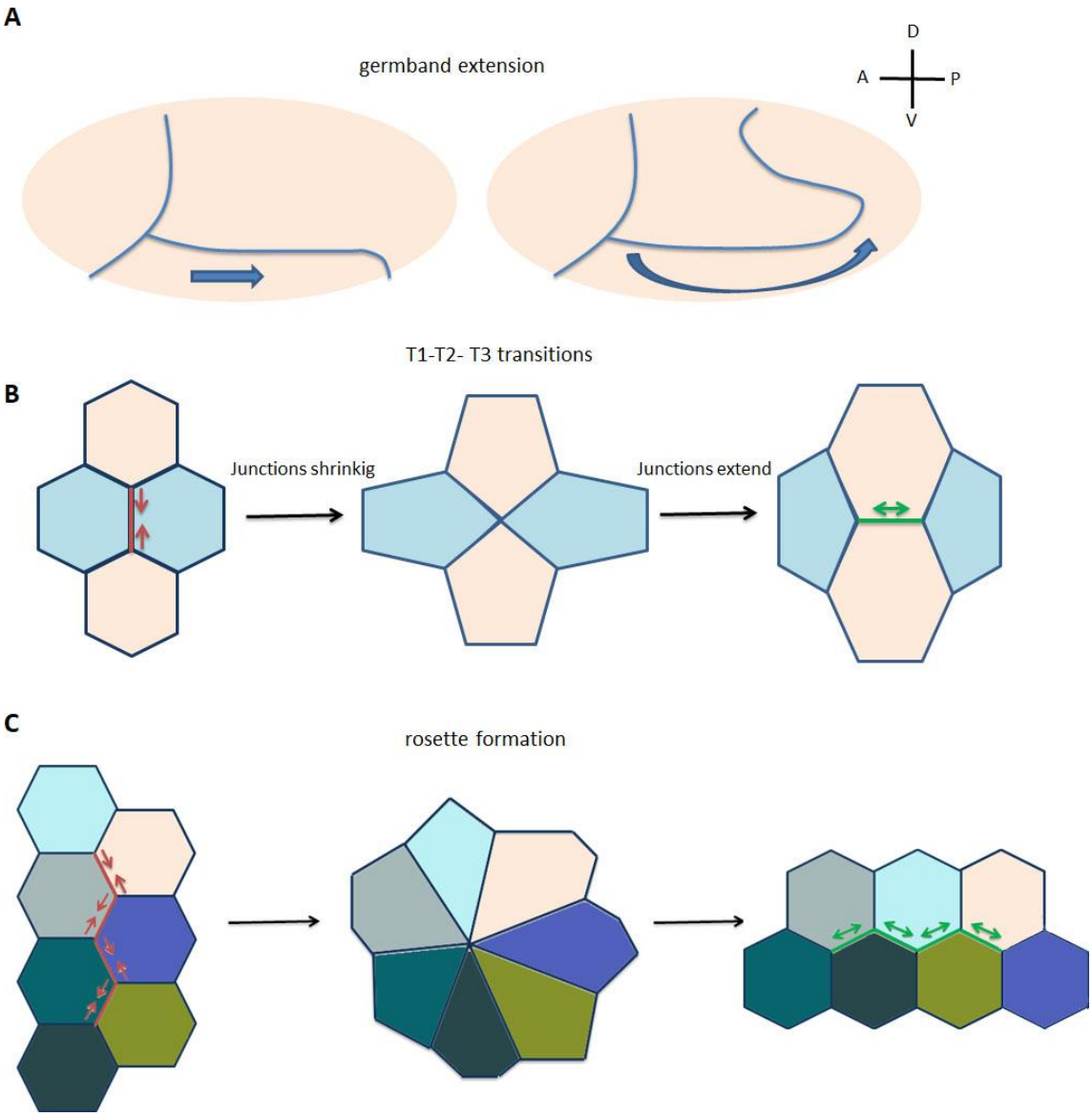

Figure 6: Neighbor change events and junction remodeling during germband extension. (A) Germband extension along the anterior-posterior body axis. (B) T1-T2-T3 transition with formation of a 4-cell vertex. Myosin II mediated shortening of junctions along the D/V axis (red arrows), followed by formation of new junctions along the A/P axis (green arrows). (C) Rosette formation. A group of cells (~7 cells) is involved, forming a rosette. Extensions of new junctions contribute to body elongation.

For proper execution of this axis elongation, the planar distribution of the dynamic components of the actomyosin network and of adherens junction associated proteins is required. F-Actin and myosin II accumulate at cell-cell contact sites in the anterior/posterior (A/P) axis, while E-Cadherin, Armadillo/β-catenin and Baz/Par3 show an enrichment at junctions between the dorsal and ventral cells (D/V axis) (Zallen & Wieschaus 2004; Blankenship et al. 2006). The Myosin II activating Rho-kinase Rok, activated by its associated Rho GTPase, is required for the right positioning of Myosin II and co-localizes with its substrate in the A/P axis (Amano et al. 1996; Bertet et al. 2004; Simões et al. 2010). The

Rok- and actin-binding protein Shroom has been shown to amplify Rok and Myosin II planar polarity, as the loss of *shroom* leads to a decreased level of junctional localization in A/P orientation (Hildebrand & Soriano 1999; Bolinger et al. 2010; De Matos Simões et al. 2014). In *shroom* mutants, also less junctional tension and defective multicellular rosette formation has been described (De Matos Simões et al. 2014), pointing to a key role to generate local myosin contractility in convergent extension. Moreover, Rok is also able to phosphorylate Baz (Simões et al. 2010), an important feature to exclude it from the A/P interfaces. Baz in turn is essential for planar polarized distribution of myosin II and Arm/β-catenin, as the loss of Baz results in a strong disruption of the planar localization of the latter (Simões et al. 2010; De Matos Simões et al. 2014).

Consequently, it has been shown, that Baz plays a key role not only in apical-basal polarity, but also in mediating planar cell polarity during cytoskeleton associated dynamic cell rearrangement events (Zallen & Wieschaus 2004).

Through this complex system of planar polarized actomyosin networks, also planar polarized forces are generated, that direct spatially organized cell rearrangements in order to elongate the body axis. The LIM protein Ajuba is recruited to AJs in a tension- dependent manner, as it localizes within seconds to sites of myosin accumulation in response to mechanical forces. Loss of Ajuba results in an increase of rosette formation and reduced rosette resolution through defective cell adhesion, reflected by gaps between interfaces in late stages of rosette formation (Razzell et al. 2018). The highly dynamic localization of Ajuba reflects the importance of the interplay between mechanical forces and the planar polarized recruitment of tension sensitive proteins.

1.4 Smallish (Smash)

The 170 kDa Lin11, Isl-1, Mec-3 (LIM) domain protein Smallish (Smash, CG43427) was first identified as a binding partner of Baz in a yeast two-hybrid screen. The three PDZ domains of Baz (aa291-737) were used as bait (Ramrath 2002; von Stein 2005). PDZ domains are protein interaction modules that often recognize short amino acid motifs at the C-terminus of target proteins, called PDZ binding motifs (PBM) (Lee & Zheng 2010). Smash exhibits a C-terminal module consisting of a LIM domain and a class I PDZ binding

motif (FSCV), as well as two predicted coiled-coil domains. The LIM domain is recognized as a tandem zinc-finger structure that functions as a protein-interaction module. These domains consist of approximately 55 amino acids with 8 highly conserved residues that contain mostly cysteine and histidine located at defined intervals (Kadrmas & Beckerle 2004).

Several isoforms of Smash have been annotated. The largest isoform PM and the smaller isoform PI share the LIM-PBM module, which is absent in Smash-PJ (Figure 7).

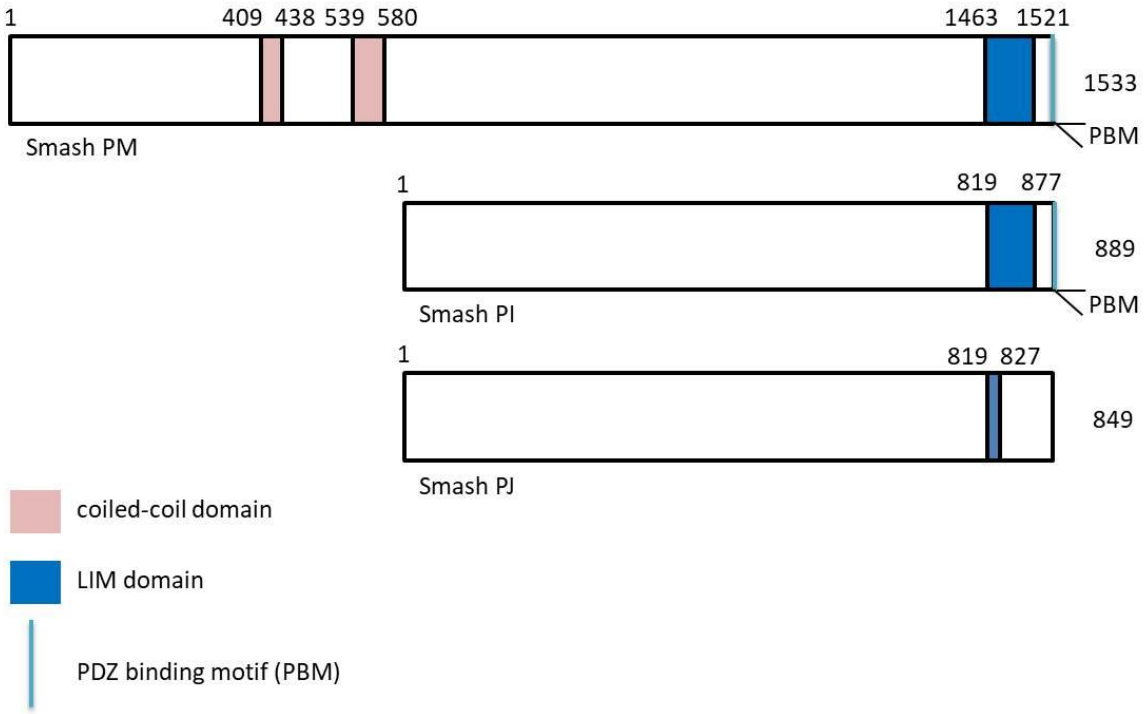

Figure 7: Smash isoforms. Smash PM contains two coiled-coil domains, a C-terminal LIM domain and a PDZ binding motif. Smash PI does not exhibit the coiled-coil domains, but the PBM module, which is absent in Smash PJ.

The interaction of Smash and Baz has been confirmed via co-immunoprecipitation (co-IP) using embryos overexpressing GFP-Smash PI and wild type embryos. The direct interplay between the PBM of Smash and the PDZ domains 2 and 3 of Baz was investigated by nuclear magnetic resonance (NMR) spectroscopy. Via this NMR study, also a direct interaction of Smash PBM and the PDZ domain of Canoe (Cno), which is a *Drosophila* homologue

of the Actin binding protein Afadin was confirmed. Smash is detectable from embryonic stage 5 onwards in all ectodermally derived epithelia, including the epidermis, the fore- and hindgut, Malpighian tubules, salivary glands, the amnioserosa and the tracheal tree. It is also expressed in the somatic musculature, as it was found in body wall muscles, the pharynx muscles and the visceral musculature surrounding the midgut. Smash, which is located on the right arm of the third chromosome got its name on the basis of its overexpression phenotype. The ectopic expression of GFP-Smash PM leads to complete lethality, while upon the overexpression of GPF-Smash PI rare escaper flies hatch, which are strongly reduced in their size. Cuticles of embryos that die during embryogenesis show massive defects, as they display dorsal open, anterior open phenotypes or both. These findings indicate the importance of Smash during epidermal development. First indication of Smash as a regulator of the actomyosin network has been shown on the cellular level, as the overexpression of Smash PM in random clones in the follicular epithelium and in the tracheal system induced apical constriction (Beati et al. 2018).

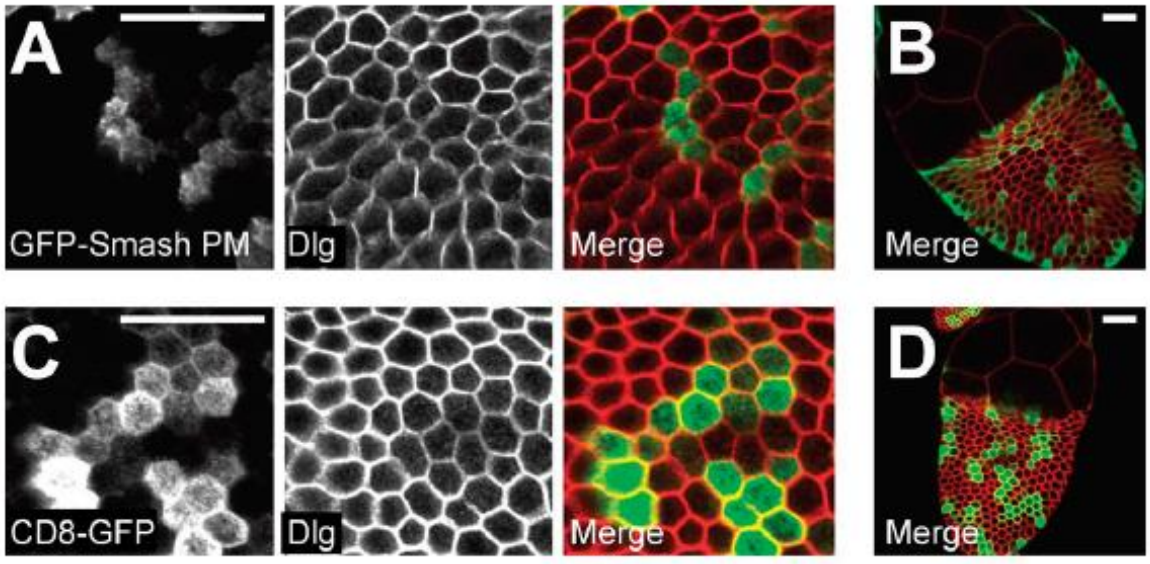

Figure 8: Overexpression of GFP-Smash PM induces apical constriction of follicular epithelial cells. (A) GFP-Smash PM (green in Merge) was overexpressed in randomly induced clones in the follicular epithelium of an egg chamber at stage 10A. Dlg (red in Merge) marks cell outlines close to the apex of the cells. (B) Overview of the egg chamber shown in A. (C) Control clones overexpressing CD8-GFP. (D) Overview of the egg chamber. Adapted from Beati et al. (2018).

Beside this overexpression phenotype, shown in Figure 8, Smash shares various similarities with the conserved actin-binding protein Shroom (Shrm). Both proteins localize to the ZA and exhibit a very similar expression pattern and subcellular localization. Shrm is a Rho kinase binding protein, which contributes to the mediation of planar cell polarity of junction associated proteins (Hildebrand & Soriano 1999; Haigo et al. 2003; Bolinger et al. 2010; De Matos Simões et al. 2014; Beati et al. 2018). However, the exact molecular-pathway of how Smash is regulating the activity of the actomyosin network during morphogenesis and if Shrm is a component of this pathway or acts in a redundant pathway is not clear.

1.5 LIM-domain only 7

The LIM domain is an evolutionarily conserved double-zinc finger motif often found in proteins mediating protein-protein interactions in the cytoplasm and the nucleus. Various LIM-domain containing proteins have been identified to play a key role in signal transduction regulating the rearrangement of the actin cytoskeleton (Khurana et al. 2002). LIM-domain only 7 (LMO7) is the vertebrate orthologue of Smash and encodes two splice variants, LMO7a and LMO7b. In addition to the C-terminal LIM domain, LMO7 also exhibits a PDZ domain, a PDZ binding motif and another protein interaction domain, called Calponin Homology domain (Holaska et al. 2006) (Figure 9). LMO7a also contains a F-box sequence (amino acids 549–590), which was shown to be critical for degradation of cellular regulatory proteins (Cenciarelli et al. 1999). LMO7, located on chromosome 13q22 in humans, shows ubiquitous expression, although tissue-specific splice forms cannot be ruled out (Ooshio et al. 2004; te Velthuis & Bagowski 2007).

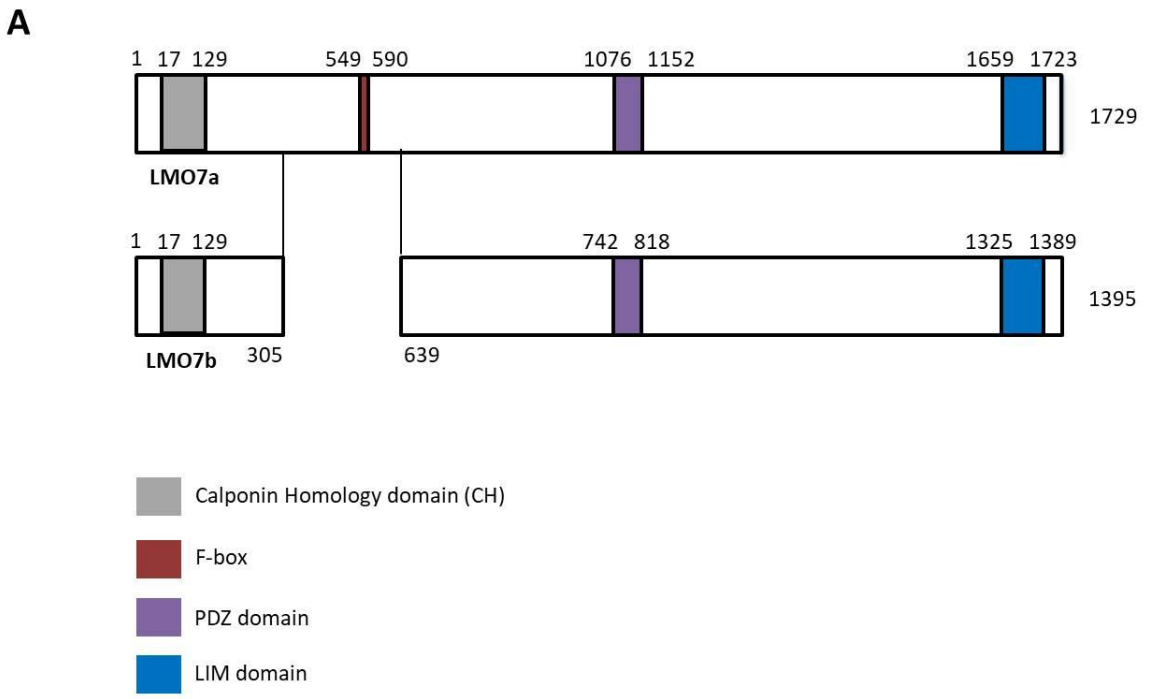

Figure 9: Isoforms of LMO7. LMO7, the vertebrate orthologue of Smash, encodes two splice variants. LMO7a contains a Calponin Homology domain, a F-box sequence as well as a PDZ domain and a LIM domain. LMO7b lacks the F-box domain.

Several studies showed that LOM7 is involved in formation and maintenance of epithelial architecture by remodeling the actin cytoskeleton. In the rat gallbladder it localizes at cell-cell interfaces at the region of the AJs (Figure 10), where it binds to the cell adhesion molecule Afadin, which in turn binds to Actin and Nectins. LMO7 also binds to the actin filament bundling protein α-Actinin, which is associated to α-catenin (Ooshio et al. 2004).

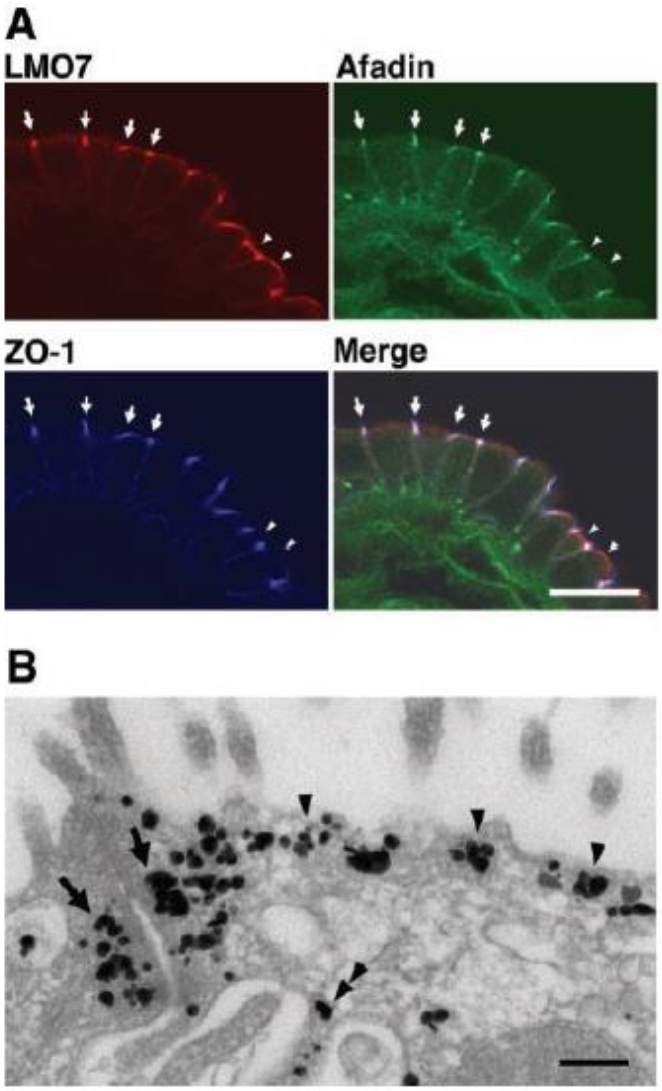

Figure 10: LMO7 localizes at AJs together with Afadin and ZO-1 in rat gallbladder. (A) Immunofluorescence microscopy of stained tissue with LMO7, Afadin and ZO-1 antibody. LMO7 localizes at AJs together with Afadin, the vertebrate homologue of *Drosophila* Canoe. (B) Electron microscopy of LMO7 in epithelial cells of rat gallbladder. Adapted from Ooshio et al. (2004).

For LMO7 a tumor suppressor function has been reported. In 22% of LMO7 full knockout mice, development of lung cancer was observed. Analysis of the cultured tumor cells showed numerical chromosome abnormalities (Tanaka-Okamoto et al. 2009). In human lung cancer a decreased expression of LMO7 in adenocarcinoma cells has been demonstrated (Nakamura et al. 2011). Furthermore, an upregulation of the expression of LMO7 has also been observed in tumors derived from liver, pancreas, prostate, colon and breast (Kang et al. 2000). Here, the fact that chromosome 13q22 is involved in hereditary breast

cancer is noteworthy, although it is not proven, that LMO7 is the only gene responsible (Kainu et al. 2000; Rozenblum et al. 2002).

Additionally, LMO7 binds directly to Emerin, an inner nuclear membrane protein. Mutations in *emerin* cause X-linked Emery–Dreifuss muscular dystrophy (X-EDMD), an inherited muscular disorder. Upon this interaction, Emerin inhibits the activity of LMO7 in *emerin* expression, indicating a negative feedback mechanism. Here, LMO7 acts as a transcription factor for *emerin* and other muscle relevant genes, shuttling between nucleus, cytoplasm and the cell surface (Holaska et al. 2006; Dedeic et al. 2011).

During zebrafish embryonic development severe defects in heart development have been reported upon the knockdown of LMO7. Morphological heart defects as well as heart mislocalization compared with control injected embryos were observed, pointing to a possible role of LMO7 in neural crest cells and their migration (Ott et al. 2008).

1.6 Src kinases

Members of the non-receptor Src family of protein tyrosine kinases (SFKs) are present in all metazoan cells and are involved in the regulation of various physiological functions (Brown & Cooper 1996). The importance of SFKs becomes clear in their pleiotropic function, as they contribute to signal transduction mediating cell growth, differentiation, cell shape, migration and survival. The Src family includes the nine members Src, Lck, Hck, Fyn, Blk, Lyn, Fgr, Yes, and Yrk (Table 1-1) (Parsons & Parsons 2004).

Table 1-1: Src family kinases.

Src family member[a]	*Pattern of expression*	*Isoforms*	*Oncogenic forms*[b]
Blk	B cells		
Fgr	Myeloid cells, B cells		Oncogenic fusion with gag sequences in feline sarcoma virus; overexpressed in some leukemias and lymphomas
Fyn	Ubiquitous	T-cell-specific isoform (Fyn T)	
Hck	Myeloid cells	Two different translational starts	
Lck	T cells, NK cells, brain		Overexpressed in T-cell acute lymphocytic leukemias
Lyn	Brain, B cells, myeloid cells	Two alternatively spliced forms	
Src	Ubiquitous	Neuron-specific isoforms	Mutated and truncated in retroviruses; truncated in colon cancer; overexpressed in mammary, pancreatic and other cancers
Yes	Ubiquitous		Oncogenic fusion with gag sequences in avian sarcoma viruses; highly expressed in colon, malignant melanoma and other cancers
Yrk	Ubiquitous		

(adapted from Parsons & Parsons 2004)

All members exhibit the conserved structure of three Src homology domains: a tyrosine kinase domain SH1, a phosphotyrosine binding domain SH2 and a N-terminal domain SH3, known to interact with proline rich regions (Figure 11). At the N-terminus a membrane targeting domain is located, carrying a myristoylation site, critical for membrane association and Src activity. The following 50-70 residues next to this SH4 domain vary among family members (Boggon & Eck 2004; Parsons & Parsons 2004; Roskoski 2004; Ia et al. 2010; Patwardhan & Resh 2010).

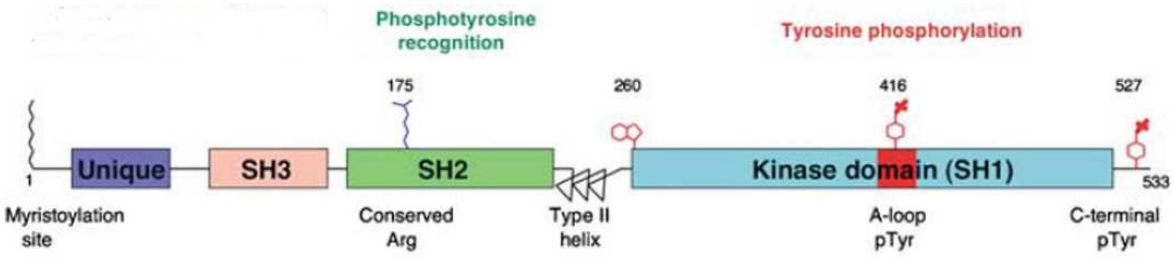

Figure 11: Structure of Src family kinases. Src kinases consist of four domains: the unique region, which differs among family members, followed by the SH3, SH2, and tyrosine kinase domains. The activation loop of the kinase domain and the activating (Tyr 416) and autoinhibitory (Tyr 527) phosphorylation sites are indicated in red. The conserved residue Arg 175 in the SH2 domain is crucial for phosphotyrosine recognition. Residue Trp 260 at the extreme N-terminus of the kinase domain is important for autoinhibition (adapted from Boggon & Eck 2004).

Src kinases are strictly regulated via phosphorylation of the respective sites. The activating phosphotyrosine 416 that results from autophosphorylation is located within the kinase domain SH1 and promotes kinase activity. At the C-terminus Src kinases display a short inhibitory phosphorylation site (Tyrosine 527), a target for the C-terminal Src kinase (Csk) and Csk homologous kinase. Phosphorylation of Tyr 527 results in intramolecular binding of the C-terminal tail to the SH2 domain and thus downregulates Src activity. (Cooper et al. 1986; Roskoski 2005; Ia et al. 2010).

Src was the first discovered oncogene encoding a non-receptor membrane-associated tyrosine kinase (Stehelin et al. 1977; Levinson et al. 1978; Varmus et al. 1989; Tice et al. 1999). Several members of Src kinases have an oncogenic form (table 1). This potential to induce cell transformation points to their important role in regulating cell growth. SFKs are involved in receptor tyrosine kinase (RTK) signaling by interaction with these growth factor receptors in DNA synthesis or survival pathways, cell motility and actin cytoskeleton rearrangement events. Ligand activation of many RTKs leads to direct activation of

SFKs (Bromann et al. 2004). For SFKs also a role in G protein coupled receptor (GPCR) signaling has been described, as SFKs are known effectors of activated G proteins. Additionally, Src activity is crucial for controlling GPCR trafficking and affects cell proliferation and cytoskeletal rearrangement (Parsons & Parsons 2004; Luttrell & Luttrell 2004; McGarrigle & Huang 2007). The importance of SFKs in cell-cell adhesion is reflected in the high number of cytoskeleton associated proteins among the substrates of Src kinases. Among them are RhoA and p120 catenin, which is known to regulate cell-cell adhesion through its interaction with the cytoplasmic tail of classical and type II cadherins and thus regulating actin dynamics (Reynolds & Roczniak-Ferguson 2004). Src also promotes epithelial-mesenchymal transition (EMT), an event characterized by the individualization of cells dissociating from epithelial structures (Boyer et al. 1997). Since this process requires alterations and turnovers of cell-cell adhesion complexes, Src kinases appear as good candidates for AJ function and remodeling. Moreover, activated Src in cultured cells leads to downregulation of E-Cad, which in turn is followed by cell-dissociation, a hallmark of invasive and metastatic cancers (Behrens et al. 1993).

1.6.1 Src42A - A *Drosophila* orthologue of Src

In *Drosophila* two Src homologues are encoded, Src42A and Src 64B. Src42A is the closest relative of vertebrate Src in *Drosophila*. It localizes along the entire plasma membrane but is enriched at the apical region of the AJs, where it forms a ternary complex with DE-Cadherin and Armadillo (Takahashi et al. 1996). Src42A has been shown to be involved in the regulation of cytoskeleton organization and cell-cell contacts in developing ommatidia (Takahashi 2005). An essential role for Src42A has been established during tracheal tube elongation, as it is required for polarized cell shape changes to orient membrane growth and cell rearrangements. The constitutive activation of Src42A leads to axial stretching and tracheal over-elongation, pointing to an instructive role in this process. Src42A seems to be the limiting factor for cell rearrangements in axial dimension of the tube (Förster & Luschnig 2012). The importance of Src42A during this morphogenetic event is also underlined in its dual role, as its activation leads to two opposing effects: On the one hand, activation of Src42A leads to reduction of E-Cad at the protein level on the other hand it enhances the transcription of E-Cad gene through the genetic interaction

with Armadillo and TCF (Shindo et al. 2008). These two main functions of Scr42A ensure the turnover and exchange of AJs and regulate the direction of anisotropic growth of the tissue (Shindo et al. 2008; Nelson et al. 2012).

Src42A mutants show a dorsal open phenotype (Takahashi 2005), pointing to an important function in cell-cell adhesion. The role of Src in dorsal closure via JNK signalling has been proven, as the activity of Src in this process is dependent on the activity of Basket (Bsk), the *Drosophila* homologue of JNK (Toyoshima et al. 1987).

Recent studies of Sun et al. (2017) showed a key role of Src42A in the formation of basolateral protrusions during rosette formation (Figure 6) in germband extension. In this process the most dorsal cell (D cell) and the most ventral cell (V cell) of the future rosette form wedge shaped protrusions in order to migrate towards each other. Embryos lacking Src42A fail to form these protrusions (Figure 12).

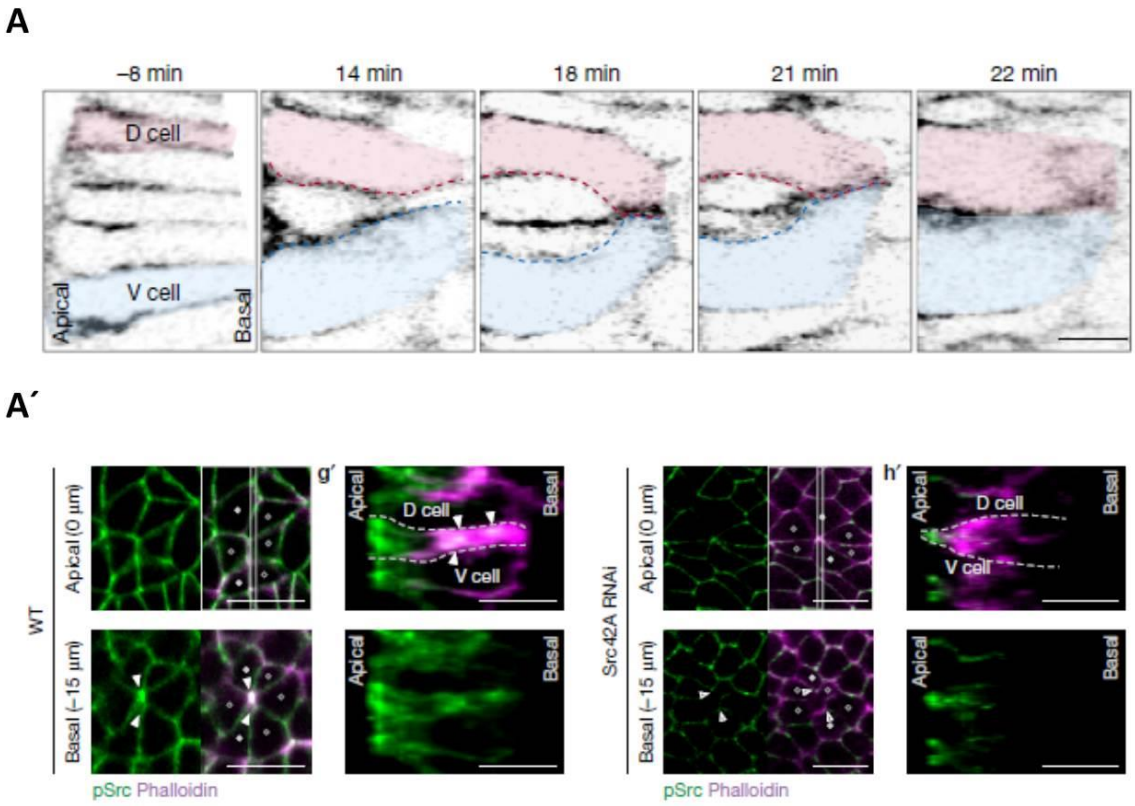

Figure 12: Src42A is involved in the formation of basolateral protrusions during germband extension. (A) Model of the formation of basolateral protrusions during formation of rosettes. The most dorsal (D) and most ventral (V) cell is highlighted in pink (D) and blue (V). (A´) In embryos lacking Src42A expression (right panel), formation of basolateral protrusions could not proceed in contrast to the wild type control (left panel). The arrowheads point to the edge of D/V cells during basolateral rosette formation. The open arrowheads show the absence of pSrc in defective protrusions (adapted from Sun et al. (2017)).

In a genome wide yeast two-hybrid screen Src42A has already been shown to interact with Smash (Giot 2003). Later studies of Beati et al. (2018) revealed that Smash is a binding partner and also a phosphorylation target of Src42A *in vitro* ad *in vivo*. Regarding to this knowledge, Src42A appears as a key candidate to elucidate the molecular pathway, in which Smash regulates cell adhesion and morphogenesis in *Drosophila* epithelial tissues.

1.7 Scope of this thesis

Dynamic cell adhesion of epithelial tissues is of fundamental importance for individual cell shape changes during morphogenesis. The establishment and maintenance of adhesion is regulated at the ZA via multiple proteins acting as molecular motors controlling the cytoskeleton. Although a range of regulators have been identified, the exact mechanism of how these tension dependent, dynamic processes are coordinated, is not clear.
The 170 kDa LIM domain protein Smash was identified as a binding partner of the key polarity determinant Baz/Par3, which has a key function in establishment of AJs during development. The vertebrate homologue of Smash, LIM-domain only 7 (LOM7) is involved in formation and maintenance of epithelial architecture by remodeling the actin cytoskeleton (Ooshio et al. 2004). Additionally, for LMO7 a possible function as tumor suppressor has been described (Tanaka-Okamoto et al. 2009; Nakamura et al. 2011), indicating a medical relevance for this so far unknown gene.

Initial results showed that overexpression of Smash induces apical constriction in epithelial cells and gave a first indication that Smash acts in a cytoskeleton associated manner (Beati et al. 2018). The aim of this study was to characterize the potential function of Smash as a regulator of actomyosin contractility during epithelial morphogenesis. For this purpose the loss-of-function phenotype of *smash* was characterized in this study. The intention was to identify proteins that interact with Smash at the ZA to elucidate the molecular mechanism of regulating cytoskeleton associated dynamics. Actomyosin activity is also coordinated by planar cell polarity (PCP), for instance in spatially directed neighbor exchange events during embryonic germband extension in order to elongate the body axis (Rauzi et al. 2010; Simões et al. 2010; Merks et al. 2018). Consequently, the aim of this work was to investigate Smash subcellular distribution and potential impact on PCP

signaling. Furthermore, the structure regarding to Smash function should be characterized.

Altogether, the purpose of this study was to resolve the molecular mechanism of how *smash* mediates actomyosin contractility at the cytoskeleton.

2 Materials and Methods

2.1 Materials

2.1.1 Chemicals, enzymes and kits

Chemicals, reagents, enzymes and kits were purchased from one of the following companies: AppliChem GmbH, Becton Dickinson GmbH, Bioline, Bio-Rad, Carl Roth GmbH, GE Healthcare, Genecraft, Gibco/BRL Life Technologies, Macherey Nagel, Merck Chemicals GmbH, Perbio Science, Roche Diagnostics, Sigma-Aldrich, ThermoFisher Scientific.

2.1.2 Fly stocks

Table 2-1: Fly stocks.

Bl = Bloomington stocknumber

Stock	Genotype	Chromosome(s)	Description	Source
Wild type fly lines				
wild type	*w*^{1118}		white eyes	Bl 5905
Gal4 driver lines				
actGal4	*actin<Gal4/CyO; MKRS / TM6b*	2,3	ubiquitous driver	Bl 4414
MTDGal4	*P{out-GAL4::VP16.R}1, w*; P{GAL4-nos.NGT}40; P{GAL4::VP16-nos.UTR}CG6325MVD1*	1,2,3	maternal triple driver the three GAL4 insertions together express GAL4 uniformly in the germarium and throughout oogenesis	Bl 31777
smallish fly lines				
smash$^{4.1}$	*smash*$^{4.1}$*/TM3*	3	*smash* mutant allele	Beati et al.

				(2018)
smash^{35}	*smash^{35}/TM6B*	3	*smash* mutant allele	Beati et al. (2018)
GFP-Smash PM	*UASp::GFP-Smash PM/Cyo*	2	expresses N-terminally GFP tagged Smash PM	Beati et al. (2018)
GFP-Smash PI	*UASp::GFP-Smash PI/Cyo*	2	expresses N-terminally GFP tagged Smash PI	Beati et al. (2018)
GFP-Smash PJ	*UASp::GFP-Smash PJ/Cyo*	2	expresses N-terminally GFP tagged Smash PJ	Beati et al. (2018)
GFP-Smash PI C-term	*UASp::GFP-Smash PI C-term/Cyo*	2	expresses N-terminally GFP tagged C terminus of Smash PI	Beati et al. (2018)
GFP-Smash PI N-term	*UASp::GFP-Smash PI N-term/Cyo*	2	expresses N-terminally GFP tagged N-terminus of Smash PI	Beati et al. (2018)
GFP-Smash PI ΔPBM	*UASp::GFP-Smash PI ΔPBM/Cyo*	2	expresses N-terminally GFP tagged Smash PI lacking the PDZ binding motif	Beati et al. (2018)
GFP-Smash PI ΔLIM	*UASp::GFP-Smash PI ΔLIM/Cyo*	2	expresses N-terminally GFP tagged Smash PI lacking the LIM domain	Beati et al. (2018)
GFP-Smash PI YmultiF	*UASp::GFP-Smash PI YmultiF/Cyo*	2	expresses N-terminally GFP tagged Smash PI with mutation of all six Y residues of GFP-Smash PI to F	Beati et al. (2018)
other				
baz mutant	*baz^{EH747}/FM7*	1	mutant allele	Krahn et al. (2010); Shahab et al.

				(2015)
BAC CH321-21P3	*BAC CH321-21P3/Cyo*	2	Bacterial artificial chromosome; contains complete genomic region of smallish	Beati et al. (2018)
sqh-GFP	*y1,w1,cv1,sqhAX3;P{sqhGFP.R}*	2	expresses N-terminally GFP tagged sqh under endogenous promoter in sqh mutant background	Bl 57144
sqh-mCherry	*sqhAX3; sqh::Sqh - mCherry*	2	expresses N-terminally mCherry tagged sqh under endogenous promoter in sqh mutant background	Martin et al. (2010)
Venus-Rok	*sqh::Venus RokK116A*	3	expresses N-terminally Venus tagged kinase dead version of Rok under sqh promoter	Simões et al. (2010)
DE-Cad-GFP	*endo::DE-Cad-GFP/Cyo*	2	expresses N-terminally GFP tagged DeCad under endogenous promoter	gift from T. Lecuit, Institut de Biologie du Développement de Marseille, Marseille,France; Huang et al. (2009)
Injection Stock GenetiVision	*y1 M {vas-int.Dm} ZH-2A w[*]; M {3xP3-*	2	2nd chromosome attP site at 22A. Expresses phiC31 integrase under	Bischof et al. (2007)

	RFP. attP}ZH-22A		the control of vasa. Insertion is marked with GFP and RFP expressed in the eye.	
FRT82Bovo^{D1}	*FRT82Bovo^{D1}/TM3, Sb*	3	Expresses dominant negative ovo to cause oogenesis arrest. Carries FRT site.	Bl 2149
hsFLP;;FRT82B*cno*^{R2}	*hsFLP;;FRT82Bcno^{R2}/TM3, Sb*	1,3	*cno* allele. Carries FRT site.	Sawyer et al. (2009)

2.1.3 Antibodies

2.1.3.1 Primary Antibodies

Primary antibodies used in this study are listed. IF = Immunofluorescence, WB = Western blotting, DSHB = Developmental Studies Hybridoma Bank.

Table 2-2: Primary Antibodies

Antigen	Host	Apllication	Dilution	Reference/Source
smash	guinea pig	IF	1:500	Beati et al. 2018
Baz	rabbit	IF	1:1000	Wodarz et al. 1999
DCAD2 DE-cadherin	rat	IF	1:5	DSHB
Src42A	rabbit	IF	1:1000	Takahashi (2005)
CF.6G11 βPS Integrin	mouse	IF	1: 10	DSHB
α-Actinin	rat	IF	1:10	Babraham Biosciences Technologies
Canoe	rabbit	IF	1:1000	Sawyer et al. 2009

phospho-Myosin light chain	rabbit	IF	1:50	Cell Signaling #36719
N2-7A1 Armadillo	mouse	IF	1:20	DSHB
anti-GFP	rabbit	WB	1:1000	A11122; Invitrogen
anti-GFP	mouse	WB	1:1000	Roche
9E10 anti-myc	mouse	WB	1:100	DSHB
anti-HA	mouse	WB	1:200	11-583-816-001; Roche
anti-PY	mouse	WB	1:1000	P3300; Sigma-Aldrich

2.1.3.2 Secondary Antibodies

For Western blotting (WB) and Immunofluorescence (IF) the following secondary antibodies were used.

Table 2-3: Secondary Antibodies

Antigen IG	Host	Conjugate	Application/Dilution	Reference/Source
guinea pig	goat	AF488	IF: 1:200	Invitrogen, A11073
guinea pig	goat	AF555	IF: 1:200	Invitrogen, A21435
guinea pig	goat	AF647	IF: 1:200	Invitrogen, A21450
rabbit	goat	AF488	IF: 1:200	Invitrogen, A11034
rabbit	goat	AF555	IF: 1:200	Invitrogen, A21429
rabbit	goat	AF647	IF: 1:200	Invitrogen, A21245
rat	goat	AF488	IF: 1:200	Invitrogen, A11006
rat	goat	AF555	IF: 1:200	Invitrogen, A21434
rat	goat	AF647	IF: 1:200	Invitrogen, A21247
mouse	goat	AF488	IF: 1:200	Invitrogen, A11029
mouse	goat	AF555	IF: 1:200	Invitrogen, A21424
mouse	goat	AF647	IF: 1:200	Invitrogen, A21236

guinea pig	goat	HRP	WB: 1:10000	Dianova, 106-035-003
rabbit	goat	HRP	WB: 1:10000	Dianova, 111-035-144
rat	goat	HRP	WB: 1:10000	Dianova, 112-035-068
mouse	goat	HRP	WB: 1:10000	Dianova, 115-035-068

2.1.4 Bacterial strains and Cell Culture Lines

Table 2-4: Bacterial strains and cell lines used in this work

E.coli XL-1 blue	Amplification and purification of plasmid DNA
S2/S2R$^+$cells	Transfection for protein-biochemical experiments

2.1.5 Plasmids

Table 2-5: Plasmids used in this work

Plasmid	**Source**
actin5c<Gal4	Beati 2013
UASp Smash-PM PAGW	Beati 2013
UASp Smash-PI PAGW	Beati 2013
UASp Smash-PJ PAGW	Beati 2013
UASp Smash-PI C-term PGW	Beati 2013
UASp Smash-PI N-term PGW	Beati 2013
UASp Smash-PI ΔLIM PGW	Beati 2013
UASp Smash-PI ΔPBM PGW	Beati 2013
UASp Rok pAMW	this work
UASp Sqh pAMW	this work
UASp Shroom PAMW	this work
UASp Moesin PAMW	this work
UASp Src42A PMW	(Beati 2013)

2.1.6 Vectors

Table 2-6: Vectors used in this work

Vector	Description	Source
pENTR/TOPO	Gateway entry vector, kanamycin resistance	Invitrogen
pAGW	act5c promoter Gateway cassette N-terminal eGFP tag	Drosophila Genomics Resource Center
pAMW	act5c promoter Gateway cassette N-terminal 6XMYC tag	Drosophila Genomics Resource Center
pAHW	act5c promoter Gateway cassette N-terminal 3XHA tag	Drosophila Genomics Resource Center

2.1.7 Oligonucleotides

Table 2-7: Primer used in this work

Primer	Sequence (5´- 3´)	Application
Rok_for	CAC CAT GCC AGC TGG ACG AGA AAC	Cloning of *Rok* fragment in expression vector for S2 cell transfection forward
Rok_rev	TCA TTT CAG CGA TGA ATT GGC TGG	Cloning of *Rok* fragment in expression vector for S2 cell transfection reverse
sqh_for	CAC CAT GTC ATC CCG TAA GAC	Cloning of *sqh* fragment in expression vector for S2 cell transfection forward
sqh_rev	TTA CTG CTC ATC CTT GTC CTT	Cloning of *sqh* fragment in expression vector for S2 cell transfection reverse
shroom_for	CAC CAT GAA AAT GCG CAA TCA	Cloning of *shroom* fragment in

		expression vector for S2 cell transfection forward
shroom_rev	CTA ACA ATC GCT TTG GAC TAG	Cloning of *shroom* fragment in expression vector for S2 cell transfection reverse
moesin_for	CAC CAT GGT CGT CGT CTC CGA	Cloning of *moesin* fragment in expression vector for S2 cell transfection forward
moesin_rev	TTA CAT GTT CTC AAA CTG ATC	Cloning of *moesin* fragment in expression vector for S2 cell transfection reverse

2.1.8 Microscopes/ Imaging Systems

Axioimager	Carl Zeiss Jena GmbH
Binocular Stemi 2000	Carl Zeiss Jena GmbH
Fluorescence Binocular	Leica MZ 16 FA
LSM 880	Carl Zeiss Jena GmbH
scanning electron microscope	Leo 1430VP

2.1.9 Technical devices

Centrifuge 5417 R	Eppendorf
Mastercycler gradient 5331	Eppendorf
ChemoCam Imager	Intas Science Imaging
Incubator B6	Heraeus
Incubation shaker Minitron	Infors HT

2.1.10 Software

Zen black	Carl Zeiss Jena GmbH
FIJI	Schindelin et al. (2012)
DNA sequence analysis	geneious 6.1.8.

2.2 Methods

2.2.1 Fly work and genetic methods

2.2.1.1 Fly breeding

Flies were kept on standard medium at 25°C, unless stated otherwise. Embryos used for live imaging or Immunostaining were collected by keeping the flies in cages on apple agar juice plates, coated with yeast.

Fly food

Standard medium (Ashburner 1989)

- Heat 9.5 L water, add
  - Agar Agar 50 g Carl Roth®
  - brewer's yeast 168 g Cenovis
  - soy flour 95 g Bauck GmbH

- Mix until foam forms
- Add the following components one by one and mix in between:
  - malt extract 450 g Arche Naturprodukte GmbH
  - treacle 400 g Grafschafter Goldsaft, Zuckerrübensirup; Grafschafter Krautfabrik Josef Schmitz KG
  - polenta 712 g HOLO, Reformhaus

- Cook for 45 min
- Cool down to 60 °C then add 45 ml propionic acid and 150 ml 10% nipagin

Apple agar plates

Agar Agar	20g	Carl Roth®
Sugar	8,5g	Raffinade, Peifer & Langen GmbH & Co. KG
Apple juice	170ml	natural juice, rio dòro
H_2O	330ml	

Mixture was cooked in microwave until the agar is in solution and cooled down to 60 °C. 10% Nipagin was added and solution was poured into big or small petri dishes, store at 4 °C, lid down.

2.2.1.2 Gal4-UAS System

The Gal4-UAS system is a binary system that was adapted from yeast. It uses the transcription factor Gal4, which binds to a specific promotor sequence called upstream activation sequence (UAS) to activate the expression of downstream gene products (Brand & Perrimon 1993). In *Drosophila* this system is utilized to drive ectopic expression of genes controlled in a temporal and spatial manner. To this aim, a driver fly line carrying the sequence for the Gal4 protein is crossed to a UAS line fused to the gene of interest.

2.2.1.3 Bacterial Artificial Chromosome

A bacterial artificial chromosome (BAC) is a DNA construct with a usual size of 150–350 kbp. Using *E. choli*, the BAC is maintained at low copy number, facilitating plasmid maintenance and recombineering, but is induced to high copy number for plasmid isolation. Recombineering allows gap repair and mutagenesis in bacteria. Gap repair efficiently retrieves DNA fragments up to 133 kilobases long from BAC clones. ΦC31-mediated transgenesis integrates these large DNA fragments at specific sites in the genome, allowing the rescue of lethal mutations in the corresponding genes. This transgenesis platform greatly facilitates structure/function analyses of most *Drosophila* genes. In this work BAC CH321-21P3 from the genomic BAC libraries engineered into the attB-P[acman]-Cm^R-BW vector was used (Venken et al. 2009).

2.2.1.4 Injection

The bacterial artificial chromosome was injected by Genetivision via ΦC31 integrase-mediated site specific transgenesis into the following docking site: VK37(2L).
Generation of transgenic flies by ΦC31-mediated targeted insertion at chromosomal position 22A was achieved by injection of attB-containing DNA constructs into embryos of the stock y1 M {vas-int.Dm} ZH-2A w[*]; M {3xP3-RFP. attP} ZH-22A (Bischof et al. 2007).

2.2.1.5 Rescue experiments

Former lethality studies showed that only 41,7% of homozygous *smash*^{35} mutant animals of the F1 generation eclosed as adults. For rescue experiments flies carrying the injected BAC CH321-21P3 were crossed in *smash*^{35} mutant background.
Full rescue was achieved when the eclosion rate of *smash*^{35} homozygous mutant adults expressing BAC CH321-21P3 achieved 100% of the expected value.

For further rescue experiments and structure function analysis, GFP-tagged Smash constructs inserted at chromosomal position 22A in *smash*^{35} homozygous mutant animals were expressed using the Gal4-UAS system. act5C::Gal4 was used as a ubiquitous driver line. Crosses for rescue experiments were set up according to the following scheme:

$$\frac{act5C :: Gal4}{CyO} ; \frac{smash35}{TM6B} \times \frac{UASp :: GFP - Smash}{CyO} ; \frac{smash35}{Tm6B}$$

According to Mendelian laws, 11.11% of the progeny should have the following genotype if all animals except for homozygous balancer animals survive:

$$\frac{act5C :: Gal4}{UASp :: GFP - Smash} ; \frac{smash35}{smash35} \quad (1)$$

The animals with genotype 1 are those that are potentially rescued by expression of the respective GFP-Smash construct. The percentage of *smash*^{35} homozygous mutant animals

carrying only the act5C::Gal4 driver or the respective UASp::GFP-Smash construct over the CyO balancer would be 22.22% according to Mendel, if all *smash*^{35} homozygous flies would survive, which is not the case. The corresponding two genotypes are as follows

$$\frac{act5C :: Gal4}{CyO} ; \frac{smash35}{smash35} \quad or \quad \frac{UASp :: GFP - Smash}{CyO} ; \frac{smash35}{smash35} \qquad (2)$$

The flies were counted with the respective genotypes and determined the percentage relative to the total number of all surviving animals. The percentage of homozygous *smash*^{35} flies not expressing the GFP-Smash construct (2) were divided by 2 to allow comparison to the percentage of potentially rescued homozygous *smash*^{35} flies (1). If the percentage of animals with genotype 1 was significantly higher than the percentage of animals with genotype 2 divided by 2, this was scored as rescue of the semilethality of *smash*^{35} animals. Normal distribution was controlled using the Shapiro–Wilk test. P-values were calculated using a two-sided paired t test.

2.2.1.6 Generation of germline clones

Germline clones were created using the FLP/FRT system (Chou & Perrimon 1992; Chou & Perrimon 1996) and the female sterile *ovo*^{D1} allele (Mével-Ninio et al. 1996). Via this method it is possible to exclude the maternal component through the generation of a homozygous mutant germ line in otherwise heterozygous mutant flies. The FLP/FRT system allows recombination between alleles containing the FRT sites thus enabling the generation of homozygous mutant flies. This catalytic reaction is mediated by the flippase, whose enzymatic activity is controlled by a heatshock promoter that is induced at 37 °C. Due to the female sterile ovo^{D1} allele, only egg chambers that are homozygous mutant for the desired allele are able to develop. Upon heat shocking L2 larvae of the genotype hsFLP;; FRT82Bcno^{R2}/FRT82Bovo^{D1} for 3 h at 37°C, mitotic recombination between FRT sites was induced, catalyzed by the heat shock flippase (hsFLP) on the first chromosome. The crossing was set up according to the following scheme:

$$\frac{w}{y} ;; \frac{FTR82B, ovoD1}{TM3, Sb} \; x \; \frac{hs :: FLP}{x} ;; \frac{FRT82B, cnoR2}{TM3, Sb}$$

$$\downarrow$$

$$\frac{w}{hs :: FLP} ;; \frac{FTR82B, ovoD1}{FRT82B, cnoR2}$$ heat shock

2.2.2 Molecular Biology Methods

2.2.2.1 Polymerase Chain Reaction

For amplification of desired coding sequences using the appropriate primer sequences, the proofreading polymerase Phusion® High-Fidelity DNA Polymerase (NEB) was used. Amplification of the constructs was performed with the following PCR-program:

Time	Temperature [°C]	Purpose	
30 sec	95	Initial denaturation	
15 sec	95	denaturation	
15 sec	primer specific	annealing	34 cycles
1 min	68	elongation	
5 min	68	final elongation	

The annealing temperature was selected based on the primer specific melting temperature, while the elongation time depended on the length of the desired DNA fragment. PCR products were confirmed by agarose gel electrophoresis.

2.2.2.2 Gel electrophoresis

Agarose gel electrophoresis was performed to analyse amplified DNA fragments based on their size. DNA molecules are separated by the fact that negatively charged DNA migrates towards the cathode in an electric field (Schwartz & Cantor 1984).

The gels used as matrix contained 1x TAE buffer supplemented with 1 % agarose. Before loading the DNA samples into the gel, they were supplemented with HDGreen Plus (Intas)

to stain DNA. For distinction of fragment size, GeneRuler 1kB DNA ladder (Fermentas) was loaded to a separate pocket. DNA molecules were separated for 30 minutes at 100 V.

TAE-Puffer (50x): 2M Tris base
50 mM EDTA pH 8,0
1M acetic acid

2.2.2.3 DNA extraction from Agarose gels

After separating DNA molecules via gel electrophoresis the band of the desired size was cut out. DNA was extracted using NucleoSpin Extract II Kit (Macherey-Nagel).

2.2.2.4 Gateway cloning

The full length coding sequences of desired genes were PCR-amplified from following clones, which were purchased from the Drosophila Genomics Resource Center are listed in the following table.

Table 2-8: cDNA clones used in this work

cDNA clone	gene
LD15203	*rok*
LD14743	*sqh*
LD13775	*shroom*
RH14719	*moesin*

For respective primer sequences refer to Table 2-7. PCR-amplified coding sequences were cloned into the pENTR vector using the pENTR Directional (SD/D-) TOPO Cloning kit (Invitrogen) following the manufacturer's instructions. N-terminally HA-/Myc-tagged constructs were generated by LR-recombination using the Gateway LR Clonase Enzyme Mix (Invitrogen) of the respective pENTR vector and the appropriate Gateway destination vectors: pAHW and pAMW (Drosophila Genomics Resource Center, see Table 2-6).

2.2.2.5 Transformation in *Escherichia coli*

For the transformation of chemically competent *Escherichia coli* (*E. coli*) cells, about 100 ng of desired plasmid DNA was added to 50 µl competent cells (XL-1 blue or One Shot®). After an incubation time of 5 minutes on ice, the cells were heat-shocked at 42°C for 45 seconds. Afterwards, the tubes were immediately transferred back on ice and incubated for another 2 minutes. 250 µl prewarmed (RT) LB-medium was added to the cells and the mixtures were incubated at 37 °C for 1h while shaking. Finally, about 80 µl of the bacterial culture was spread on a prewarmed selective agar plate and incubated overnight before colonies were screened.

LB-Medium:	1% Trypton
	0,5% yeast extract
	1%NaCl
LB-Agar plates:	LB-Medium
	1% Agar-Agar
	100µg/ml Ampicillin or 50µg/ml Kanamycin

Agar plates for selection of bacteria with antibiotic resistance. Autoclave directly after adding water. Cool down until hand warm (50 °C) and add antibiotics in the required concentration. Pour into petridishes and store lid down at 4 °C.

2.2.2.6 Plasmid purification

The preparation of plasmid DNA was performed via mini-preparation for smaller amounts or via midi-preparation for bigger amounts of DNA required. Midi-preparation was done following the manufacturer's instructions of the Nucleobond AX Kit (Macheray-Nagel). For mini-preparation 1.5 ml of an overnight culture were centrifuged (13000 rpm, 1 min) and the obtained pellet resuspended in 150 µl buffer S1 (50mM Tris pH 8.0, 10mM EDTA, 100 µg RNAse A per ml). Another 150 µl of buffer S2 20mM NaOH, 1% SDS) were added

and the reaction was inverted 5 times with following 5 minutes incubation time at RT. Subsequently, 150 µl buffer S3 (3.0M KAc pH 5.5) were added and the tubes were inverted 5 times. After centrifuging the reaction 20 minutes at 13000 rpm, the supernatant was transferred into a new tube and precipitated with 400 µl isopropanol. After centrifugation of 30 minutes at 13000 rpm, the supernatant was discarded and the pellet was washed with ice-cold 70% ethanol. The air-dried pellet was resuspended in distilled water.

Buffer S1: 50mM Tris pH 8.0
10mM EDTA
100µg RNAse A/ml

Buffer S2: 20mM NaOH
1% SDS

Buffer S3: 3M KAc pH 5.5

2.2.3 Biochemical Methods

2.2.3.1 Embryonic protein extraction

Flies were kept in cages to allow to them to lay their eggs on apple juice agar plates overnight. Embryos were collected, washed with dH_2O, dechorionated with sodium hypochlorid for 4 min and transferred into a microtube. 200 µl lysis buffer containing proteinase inhibitors was added and embryos were homogenized using a biovortexer.
The lysate was incubated on ice for 20 min and centrifuged at 14.000 rpm for 10 min at 4°C. The supernatant was transferred into a new microtube and protein concentration was determined. If protein lysates were not used directly, they were stored at -20°C.

Lysis buffer: 150mM NaCl
50mM Tris pH 8.0
1% Triton X-100

Proteinase Inhibitors:

2 µg of the following Proteinase inhibitors were added to the lysis buffer.

Aprotinin

Leupeptin

Pepstatin A

Pefabloc SC

2.2.3.2 Protein lysate from S2 cells

Cells were harvested and centrifuged at 1000 rpm for 5 min. Supernatant was discarded and the obtained pellet was resuspended in 300 µl lysis buffer with proteinase inhibitors (1:500). The cell lysate was transferred to a new microtube and incubated on ice for 20 min. After centrifugation at 14000 rpm at 4°C for 10 min the supernatant was again transferred into a new microtube and the protein concentration was determined.

2.2.3.3 Determination of Protein concentration

The concentration of proteins was determined using the Pierce BCA Protein Assay Kit (Thermo Scientific). Therefore, a reference series was defined. The protein lysates were diluted 1:5 in lysis buffer. 250 µl of standards and samples were transferred to a 96 well plate that already contained 200 µl of BCA reagent. After incubation for 30 min at 37°C, the plate was cooled down to room temperature for 5 min and absorbance was measured at 562nm.

2.2.3.4 Co-Immunoiprecipitation

Co-immunoprecipitation was performed from protein lysate from previously (co-) transfected *Drosophila* S2R+ cells using GFP-Trap® beads (Chromotek). Beads were washed three times with TNT buffer and centrifuged for 2 min at 2500 g at 4°C. Before incubation with the protein lysate (1µg protein applied) for 1h at 4 °C, an input sample of 30 µl was taken. Afterwards, the beads were centrifuged at 2500 g and washed three times with TNT buffer. Subsequently, the beads were centrifuged down at 2500 g at 4°C and the supernatant was discarded. The immunoprecipitated GFP-tagged protein is coupled to the beads and interaction partners also remain bound to the precipitated protein. After de-

naturation of the proteins bound to agarose beads with 15 µl of 2x SDS loading buffer, proteins were separated via SDS-PAGE and interaction partners could be detected by Western Blot.

TNT buffer: 50mM Tris-HCl pH 8,0
150mM NaCl
1% Triton-X

2.2.3.5 SDS PAGE

Sodium dodecyl sulfate-polyacrylamide gel electrophoresis (SDS PAGE) is a technique to separate proteins based on their molecular weight. SDS binds to the proteins to achieve a negative charge of all proteins. In an electric field, these proteins migrate towards the positively charged cathode with different mobility, depending on their size. In the SDS-polyacrylamide gel electrophoresis this migration happens in a gel containing polyacrylamide, whereas the density of the gel can be controlled by the amount of acrylamide. In this polyacrylamide mesh smaller proteins migrate faster while larger proteins migrate slower.

SDS PAGE

Component	for 7,5%	for 10%	for 12,5%
30% Acrylamide	1.9 ml	2.5 ml	3.1 ml
1 M Tris-HCl pH 8.8	2.8 ml	2.8 ml	2.8 ml
20% SDS	38 µl	38 µl	38 µl
dH_2O	2.7 ml	2.1 ml	1.5 ml
10% APS	30 µl	30 µl	30 µl
TEMED	8 µl	8 µl	8 µl

Stacking gel

Component	Amount
30% Acrylamide	310 µl
1 M Tris-HCl pH 6.8	235 µl
20% SDS	10 µl
dH_2O	1.3 µl
10% APS	10 µl
TEMED	5 µl

Gels were placed into BioRad Mini Protean III electrophoresis chamber containing 1x SDS running buffer. The protein samples and a protein ruler for size determination were loaded into the gel pockets and the gel was run at 200V for 1h.

1x SDS running buffer: 192mM Glycin
25mM Tris
0,1% SDS

2X SDS loading dye: 125mM Tris-HCl pH 6,8
3mM EDTA
0,05% Bromphenolblue
10% β-Mercaptoethanol
5% SDS
20% Glycerol

2.2.3.6 Western Blot

In a Western Blot proteins that are separated via SDS PAGE are transferred to a nitrocellulose membrane and can be detected by specific antibodies. The horizontal transfer of the proteins occurs in transfer buffer via the BioRad system at 100V at 4°C for 1h. The proteins, which are negatively charged due to the SDS, run towards the nitrocellulose membrane, which is placed on the positively charged cathode side of the blot. The transfer was confirmed with Ponceau staining of the nitrocellulose membrane.
Subsequently, the membrane was blocked for 30 min with Western blot blocking buffer to prevent unspecific binding of the antibodies. Afterwards, the membrane was incubated overnight at 4 °C with the primary antibody in Western blot blocking buffer in a sealed plastic bag while shaking.
The membrane was washed three times for 10 min with TBST while shaking. The secondary HRP-conjugated antibody was diluted in Western blot blocking buffer and the membrane was incubated at RT for 2 h under shaking. After washing the membrane three times for 10 min with TBST, protein detection was performed using a chemiluminescence substrate (BM Chemiluminescene Blotting Substrate (POD), Boehringer/Roche Diagnostics). Detection of the signal was performed using the ChemoCamImager by Intas Science Imaging. For reprobing, the primary and secondary antibodies were removed from the membrane using a stripping buffer. Therefor the western blot membrane was incubated with 10 ml of fresh stripping buffer while shaking. Afterwards, the membrane was washed two times with PBS for 10 min and two times with TBST for 5 min. The membrane was blocked with Western blot blocking buffer and the procedure continued like described above.

Transfer buffer: 25mM Tris
192mM Glycin
20% MeOH

TBST: 20mM Tris pH 8.0
150mM NaCl
0,2% Tween-20

Blocking buffer: 3% Skim Milk Powder
1% BSA in TBST

Stripping buffer: 200mM Glycin
0,1% SDS
1% Tween20
pH 2,2

2.2.4 Histology

2.2.4.1 Formaldehyde fixation of embryos

Flies of the desired genotype were kept in cages to allow them to deposit their eggs on apple agar plates over night at 25°C. Embryos were loosened from the plates with water using a brush and dechorionated by adding 3 ml of sodium hypochlorite for 4 min. The embryos were washed with water and transferred to a glass vial containing equal volume of heptane and fixing solution consisting of 1xPBS and 4% formaldehyde. The fixation was performed for 17-20min while shaking. Afterwards the fixation solution was removed and replaced by 3ml methanol. The embryos were vigorously shaken to remove the vitelline membrane and sank down to the glass vial bottom. Embryos were transferred into 1,5ml microtubes and washed three times with methanol. If they were not used for Immunostaining immediately, they were stored in methanol at -20°C.

PBT: 1x PBS
0,1% Tween 20

PBTX: 1x PBS
0,5% Triton X-100

Mowiol: 5g Mowiol in 20ml PBS mixed 16h at RT, add 10ml Glycerin, mix again 16h at RT

4% Formaldehyde: 110µl 37% Formaldehyde
890µl PBS

2.2.4.2 Heat Fixation of embryos

An overnight embryo collection was dechorionated and washed as mentioned before (2.2.4.1). A small bottle of 1x Triton salt solution was put on ice. 1-2ml of this solution was transferred to a scintillation vial, which was placed in a small beaker with water to heat it on a hot plate (vial cap should be 1/2 screwed on). The collected embryos were dropped into the vial with hot solution, which was quickly recapped and shaken once. Afterwards 10-15 ml of ice-cold 1x Triton solution was quickly added and the vial was kept on ice for 1min. The vial was removed with tweezers, the solution was poured off and replaced by heptane and methanol to remove the vitelline membrane by shaking. The embryos were incubated in methanol for at least 1h and stored at -20°C in methanol, unless they were used for Immunostaining immediately.

Triton salt solution: 3% Triton-X
0,6 M NaCl

2.2.4.3 Immunostaining

The embryos or tissues were washed three times for 10 min in either 0,1% PBTw in case of embryos, or PBS with 0,2% Triton X-100 in case of other tissues. After blocking with blocking solution (washing buffer containing 5% Normal Horse Serum (NHS)) to prevent unspecific binding for 1 h, the respective primary antibody was added in blocking solution over night at 4°C. The embryos or tissues were washed again three times for 10 min, before the secondary fluorophor-coupled antibody diluted blocking solution was added and the tissue was incubated for 2h at RT while shaking. Subsequently, the tissue was washed once for 20 min in washing buffer containing Hoechst dye. After washing twice for 10 min the tissue or embryos were mounted in Mowiol.

2.2.4.4 Analysis of planar cell polarity

Planar polarity was analyzed by measuring the mean intensity of AP cell edges (60°–90°) relative to the AP axis) and the mean intensity of D/V cell edges (0°–25° relative to the A/P axis) at embryonic stage 8. Using ImageJ software (Schneider et al. 2012), the mean pixel intensity and orientation for each junction were analyzed. In each image, intensities were determined by 20 randomly chosen user-drawn lines for both edges parallel and perpendicular to the AP axis. A representative number of images was quantified for each experiment (n = 4 embryos for WT; n = 6 embryos for mutant). A mean value was obtained for each embryo. P-values were calculated using a two-sided unpaired t test.

2.2.5 Cell Culture

2.2.5.1 Cultivation of S2 cells

Schneider S2 or S2R+ cells, an immortalized culture of *Drosophila* embryonic cells (Schneider 1972) were used for biochemical experiments. The cells were grown at 25 °C in *Drosophila* S2 medium (Life technologies) containing fetal bovine serum (FBS) and antibiotics (Pen/Strep). Cells were counted using a Neubauer improved counting chamber and passaged twice a week.

S2-Medium:	Schneider´s Drosophila Medium	Life technologies
	10% FBS (Fetal Bovine Serum)	Life technologies
	50U/ml Penicillin, 50µg/ml Streptomycin	

2.2.5.2 Transfection of S2 cells

Transfection of Schneider S2 or S2R+ cells was performed using the FuGENE® HD transfection reagent (Promega). The transfection reagent was preincubated with 1 µg of the desired DNA for each sample for 15 min. The mixture was transferred to two wells containing 1-5x10^6 cells each and incubated for 72h at 25°C before the cells were harvested.

2.2.6 Imaging

2.2.6.1 Electron Microscopy

Embryos were fixed like described before (2.2.4.1). After washing with methanol, the embryos were washed with PBS several times. Dehydration of the embryos was achieved by immersion in ethanol series (5 min each step). Afterwards they were washed twice with 100% acetone, before they were preinfiltrated in 1:1 acetone:tetramethylsilane solution (TMS) for 30 min. In the next preinfiltration step, the embryos were transferred into a 1:2 acetone:TMS solution for another 30 min, before they were incubated in pure TMS for 30 min. Subsequently, some of the TMS was removed and replaced by fresh TMS. The microtubes were put under the hood to allow the embryos to air dry. For imaging the embryos were transferred to plates and sputtered with gold particles.

2.2.6.2 Laser Ablation

Immobilization of early L3 larvae was performed as described (Kakanj et al. 2016). The larvae had the genotype endo:DE-Cad-GFP, sqh::Sqh-mCherry or endo::DE-Cad-GFP, sqh::Sqh-mCherry; *smash*^{35}/*smash*^{35}. Only the 488nm channel was imaged. Laser ablation of cell bonds was performed on an inverted spinning disk confocal microscope (UltraView VoX [PerkinElmer] or Inverse TiE [Nikon]) with a 60×/1.2 NA water-immersion objective equipped with 355-nm pulsed ultraviolet laser (DPSL-355/14; Rapp OptoElectronic, 14-mW meanpower, 70-µJ per pulse). Laser ablation was induced at the plane of the AJs

in the dorsal midline of abdominal segment A3, A4, or A5 with laser power of 0.25 µJ pulsed energy (measured after the objective). Laser ablation was conducted during time-lapse imaging. Larvae were imaged at ~25°C on a spinning disk confocal microscope (Ultra-View VoX or Inverse TiE) with a single plan 60×/1.2 NA water-immersion objective and an attached CCD camera (C9100-50 CamLink; 1,000 × 1,000 pixels) controlled by Volocity software v.6.3. Images were taken every 0.5 s for 2–3 min, started ~2 min before ablation, and finished ~5 min after ablation. Images were processed using Fiji (National Institutes of Health). To analyze the vertex displacements of ablated cell bonds, the vertex distance increase from different ablation experiments were averaged in four time intervals of 20 s. First measurement point was defined as time of ablation. Standard errors were determined.

2.2.7 Statistical analysis

For statistical analysis Excel (Microsoft office package 2010) was used.

3 Results

3.1 Loss of maternal and zygotic *smash* leads to severe morphogenetic defects

In Beati et al. (2018) two deletion alleles were generated. The allele *smash*^{35} lacks the whole coding region of *smash*, while in the allele *smash*$^{4.1}$ a portion of the 3´-coding region including the LIM-PBM module is removed.

In order to study the function of the LIM domain protein Smash, maternal and zygotic mutants were generated (*smash*$^{35m/z}$). Embryos of this genotype were stained for Baz and DAPI and visualized via confocal microscopy. The majority (68%) of *smash*$^{35m/z}$ embryos showed severe defects in morphogenesis reflected by uncoordinated furrows and invaginations. During gastrulation, many exhibited an incorrectly formed ventral or cephalic furrow, whereas ectopic furrows were formed in unpredicted positions. In later developmental stages completely irregular shaped bodies were observed, as they were twisted or segmentation did not occur properly. Furthermore, tubular organs like fore- and hindgut, salivary glands or the tracheal tree were not formed correctly. These results were confirmed via scanning electron microscopy on *smash*$^{35m/z}$ and wild type embryos (Figure 13). Embryos of the genotype *smash*^{35}/*smash*$^{4.1}$ showed very similar phenotypes. Figure 14 shows two embryos at stage 7 and stage 13 with typical morphogenetic defects upon the loss of *smash* in contrast to control wild type embryos.

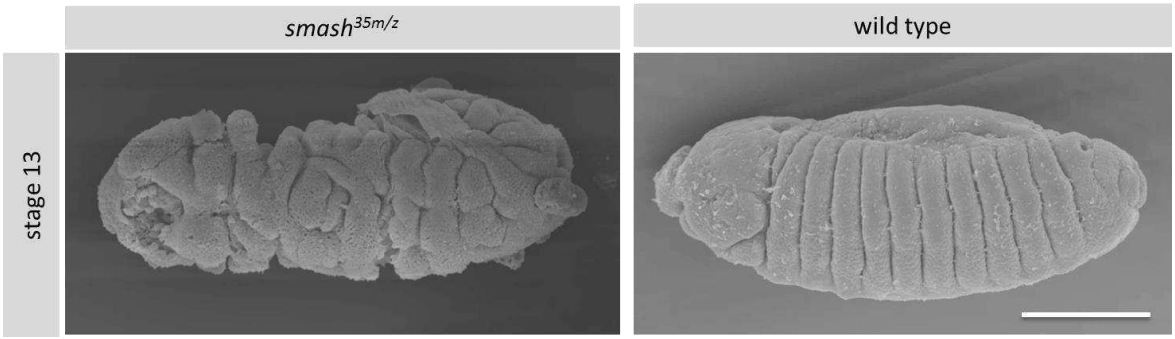

Figure 13: Scanning EM of *smash*$^{35m/z}$ and wild type embryos at stage 13. *smash*$^{35m/z}$ mutant embryo shows extremely irregular shape and surface structure in contrast to the wild type control. Bars: 100µm.

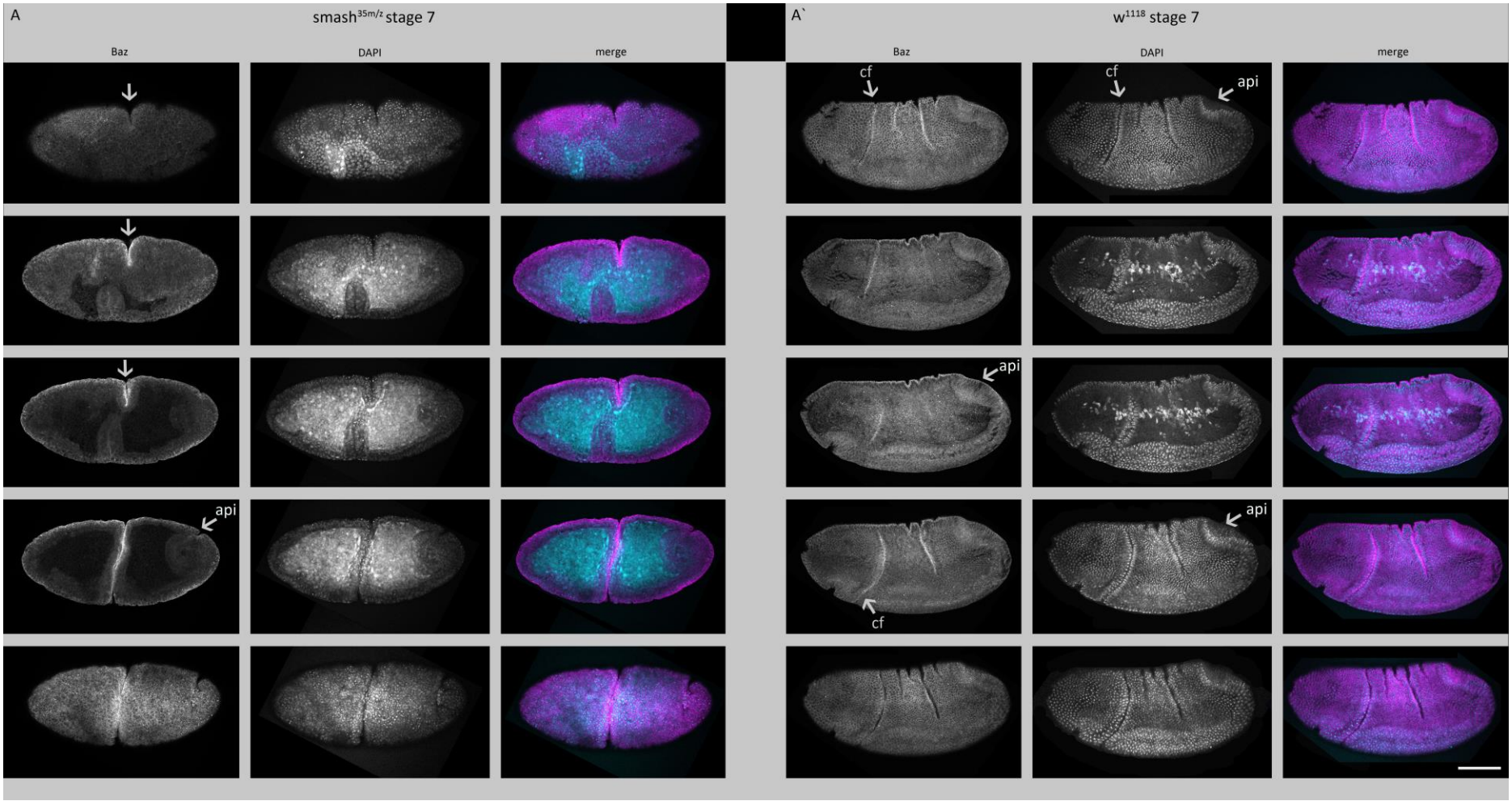

Figure 14A: Embryos lacking maternal and zygotic *smash* show severe defects in morphogenesis. (A) *smash*$^{35m/z}$ mutant embryos at stage 7 stained for Baz and DAPI in comparison to (A´) wild type control. Five optical sections of the same embryo are shown. The upper panel shows the most superficial section, followed by deeper sections showing the inside organs of the embryo. The *smash*$^{35m/z}$ mutant embryo failed to form the cephalic furrow (cf) and a correct amnioproctodeal invagination (api; arrow panel 4). It shows a deep ectopic furrow in the middle of the embryo (arrows panel 1 and 2). Bars: 100 µm.

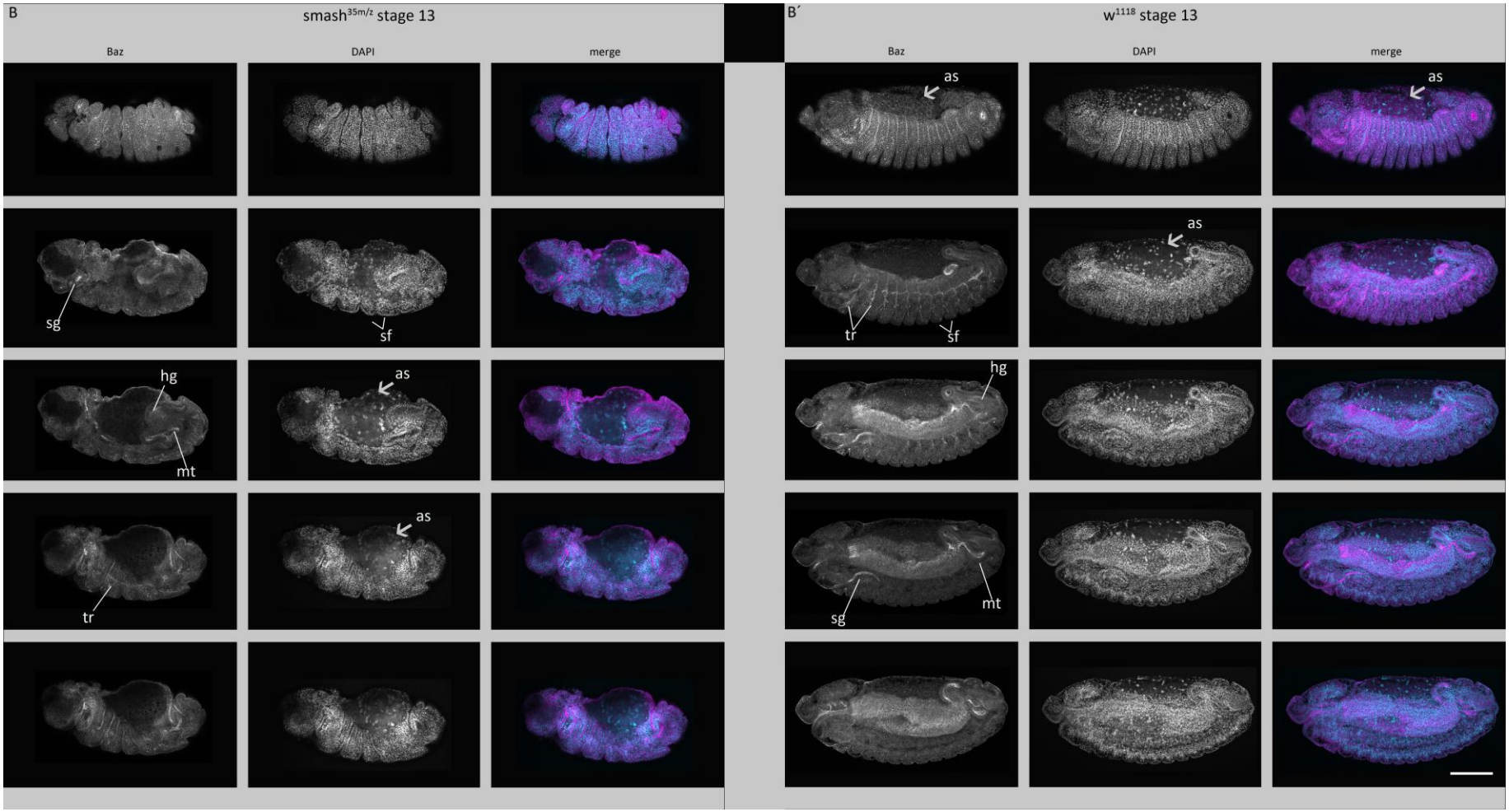

Figure 14B: Embryos lacking maternal and zygotic *smash* show severe defects in morphogenesis. (B) *smash*$^{35m/z}$ mutant embryos at stage 13 stained for Baz and DAPI in comparison to (B´) wild type control. Five optical sections of the same embryo are shown. The upper panel shows the most superficial section, followed by deeper sections showing the inside organs of the embryo. The *smash*$^{35m/z}$ mutant embryo exhibits an extremely irregular shape with random clefts in its surface. Segmental furrows (sf) are formed irregularly in their shape and depth. Inner organs like hindgut (hg), tracheae (tr), salivary glands (sg) and malpighian tubules (mt) show extreme defects in morphogenesis. The yolk covered by the amnioserosa (as) bulges out of the dorsal side of the embryo. Bars: 100 µm.

3.2 Rescue of semilethality of *smash* mutant animals

Despite this strong phenotype appearing in 68% of *smash*$^{35m/z}$ mutant embryos (shown in 3.1), occasionally escaper flies hatched, which completed embryogenesis and developed into viable, fertile adults. However, the fitness of these animals was strongly reduced, as they were weak and short-lived. Former lethality studies showed that only 41,7% of homozygous *smash*^{35} mutant animals of the F1 generation eclosed as adults, while this number dropped to 25% in the F2 generation (Beati et al. 2018), pointing to a strong maternal effect.

To confirm that this semilethality is indeed a result of the loss of *smash* and not due to a second site hit on the *smash*^{35} chromosome, rescue experiments were conducted.

For this purpose Smash-GFP constructs, including the three full length isoforms and several deletion constructs, were expressed in *smash* mutant background via the Gal4-UAS system using the ubiquitous driver actin5C::Gal4. Semilethality was fully rescued by the ubiquitous expression of full length GFP-Smash PM, as well as by the overexpression of the shorter isoform PI. The third isoform Smash PJ, which lacks the LIM-PBM module, was not able to raise the hatching rate significantly, which underlines the importance of these two domains (Figure 16A). Semilethality of *smash*^{35} mutants was also rescued by chromosomal insertion of bacterial artificial chromosome CH321-21P3, which carries the whole genomic locus of *smash* (Figure 15)

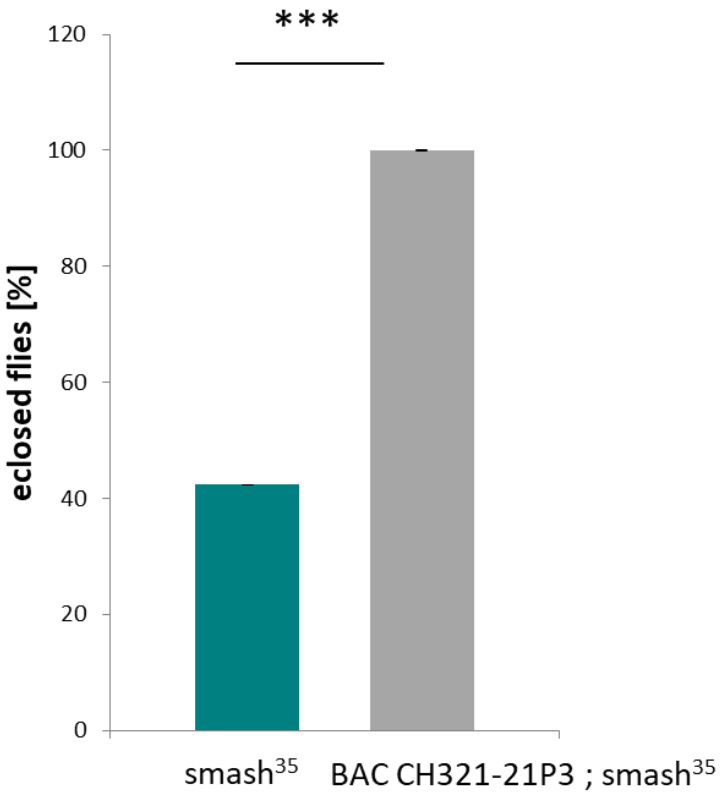

Figure 15: Bacterial artificial chromosome CH321-21P3 rescues semilethality of *smash*^{35} mutants. Grey bars: mean percentage of *smash*^{35} animals ± SEM. Green bars: mean percentage of animals carrying BAC CH321-21P3 ± SEM. Rescue was achieved when the eclosion rate of *smash*^{35} homozygous mutant adults expressing BAC CH321-21P3 achieved 100% of the expected value. *smash*^{35}: n=490; BAC CH321-21P3: n=426. (***: p < 0,001; **: p < 0.01; *: p < 0.05; ns: not significant). n= x flies in 3 repeats of crossing.

To investigate which protein domains are functionally required, a structure-function analysis was conducted, using several transgenic fly lines carrying different deletion constructs of GFP- Smash PI (Figure 16B). A version of Smash PI lacking the N-terminal part of Smash and just expressing the C-terminus containing the LIM-PBM module was able to rescue the semilethality of *smash*^{35}, whereas a construct just carrying the N-terminus failed to rescue. Deletion constructs lacking only the LIM domain or just the PDZ binding motif both rescued, demonstrating none of these domains alone are essential. Finally, as described before Smash is bound and phosphorylated by Src42A. To test the functional importance of Smash phosphorylation, a construct in which six potential phosphorylation sites were mutated (GFP-Smash PI YmultiF) was expressed in *smash*^{35} mutant background in order to rescue. Indeed, even this version of GFP-Smash PI was able to rescue, meaning

that phosphorylation of these sites by Src42A is dispensable for the rescue of semilethality.

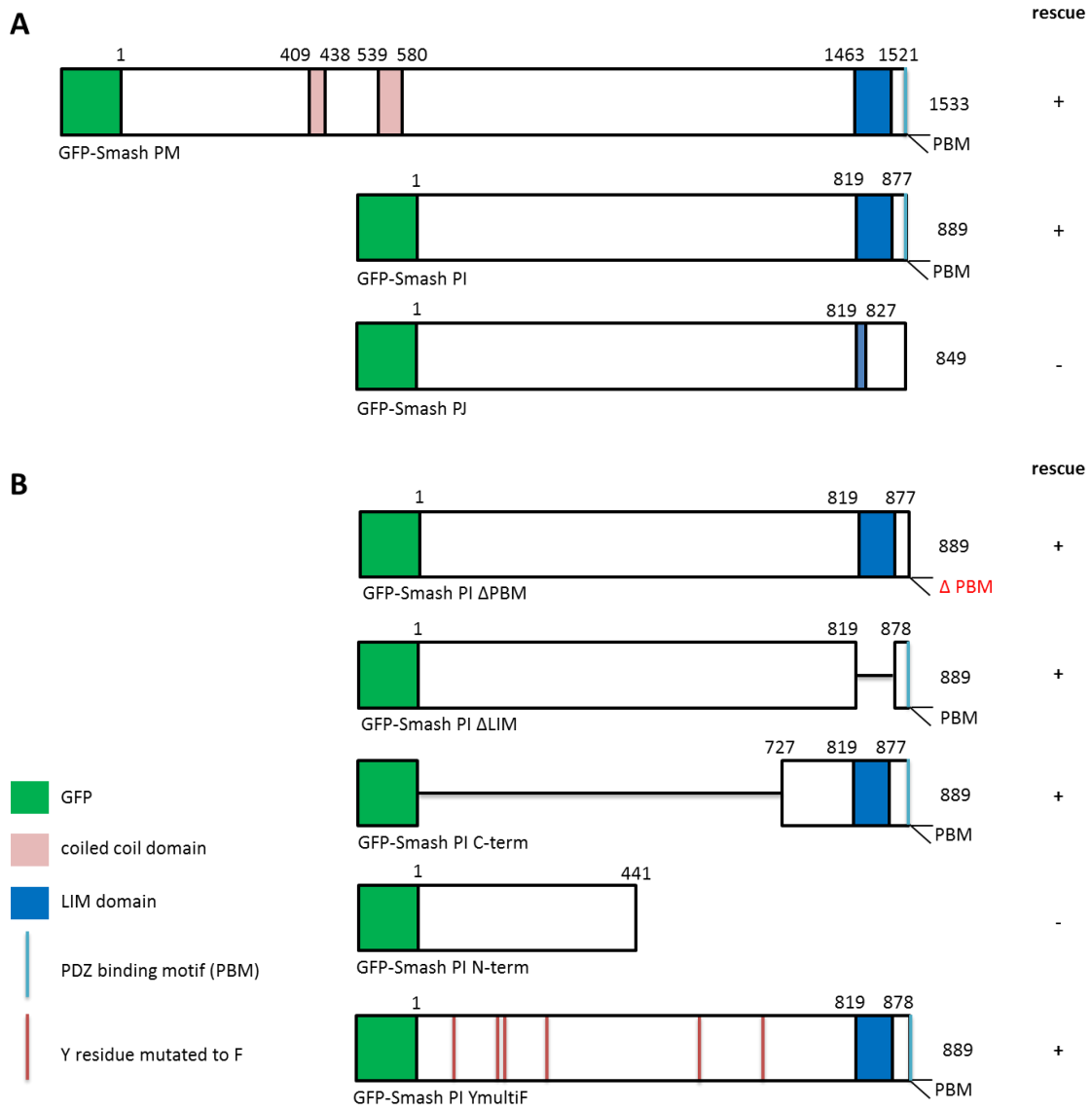

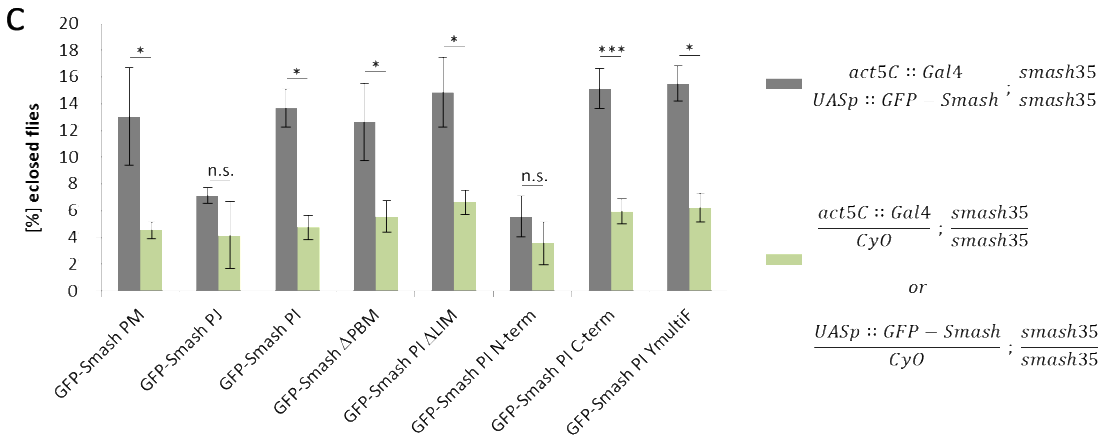

Figure 16: Overexpression of Smash PM and Smash PI rescues semilethality of *smash*^{35} mutant animals. (A) GFP-tagged isoforms Smash PM, Smash PI and Smash PJ. + or – in the column to the right indicates whether semilethality of *smash*^{35} was rescued by overexpression. (B) GFP-tagged deletion constructs of GFP-Smash PI. + or – in the column to the right indicates whether semilethality of *smash*^{35} was rescued. (C) Quantification of the rescue assay. Grey bars: mean percentage of animals with the respective genotype ± SEM. Green bars: mean percentage of animals with the respective genotype divided by 2 ± SEM. The number of eclosed *smash*^{35} homozygous adults expressing the respective GFP-Smash construct under control of the ubiquitous act5C::Gal4 driver line was counted and compared with the number of eclosed *smash*^{35} homozygous mutant adults from the same cross carrying only act5C::Gal4 or the respective UAS::GFP-Smash construct as negative control. Rescue was achieved when the eclosion rate of *smash*^{35} homozygous mutant adults expressing the rescue construct was significantly ($p<0.05$) higher than in the negative control (***: $p < 0{,}001$; **: $p < 0.01$; *: $p < 0.05$; ns: not significant). GFP-Smash PM: $p = 0.041$, $n = 663$; GFP-Smash PJ: $p = 0.143$, $n = 525$; GFP-Smash PI: $p = 0.014$, $n = 579$; GFP-Smash PI ΔPBM: $p = 0.045$, $n = 626$; GFP-Smash PI ΔLIM: $p = 0.033$, $n = 613$; GFP-Smash PI N-term: $p = 0.071$, $n = 875$; GFP-Smash PI C-term: $p = 0.009$, $n = 1072$; GFP-Smash PI YmultiF: $p = 0.021$, $n = 632$. n= x flies in 3 repeats of crossing.

3.2.1 GFP-Smash PI deletion constructs show various subcellular localizations

With regard to the results of the rescue experiments and thus to further analyze the importance of the distinct domains of Smash, the subcellular localization of these GFP-Smash PI deletion constructs where characterized (Figure 17). For this purpose an amnioserosa specific Gal4 driver was used, whose function was confirmed by the expression of the transmembrane protein CD8-GFP under UAS control. As expected, GFP-Smash PI localizes at the apical ZA associated to the AJs, where it shows a co-localization with DE-Cad and Armadillo. Interestingly, GFP-Smash PI ΔPBM and GFP-Smash ΔLIM showed a slightly different distribution. Junctional staining was still detectable, but in contrast to full length GFP-Smash PI a clear detachment from cell-cell borders was noticeable. This phenotype was stronger in case of the deletion construct lacking the LIM domain. GFP-Smash N-term, which was not able to rescue semilethality of *smash*^{35} mutants, encodes

for the N-terminal part only and thus misses the entire C-terminus containing the LIM-PBM unit. This construct completely lost its AJ-association and showed an evenly cytoplasmic distribution, pointing to the importance of the junctional attachment of Smash for proper functionality. Surprisingly GFP-Smash PI C-term, which in fact was able to rescue semilethality, also showed a clear detachment from the junctions and was detectable in the cytoplasm.

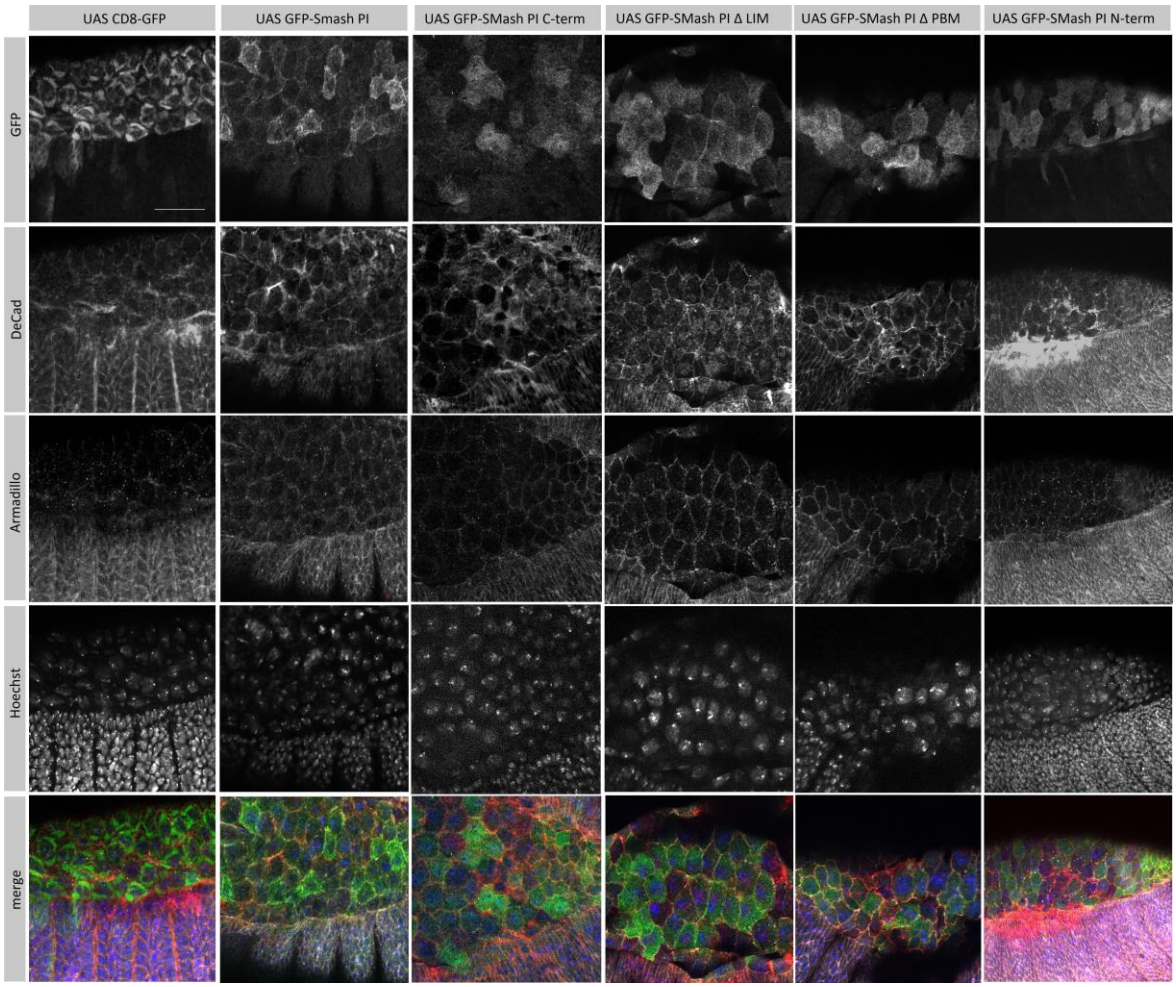

Figure 17: GFP-Smash PI deletion constructs show different subcellular localizations. Embryonic amnioserosa cells expressing GFP-Smash PI deletion constructs stained for GFP, DE-Cadherin and Armadillo. DNA was stained with Hoechst. GFP-Smash PI full length localizes to AJs; GFP-Smash PI ΔPBM showed slight cytoplasmic localization, but was mainly retained at AJs; GFP-Smash PI ΔLIM was even more cytoplasmic distributed. GFP-Smash PI N-term and GFP-Smash PI C-term were distributed cytoplasmic; CD8-GFP was used as membrane marker control. Bars 20µm.

3.3 Cortical tension is reduced in *smash* mutant epidermis

Recent studies showed that the overexpression of Smash in randomly induced clones in the follicular epithelium leads to apical constriction of epithelial cells (Beati et al. 2018). In contrast, embryos lacking maternal and zygotic *smash* showed irregular serpentine shaped junctions instead of straight, tautly ones (Figure 18).

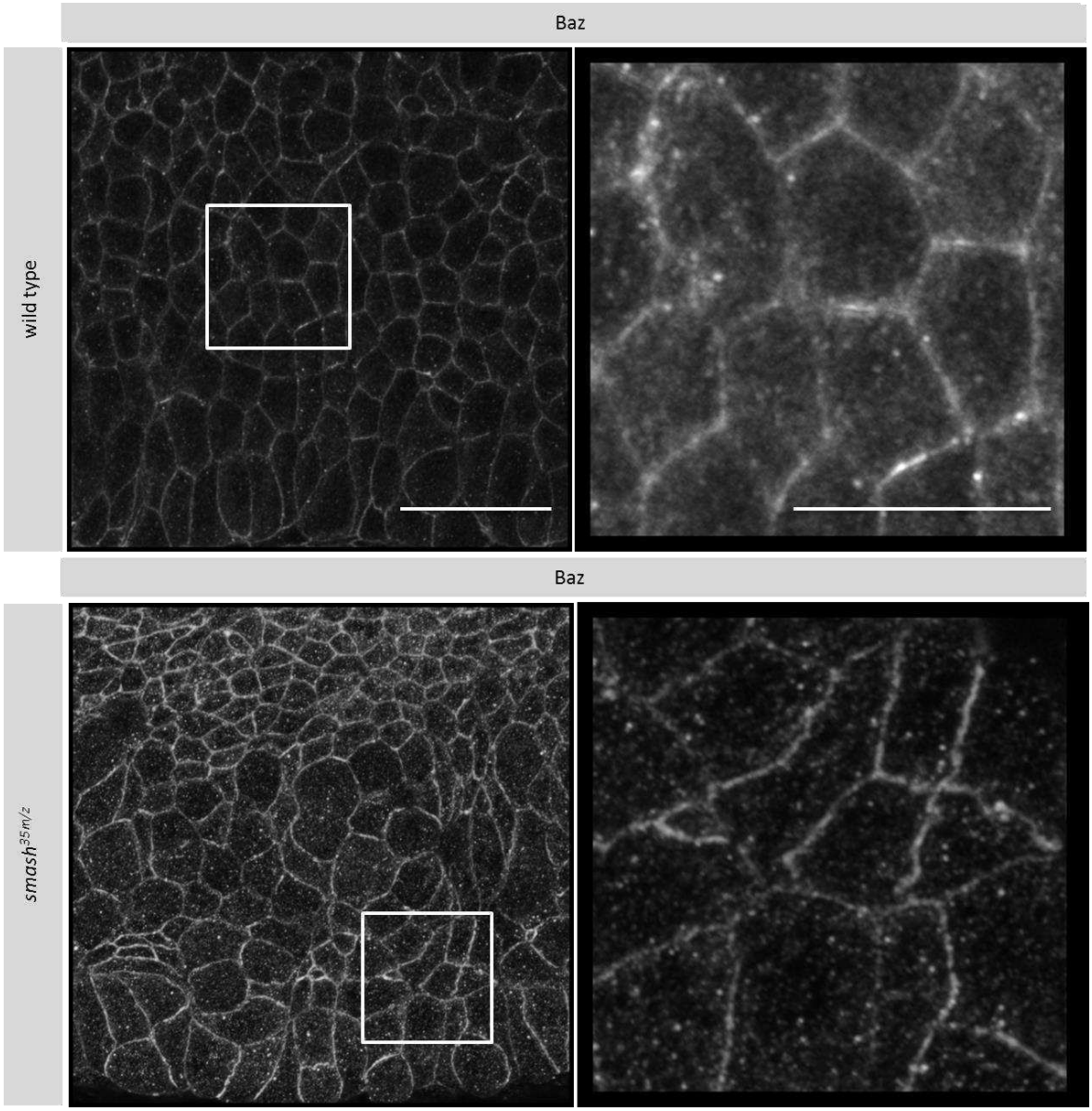

Figure 18: Junctions show serpentine shaped phenotype upon the loss of *smash*. Immunostaining for Baz in wild type and *smash*$^{35m/z}$ mutant embryos stage 8. Due to the loss of *smash*, junctions are not straight anymore, pointing to a loss of tension. Anterior is to the left and dorsal is up. Bars 10µm.

Since the process of apical constriction is accompanied by a gain of tension in those cells, it seems likely that the loose and slack junction phenotype in the *smash* mutant is due to a loss of cell bond tension. To confirm this hypothesis, laser ablation experiments in living wild type and *smash*^{35} larvae were performed. To validate that larval (L3) epidermal cells are an appropriate cell type to study Smash, the expression of Smash in the epidermis of wild type L3 larvae was examined via Immunostaining (Figure 19A). During laser ablation, the cortical actin belt of those cells was cut by a pulsed UV laser in the region of the ZA, marked by DE-Cad-GFP. The displacement of opposing cell vertices was followed over time by live imaging, whereby a higher vertex displacement speed correlates with higher cell bond tension (Landsberg et al. 2009).

In wild type situation, cell vertices were moving faster compared to *smash* mutant larvae (Figure 19B). This observation was quantified by analyzing the average vertex distance increase from different ablation experiments in four time intervals of 20s, while the first measurement was the time of ablation. A significant reduction of the vertex displacement speed and amplitude in *smash*^{35} larvae was determined, indicating that indeed the loss of *smash* leads to a reduction of cell bond tension (Figure 19C).

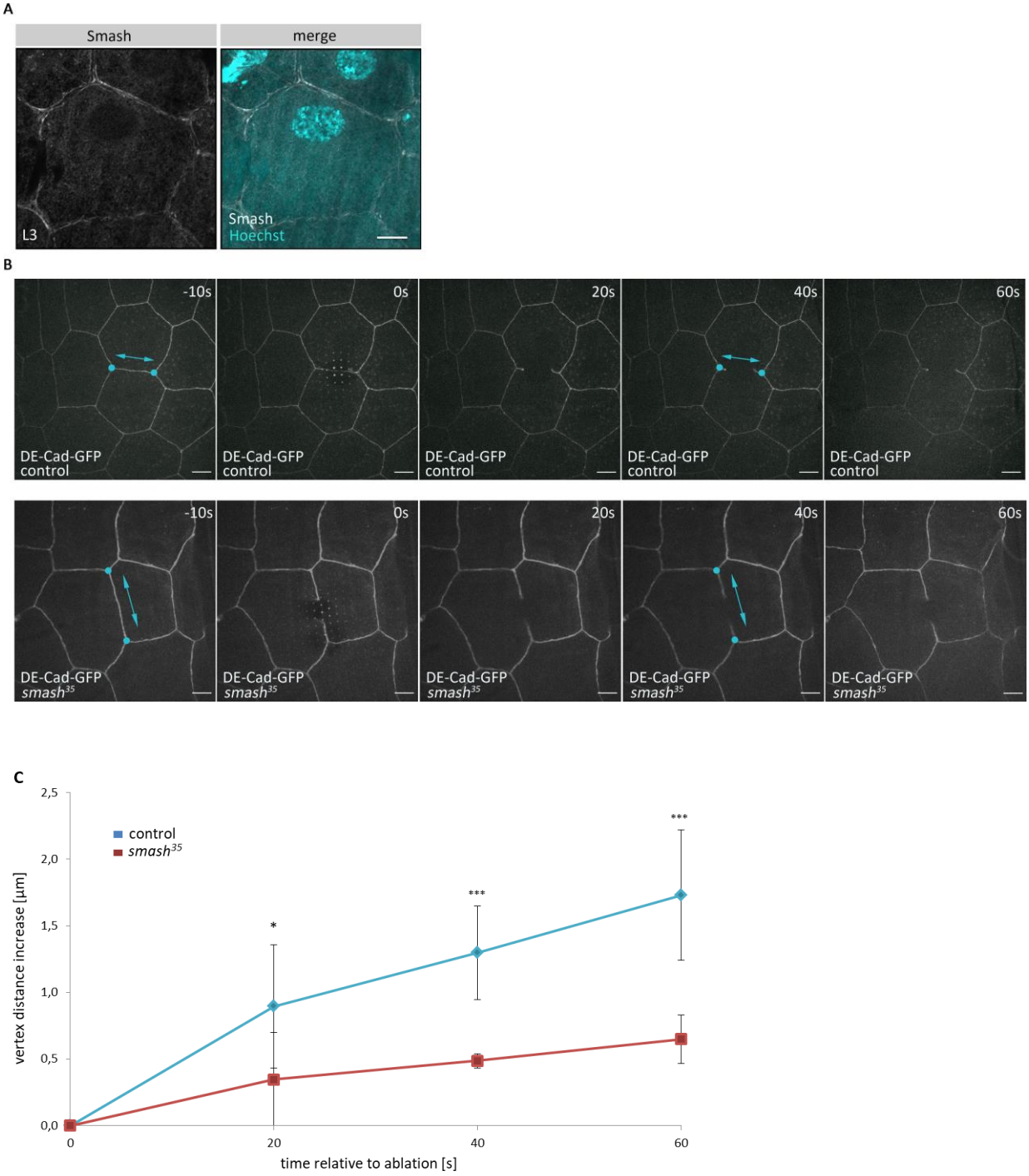

Figure 19: Cell bond tension is reduced upon loss of *smash* function. (A) L3 wild type larvae stained for Smash and Hoechst to confirm Smash expression in larval epidermis. (B) Live imaging of laser ablation of single cell bonds in the epidermis of *smash*^{35} and control third instar larvae. The ZA was marked with DE-cad-GFP. The time (seconds) relative to the time point of laser ablation (0) is given in each panel. The distance (double-headed cyan arrows) between vertices (cyan dots) of the ablated cell bond was measured over time. (C) Quantification of vertex distance increase over time in wild type and *smash*^{35} larvae. Mean vertex displacement amplitude ± SEM: wild type (20 s) 0.896 ± 0.462 µm, *smash*^{35} (20 s) 0.346 ± 0.353 µm; *, p = 0.0279; wild type (40 s) 1.297 ± 0.352 µm, *smash*^{35} (40 s) 0.485 ± 0.055 µm; ***, p = 5.998 × 10−5; wild type (60 s) 1.729 ± 0.490 µm, *smash*^{35} (60 s) 0.649 ± 0.182 µm; ***, p = 0.00014; mean vertex displacement speed ± SEM in first 60 s: wild type 0.029 ± 0.007 µm/s, *smash*^{35} 0.011 ± 0.003 µm/s; ***, p = 0.00014. p-values were determined using the two-sided unpaired t test. n = 7 representative videos were analyzed for each genotype. Bars 20µm.

3.4 Subcellular localization of Smash within the actomyosin network

In *Drosophil*a embryos, Smash is detectable from stage 5 onwards in all ectodermally derived epithelia, including the epidermis, the fore- and hindgut, amnioserosa, malpighian tubules and the tracheal tree. Smash expression was also found in the somatic body wall muscles, the pharynx muscles and the visceral muscles surrounding the midgut (Beati et al. 2018). In the somatic musculature, Smash was strongly enriched at the cell-cell contact sides between the epidermal tendon cells and the muscle fibers, called myotendinous junctions. Here a strong co-localization with α-Actinin and β-PS Integrin could be detected (Figure 20).

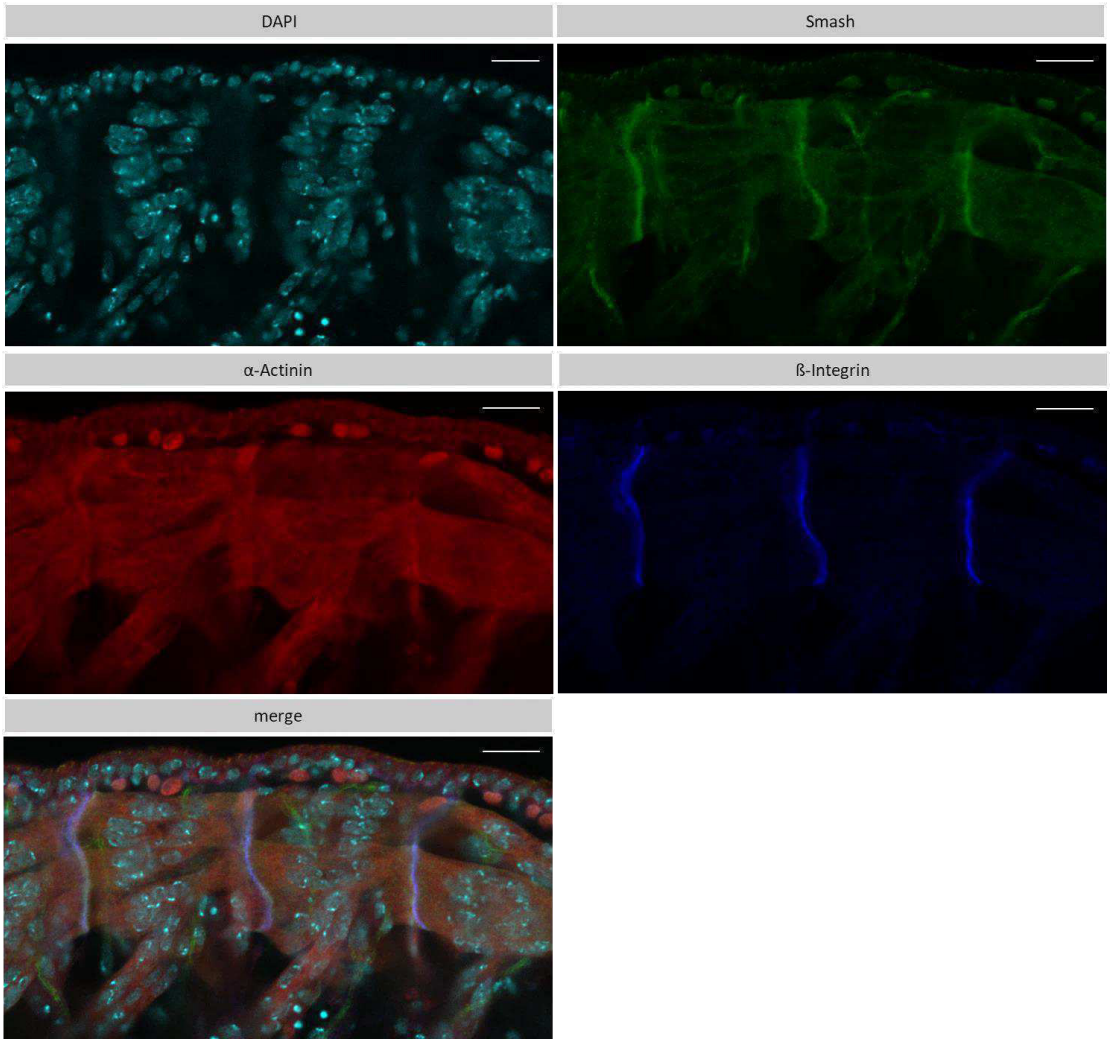

Figure 20: Smash is enriched at myotendinous junctions. Immunostaining of a stage 16 embryo. Smash accumulates at myotendinous junctions where it colocalizes with α-Actinin and β-Integrin. Bars 20µm.

On the subcellular level, Smash localizes at the apical ZA in the region of the AJs together with Baz, Rok and Sqh, the *Drosophila* myosin light chain. These proteins are not only restricted to the apical part of the cells, they also show a polarization within a plane. Baz shows an enrichment at AJs present in the dorsal/ventral (D/V) axis (Simões et al. 2010), while Venus-Rok and Sqh-mCherry localize to junctions positioned in the anterior/posterior (A/P) axis. Smash was also found planar polarized in the embryonic epidermis during germband extension as it shows a significant enrichment at A/P cell borders, where it co-localizes with Venus-Rok, Sqh-mCherry and also Cno (Figure 21).

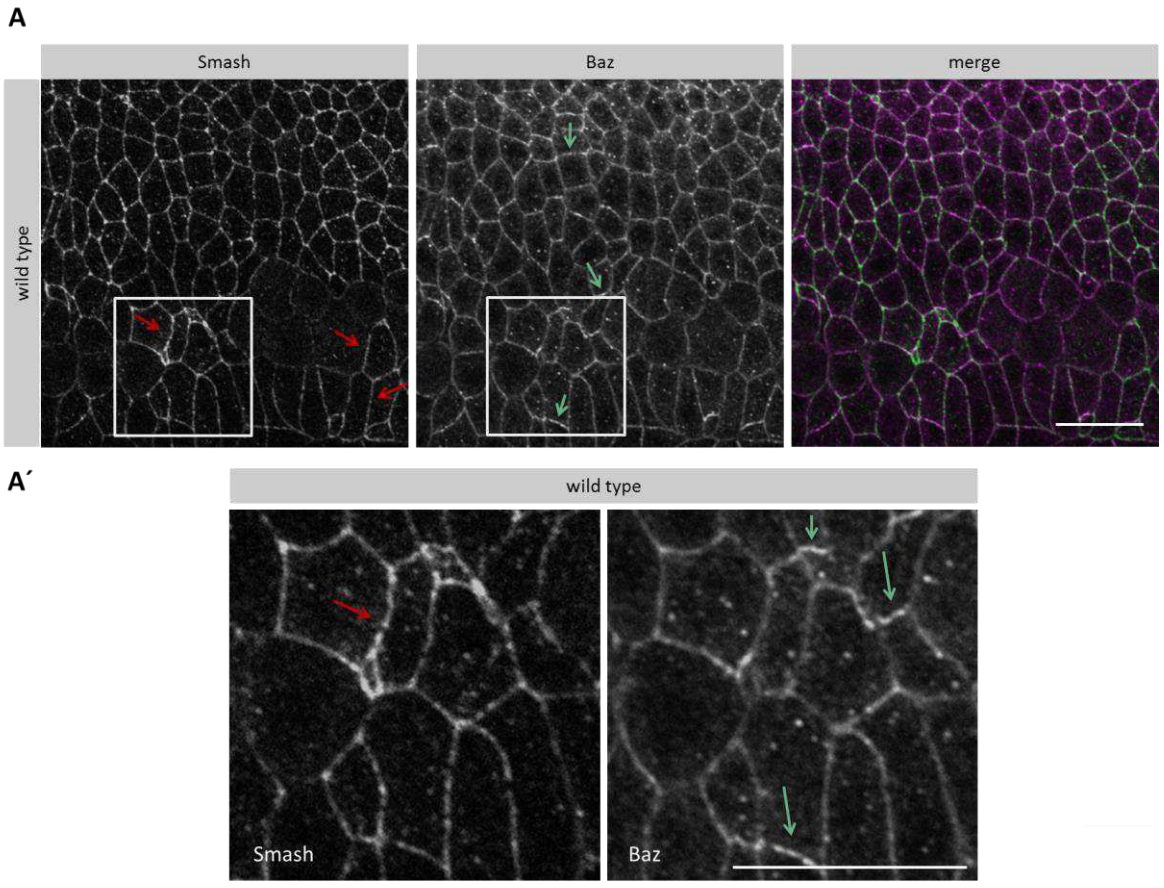

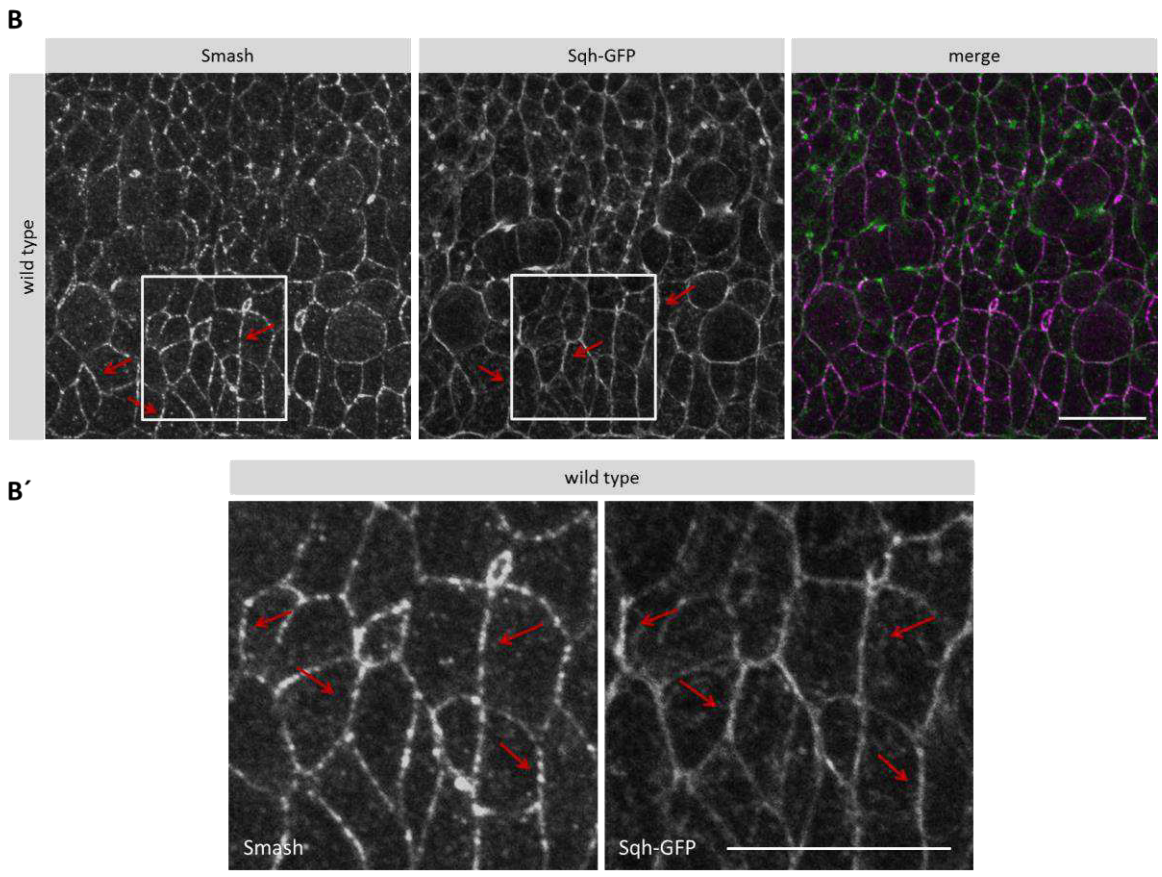
B
Smash
Sqh-GFP
merge
wild type
B´
wild type
Smash
Sqh-GFP

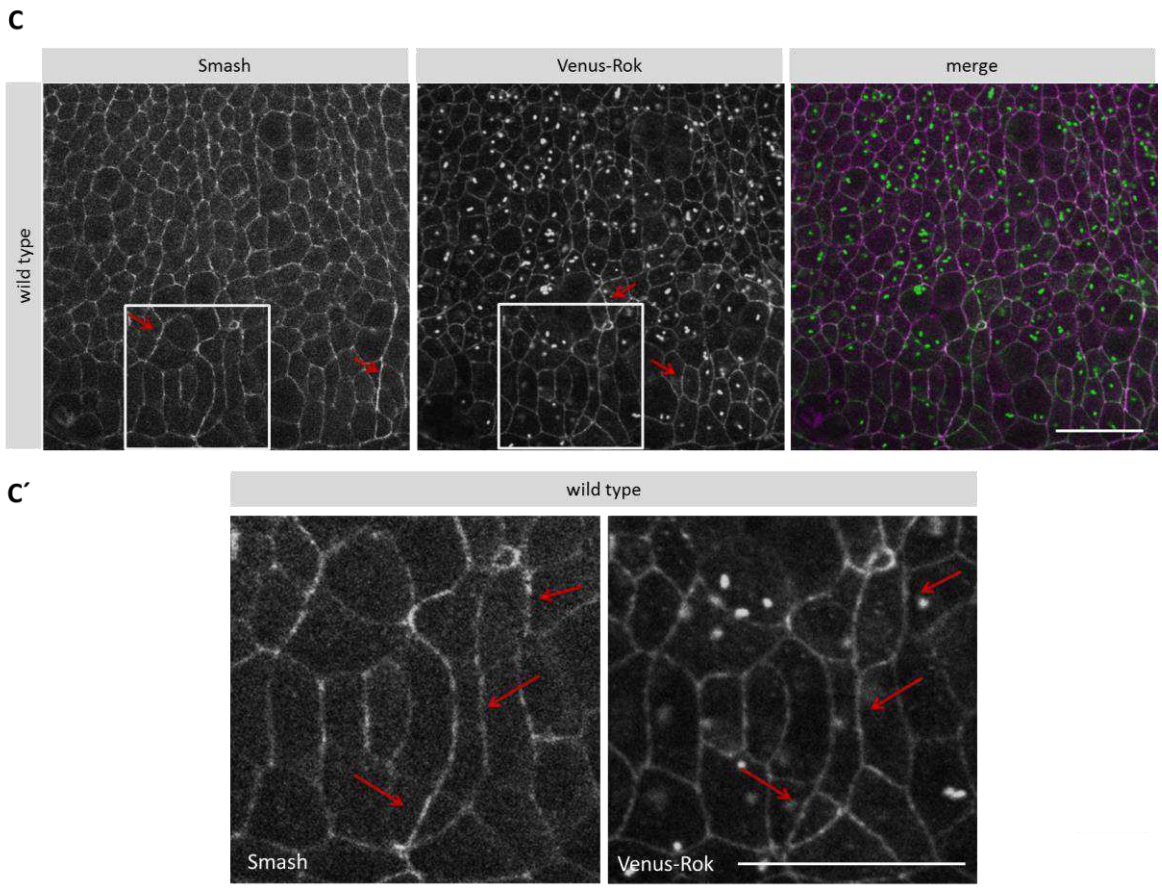
C
Smash
Venus-Rok
merge
wild type
C´
wild type
Smash
Venus-Rok

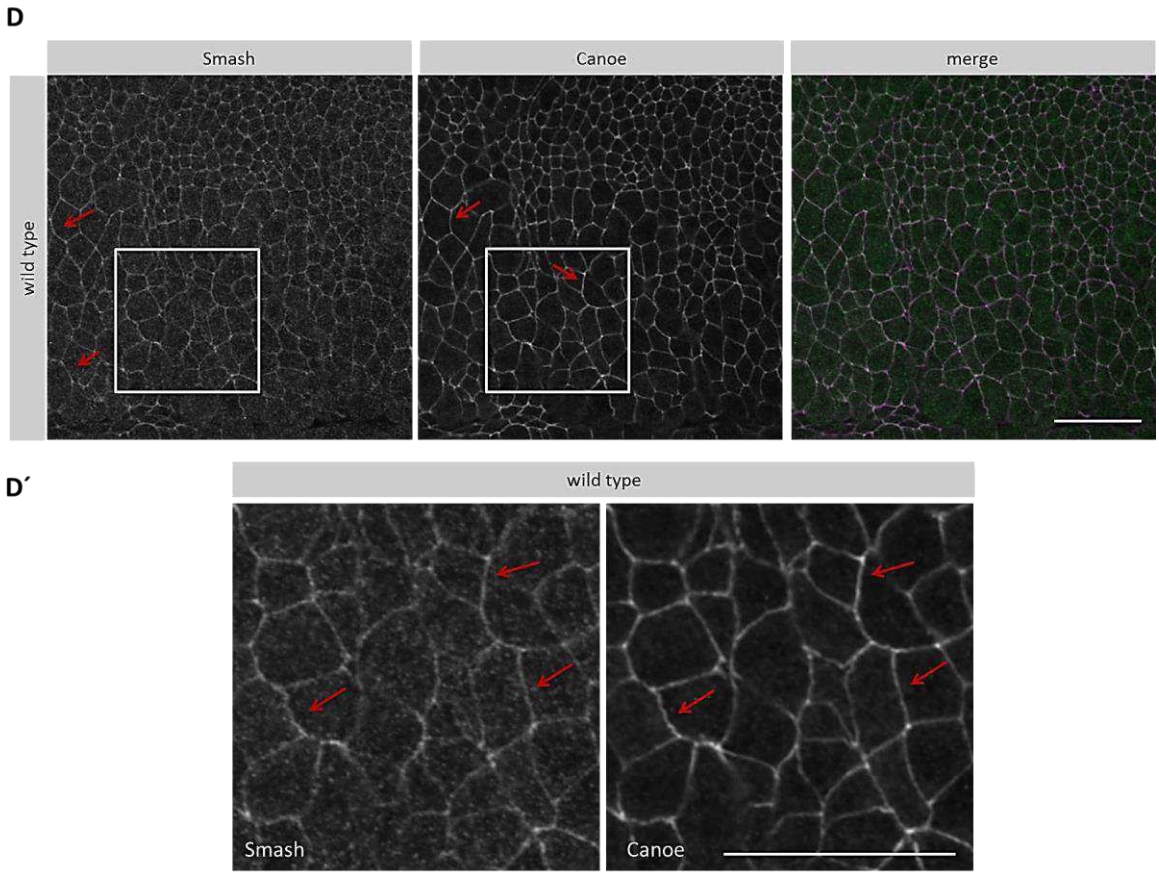

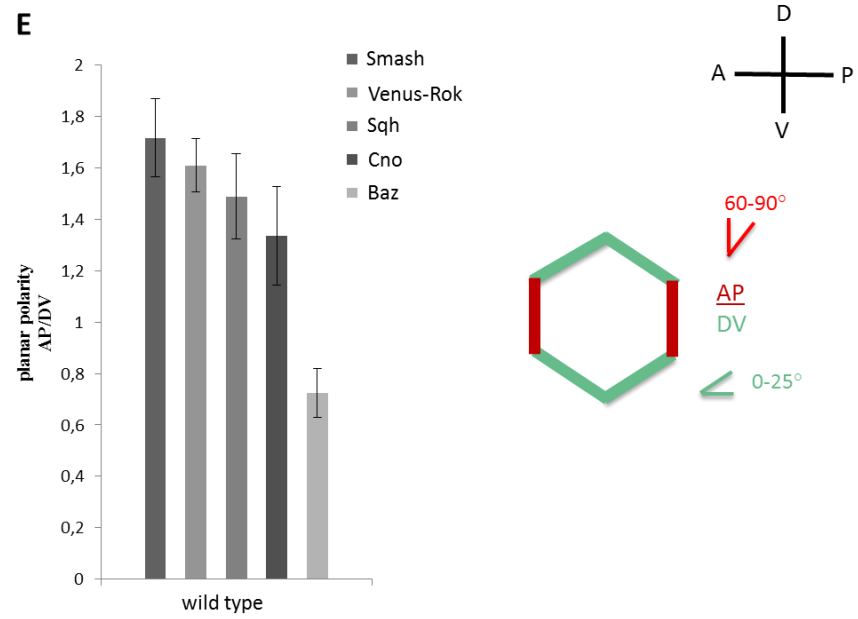

Figure 21: Smash is planar polarized in embryonic epidermis. (A)-(D) Smash is planar polarized and enriched at A/P junctions. Embryos at stage 8 were stained for Smash and Baz. For analysis of the subcellular localization of Sqh, Sqh-GFP fly line was used. Some A/P junctions are marked by red arrowheads and some D/V junctions are marked by green arrowheads. (A´-D´) Higher magnifications of grey boxes in (A)-(D). (E) Quantification of PCP of Smash, Sqh, and Baz in stage 8 embryonic. n = 200 cell contacts analyzed for each protein. Bars 20 µm.

3.4.1 Planar cell polarity is reduced or lost in *smash* mutant embryos

In order to study the loss-of-function phenotype in *smash*$^{35m/z}$ mutants on the cellular level, the distribution of several cortical junction-associated proteins that show a planar polarization were examined in the wild type and *smash*$^{35m/z}$ mutant embryonic epidermis. Although apical-basal polarity of Baz seemed to be unaffected in *smash*$^{35m/z}$ mutant embryos, planar polarity was abolished. Instead of being enriched at junctions in the D/V axis as in wild type embryos, Baz showed a slight enrichment at the A/P junctions, indicating that Smash is required for preventing Baz-recruitment to the A/P edges. The distribution of Venus-Rok seemed to be unaffected in *smash*$^{35m/z}$ mutant embryos and remained in its A/P enriched localization. However, Sqh-mCherry and Cno, which also show an accumulation at the A/P cell borders in wild type situation, lost their planar polarization upon the loss of *smash*, as they were evenly distributed at both A/P and D/V junctions in the *smash*$^{35m/z}$ mutant (Figure 22).

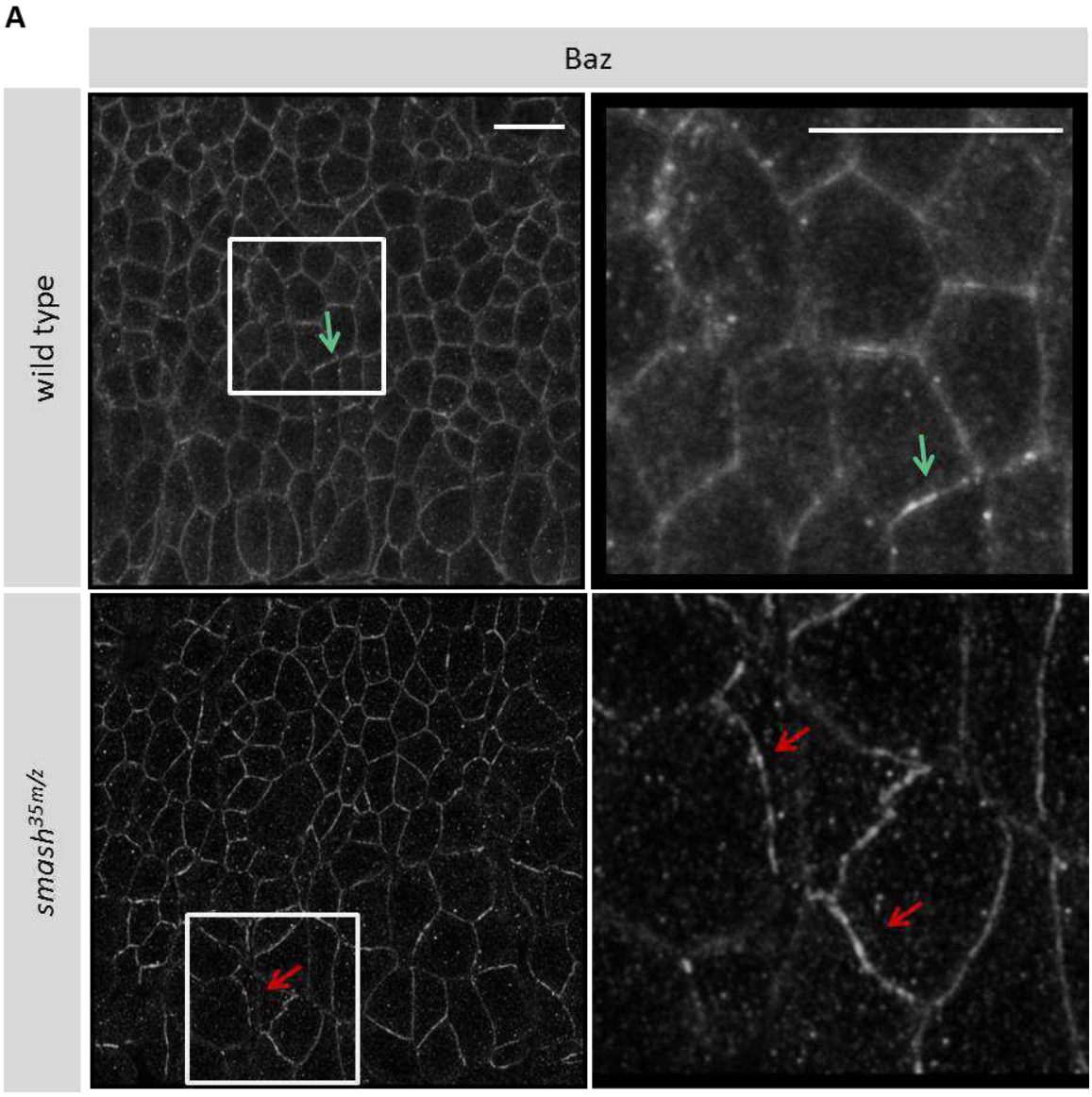
A
Baz
wild type
smash35m/z

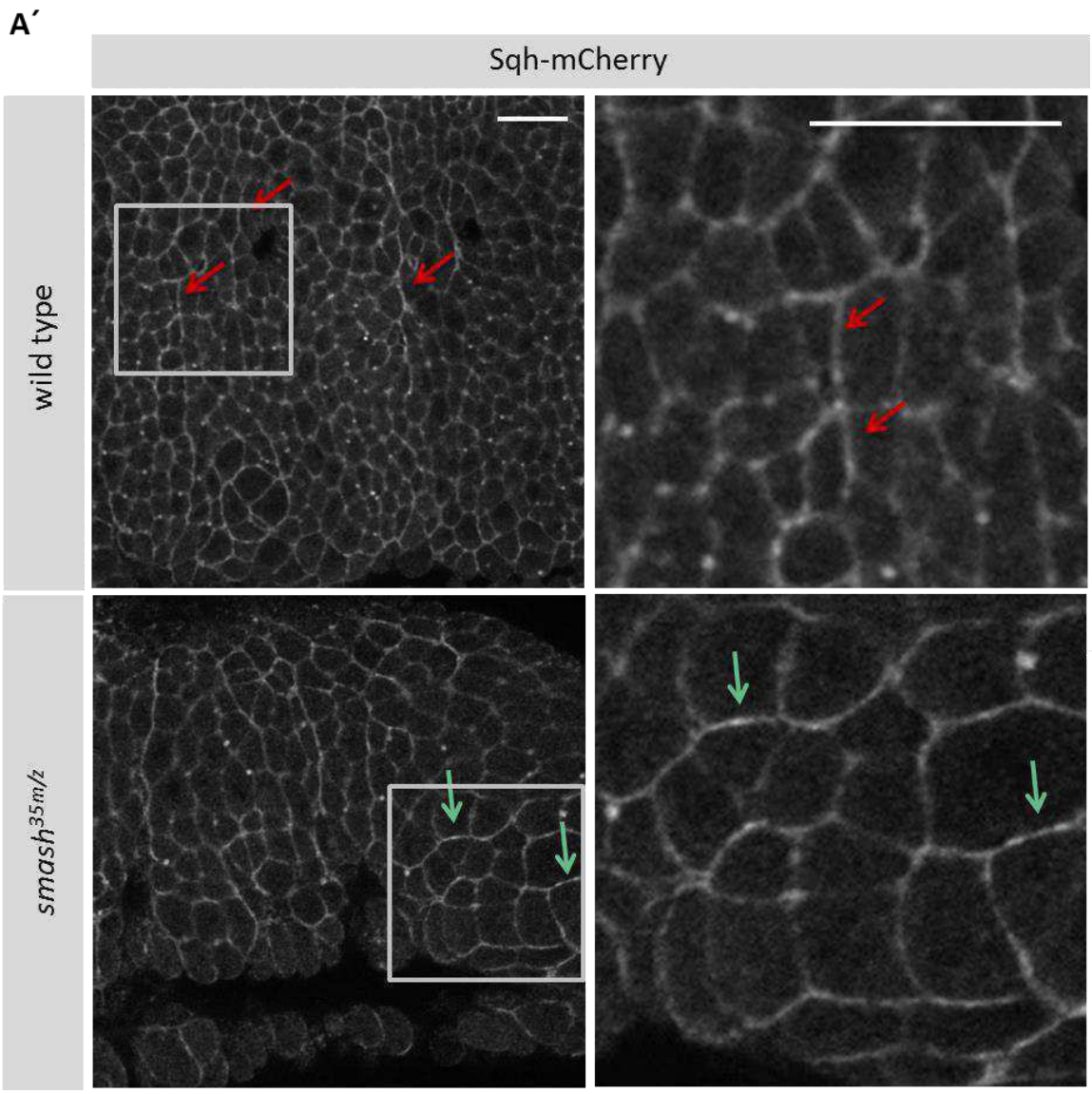
A´
Sqh-mCherry
wild type
smash35m/z

A''

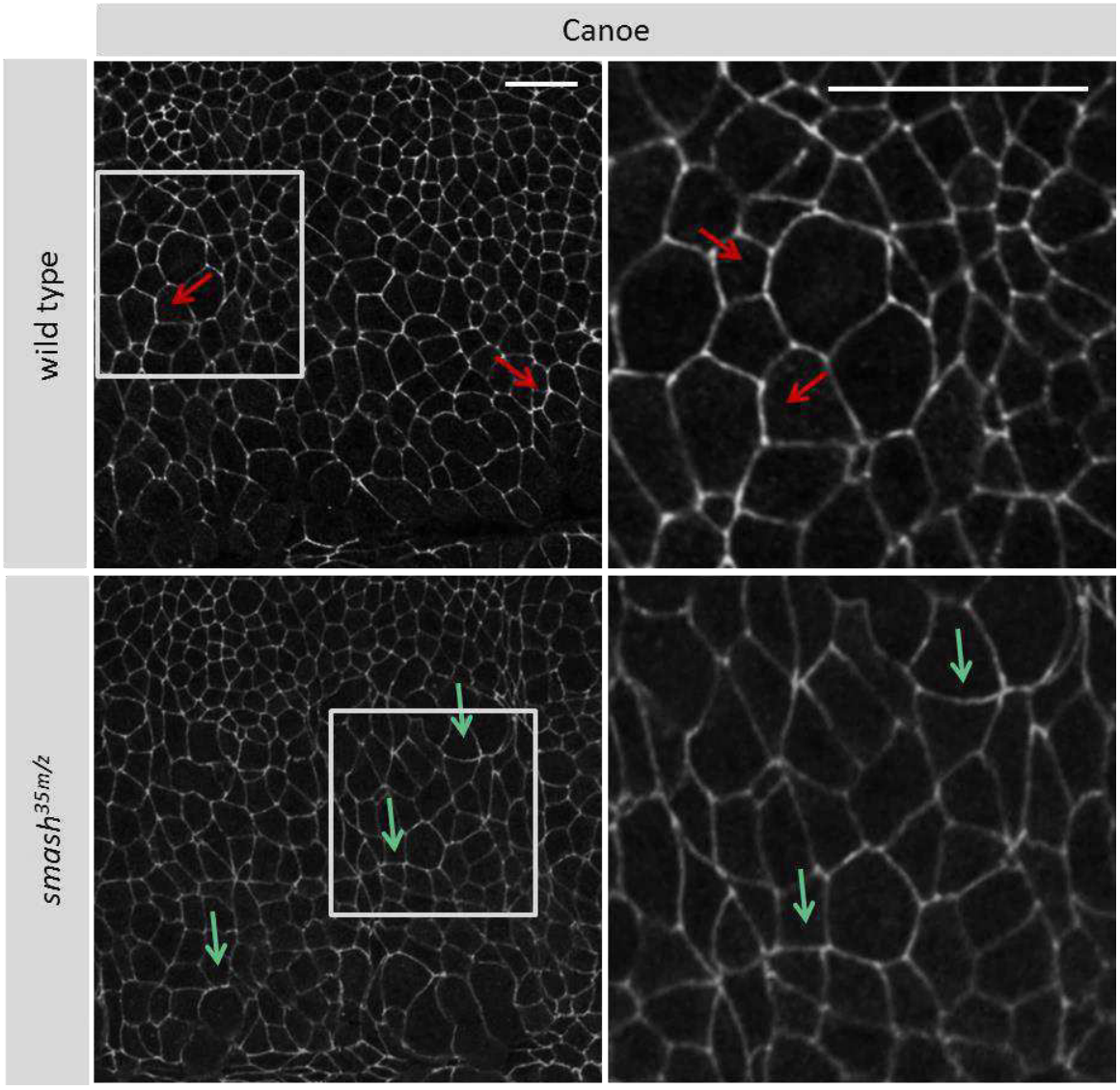

A‘‘‘

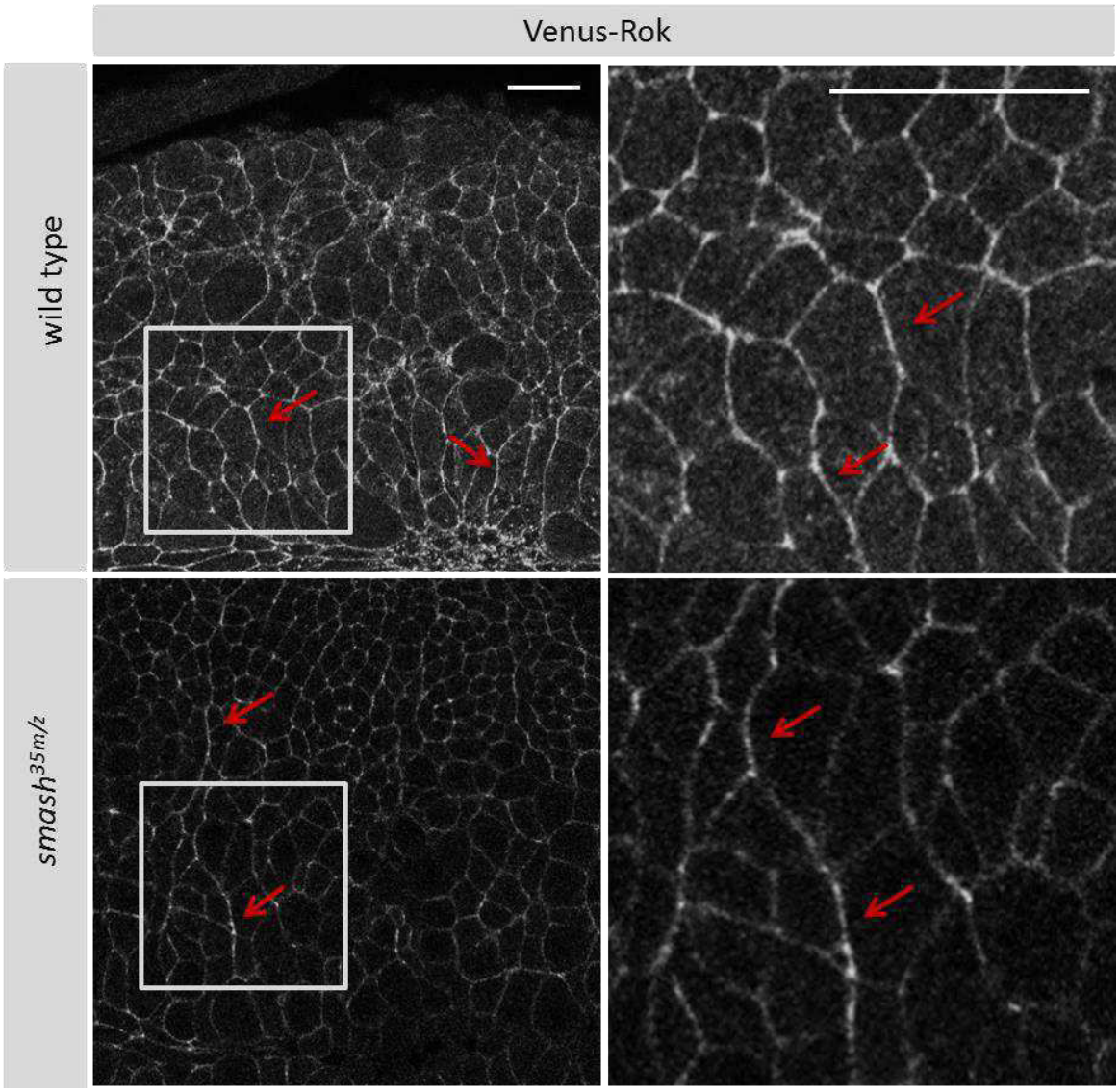

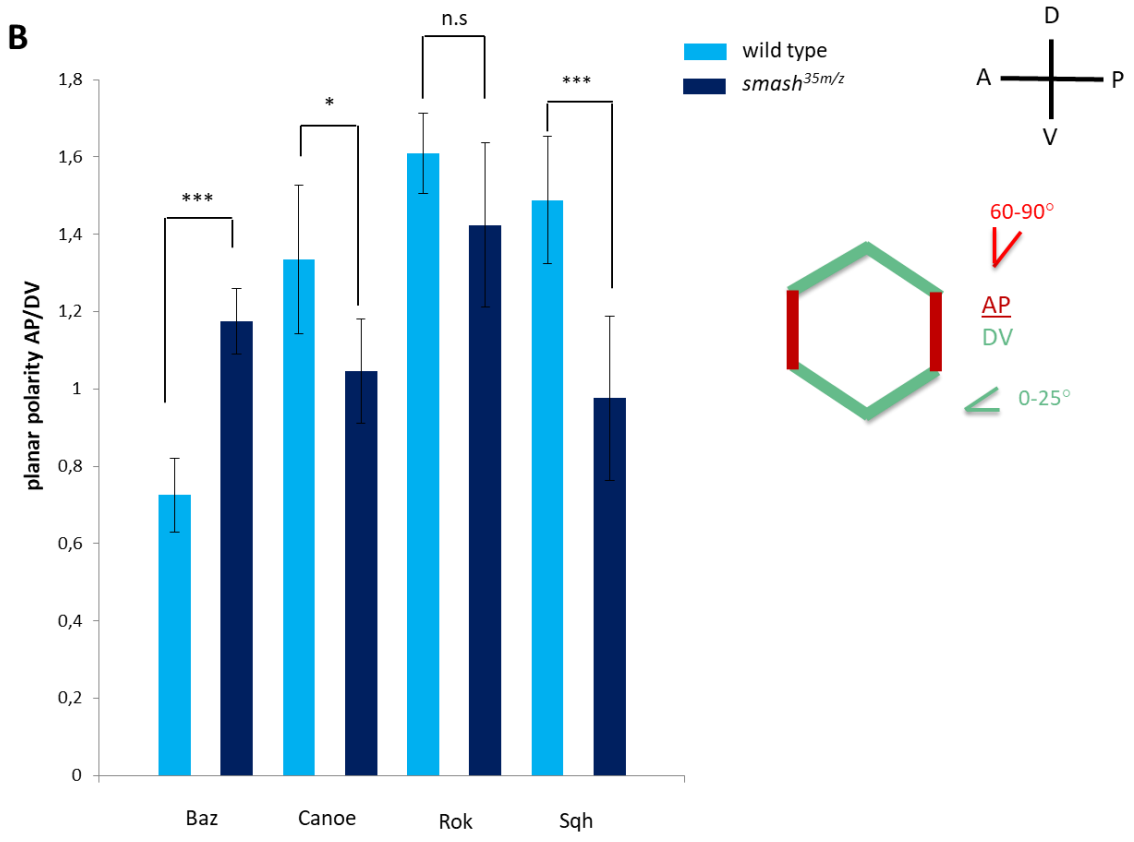

Figure 22: Planar cell polarity is abolished in *smash*$^{35m/z}$ mutant embryos. (A)-(A´´´) *smash*$^{35m/z}$ mutant (lower panel) or wild type (upper panel) stage 8 embryos were stained for Baz and Cno. Analysis of Sqh and Rok localization was conducted using Sqh-mcherry and Venus-Rok fly lines crossed in *smash*$^{35m/z}$ mutant background. Exemplary A/P junctions are marked by red arrows and D/V junctions are marked by green arrows. Higher magnification of grey boxes in respective lower panels. (B) Quantification of planar polarization of Baz, Cno, Sqh, and Rok in stage 8 embryos (***: $p < 0{,}001$; **: $p < 0.01$; *: $p < 0.05$; ns: not significant). For Baz, n = 160 cell contacts analyzed per genotype; for all other proteins, n = 200 cell contacts analyzed per genotype. Bars 20µm.

3.5 Smash associates with multiple actomyosin components at the ZA

In order to unravel the molecular mechanism of how *smash* regulates the actin-myosin network at the ZA and thus epithelial morphogenesis, the genetic interaction with known regulators of actomyosin contractility was studied. In further experiments the potential association of Smash with some actomyosin interactors at the protein level was investigated.

3.5.1 Smash is lost upon the loss of Baz

As described before, Smash co-localizes and binds to Baz at the ZA via its PDZ domains. However Smash and Baz do not show the identical localization, as Smash is enriched at junctions in the A/P axis, while Baz accumulates at cell-cell contacts in the D/V axis in wild type situation. In order to clarify the genetic interaction between Smash and Baz, Smash localization in *baz* zygotic mutant baz^{EH747} embryos was examined. These mutant embryos develop normally due to the maternal load of Baz until stage 10 (Krahn et al. 2010). Afterwards epidermal cells lose Baz protein and herewith epithelial integrity. Figure 23 shows that in these cells Smash localization is completely abolished.

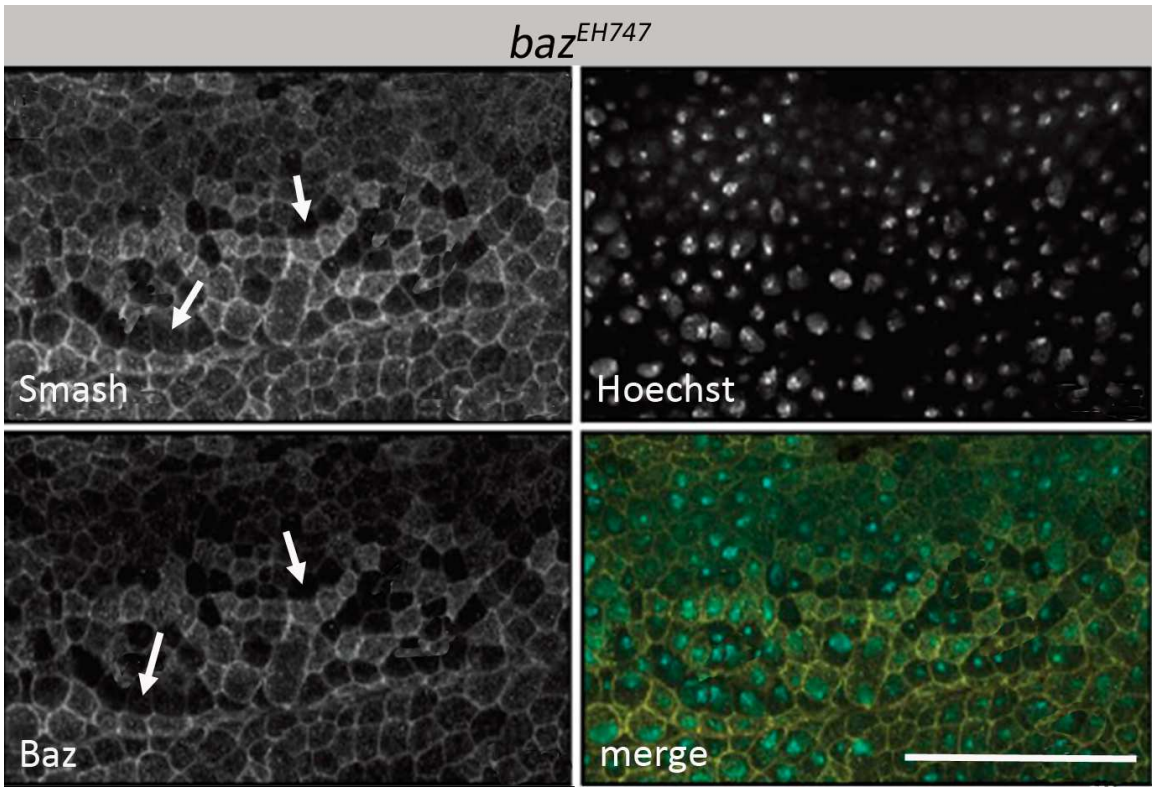

Figure 23: Smash is abolished in *baz* zygotic mutant embryos. Epidermis of stage 11 baz^{EH747} mutant embryos stained for Smash, Baz and DAPI. In cells lacking Baz also Smash is lost at the ZA. Bars 10 µm.

3.5.2 Loss of *canoe* leads to defects in Smash localization

Smash has been shown to bind the ZA-associated actin-binding protein Canoe via its PDZ binding motif (Beati et al. 2018). Loss of Canoe disrupts junctional dynamics and leads to cellular defects, as Canoe links AJs to the cytoskeleton through its actin and echinoid

binding domain (Sawyer et al. 2009). According to the assumption that these two proteins may act together in a molecular network involved in regulation of planar cell polarity and actomyosin dependent contractility, Smash localization upon the loss of Canoe was investigated. To this aim germline clones lacking maternal and zygotic *canoe* (*cno*$^{R2\ M/Z}$) were generated. Planar polarity of Smash was affected due to the complete removal of Canoe. Uniform association along the junctions with enrichment in the A/P axis was lost, as Smash seemed to be scattered along the plasma membrane in a dotted pattern, in contrast to wild type control (Figure 24).

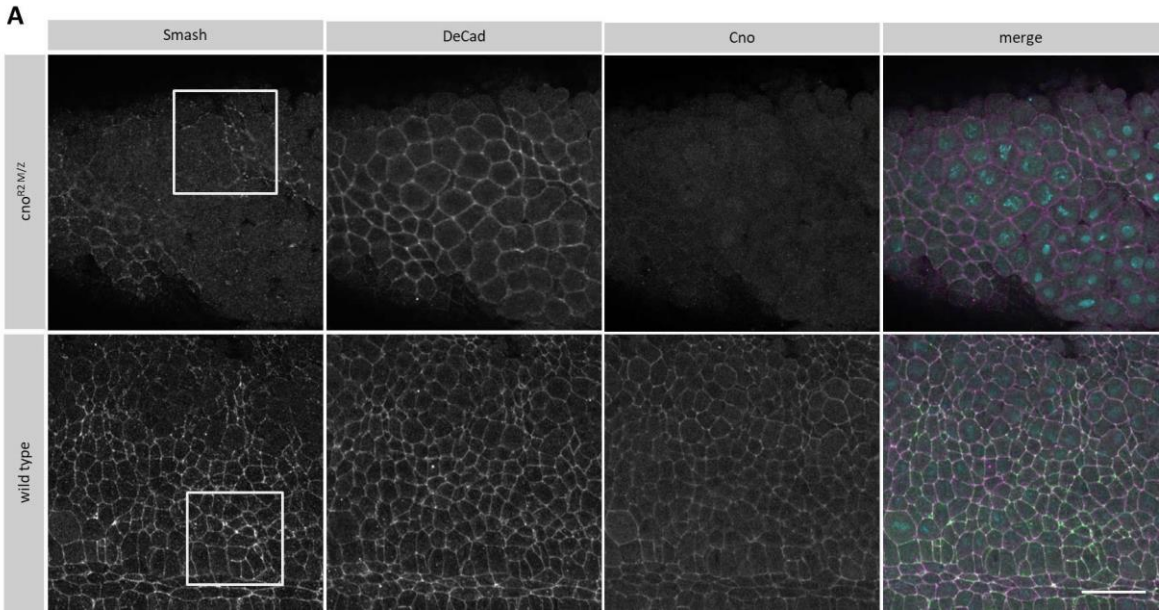

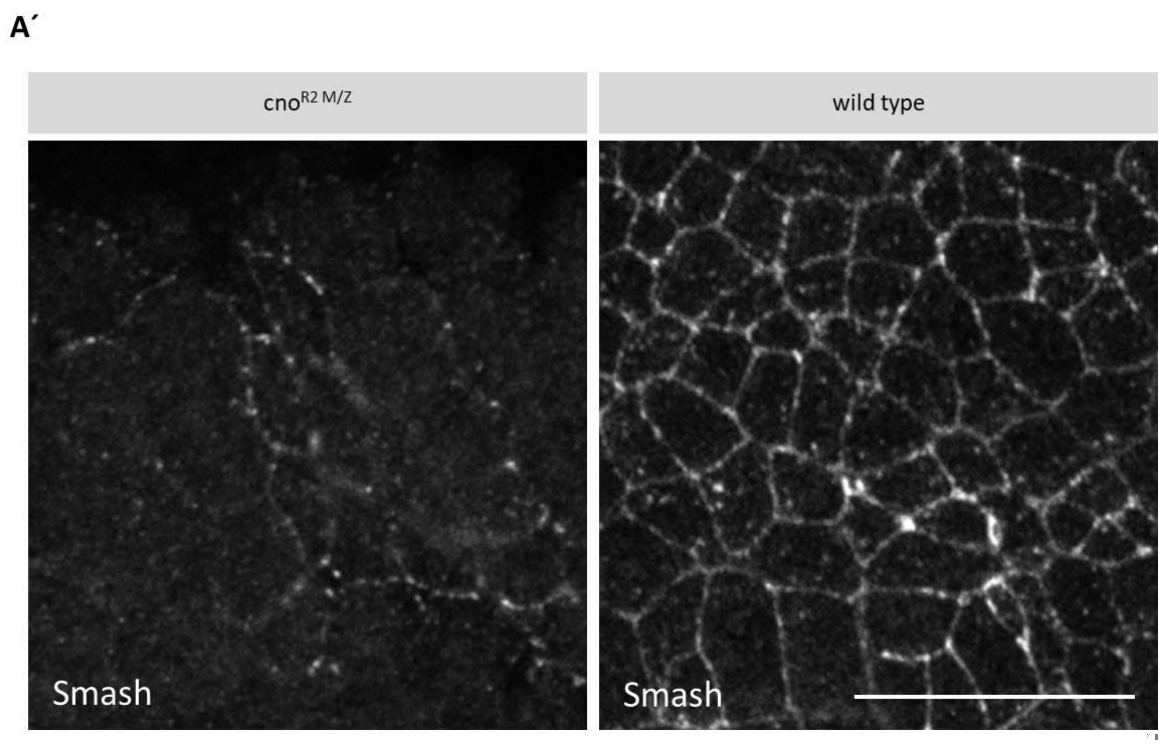

Figure 24: Smash localization is effected upon loss of Cno. (A) Immunohistochemistry of embryos lacking maternal and zygotic Cnoe and wild type embryos stage 8 stained for Smash, DE-Cad and Canoe. Smash appears in a dotted pattern. (A´) Higher magnification of grey boxes in (A). Bars 20 µm.

3.5.3 Phosphorylation of Myosin II is affected in *smash* mutant embryos

One of the primary roles defined for Rok is the regulation of actin-myosin cytoskeletal organization by phosphorylating Sqh, the *Drosophila* myosin II regulatory light chain. Phosphorylated myosin II regulatory light chain promotes actomyosin contractility by activating myosin ATPase, thus enabling its interaction with F-actin to generate a contractile force (Julian & Olson 2014). Rok has also been shown to be required for planar polarization of Baz, as it destabilizes Baz at A/P junctions by specific phosphorylation (Simões et al. 2010). Rok is planar polarized itself, as it is enriched at A/P junctions, where it shows a co-localization with Smash. This distribution was unaffected upon the loss of Smash (Figure 22). In order to study, whether Smash is mediating tension by intervening in phosphorylation of Myosin II, *smash*$^{35m/z}$ and wild type embryos at stage 8 were stained using an anti-phospho Myosin (p-Myosin) antibody. Figure 25 shows that indeed in *smash*$^{35m/z}$ mutant embryos less activated junctional Myosin was detected, while DE-Cad

staining showed an unaffected junctional localization. This result supports the hypothesis that Smash regulates epithelial morphogenesis in a Myosin II dependent manner.

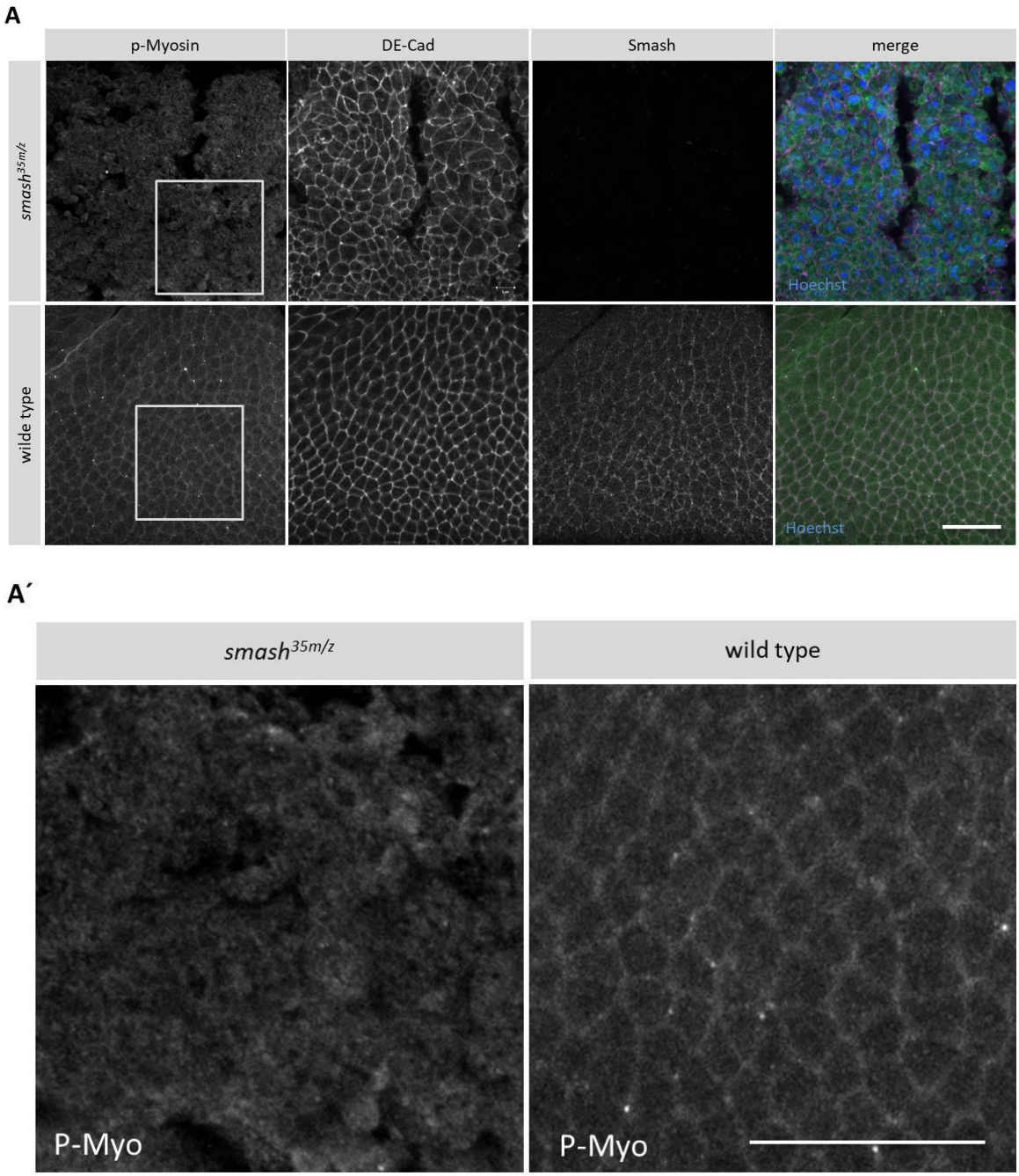

Figure 25: Phosphorylation of Myosin II is downregulated in *smash*$^{35m/z}$ mutant embryos. *smash*$^{35m/z}$ and wild type embryos stage 8 stained for Smash, DE-Cad and p-Myosin. Junctional staining is reduced in *smash*$^{35m/z}$ mutant embryos. (A´) Higher magnification of grey boxes in (A). Bars 20µm.

3.5.4 Smash binds to Rok, Shrm and Moe *in vitro*

To analyze whether Smash interacts with Rok on the protein level, full length GFP-Smash PM was co-transfected with a myc-tagged version of Rok in S2 cells. GFP-Smash PM was pulled down by co-IP followed by western blot using an anti-myc antibody. A clear signal in the size of Rok (156,5 kDa) was detectable, while no or just a weak band was observed in the lanes, in which Rok was co-transfected with control CD8-GFP (49,5 kDa) (Figure 26). This confirmed that Smash indeed binds to Rok on the protein level. These results give more insight in the mechanism of how epithelial cell contractility is established and maintained, whereby Smash seems to play a key role as possible cofactor, potentially providing substrate specificity towards sqh (Myosin II) or as phosphorylation target itself.

To further investigate the presumption that Smash may act as an adapter protein between Rok and Sqh, additional co-IP experiments were conducted. After pulling down GFP-Smash PM, in most experiments no band of myc-Sqh at the predicted size of 25,8 kDa was observed in western blot analysis (Figure 26). Thereby no direct interaction in cell culture between Smash and Sqh was confirmed. However, in some experiments a slight signal could be detected in the size of myc-Sqh after pulling down Smash-GFP. This result was not reproducible in all repeats.

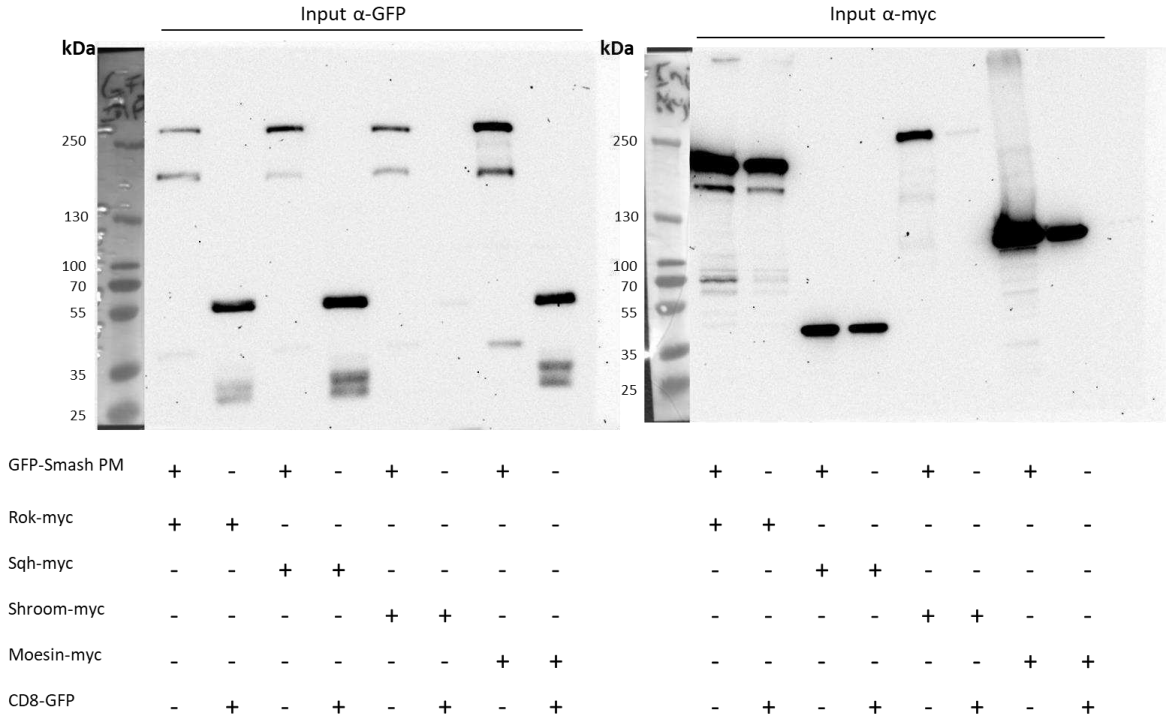

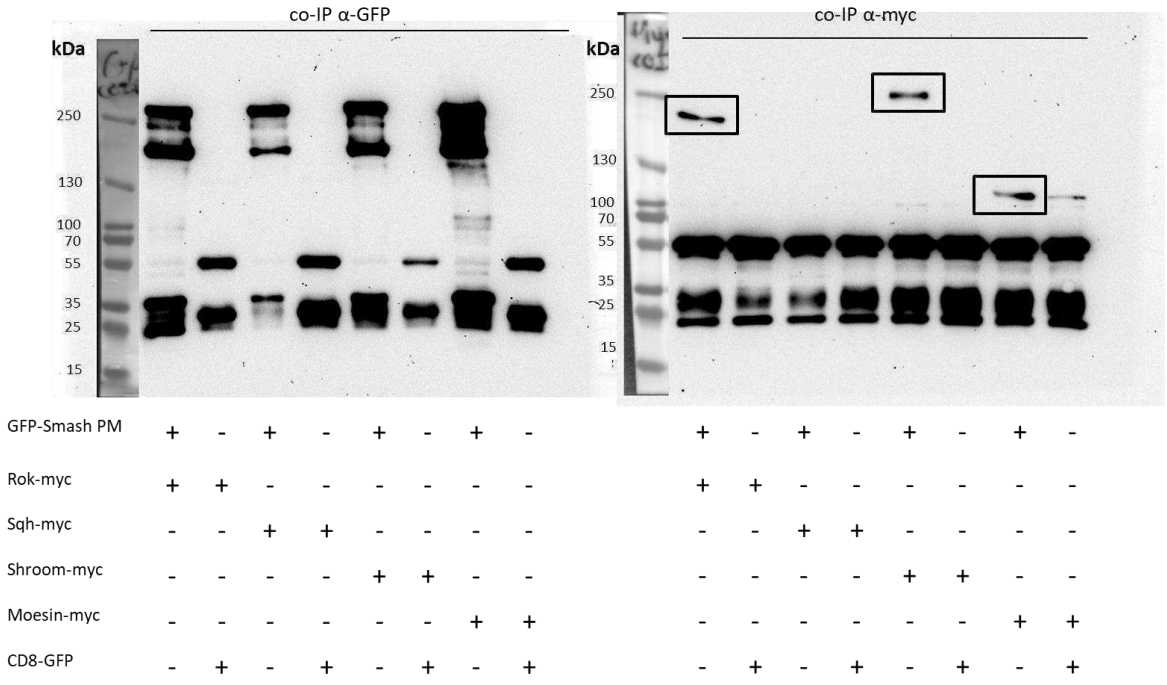

Figure 26: Smash binds to Rok, Shrm and Moe *in vitro*. S2 cells were co-transfected with GFP-Smash PI and the respective myc-tagged protein. GFP- was pulled down and potential binding was confirmed using an anti-myc antibody. A clear signal could be detected in case of Rok, Shroom and Moesin.

The conserved actin-binding protein Shroom shares several similarities with Smash, as it induces apical constriction upon overexpression in *Drosophila* and vertebrate cells. Also the expression pattern and subcellular localization of Shroom and Smash are almost identical, since both localize at the apical region at the ZA in a planar polarized fashion (Hildebrand & Soriano 1999; Haigo et al. 2003; Bolinger et al. 2010; De Matos Simões et al. 2014). To investigate a possible interaction of Shroom and Smash, co-IP experiments with subsequent western blot analysis were performed. S2 whole cell lysate from S2 cells co-transfected with GFP-Smash PM and myc-tagged Shroom was used. GFP-Smash PM was pulled down by co-IP and anti-myc antibody was used to detect a potential binding of myc-Shroom at the size of 179,5 kDa. An obvious protein interaction could be detected (Figure 26), so it seems likely, that these two proteins may act together in the same pathway.

Another candidate which has been tested for interacting with Smash is the actin binding protein Moesin (Moe). Moe belongs to the ERM family, which consists of three closely related proteins, ezrin, radixin, and moesin that are thought to act as cross-linkers be-

tween plasma membranes and the actin cytoskeleton (Tsukita et al. 1997). Here, also an intense signal corresponding to the size of myc-Moe protein (69,9 kDa) could be detected. These interactions on the protein level point to a close relation of Smash to a mechanism regulating the actomyosin network.

3.6 Interaction of Smash and Src42A

Smash is a binding partner and a phosphorylation target *in vitro* and *in vivo* of the well-known regulator of cell-cell adhesion and morphogenesis Src42A (Tateno et al. 2000; Förster & Luschnig 2012; Nelson et al. 2012; Beati et al. 2018) To analyze this relationship in more detail, further experiments regarding to structure-function correlation and subcellular distribution were performed.

3.6.1 Phosphorylation of Smash by Src42A is independent of its interaction as binding partners

Interestingly, Src42A phosphorylates the smallest isoform GFP-Smash PJ to only a very low extent. Since Smash-PJ is lacking the LIM-PBM module, this result points to an important function of these domains mediating the interaction between Smash and Src42A (Beati et al. 2018). To test if the phosphorylation is dependent on the direct interaction and if Src42A actually also binds to Smash PJ, co-IP experiments were performed. An HA-tagged version of Src42A (63,5 kDa) was co-expressed with full length GFP-Smash PM (195,5 kDa), GFP-Smash PI (124,7 kDa) and GFP-Smash PJ (120,3 kDa) in S2 cells and GFP-Smash constructs were pulled down by co-IP. In all cases, including GFP-Smash PJ, a clear signal corresponding to the size of Src42A-HA was detectable in a western blot using an anti-HA antibody (Figure 27). Phosphorylation of GFP-Smash PM and GFP-Smash PI was confirmed by using an anti-Phosphotyrosine antibody (PY) after stripping the membrane. Here, a weak signal at the size of GFP-Smash PJ was detectable compared to the other isoforms, meaning that phosphorylation is strongly reduced. Consequently, phosphorylation of Smash requires the LIM-PBM module, while Src42A binding to Smash is independent of the presence of this domain.

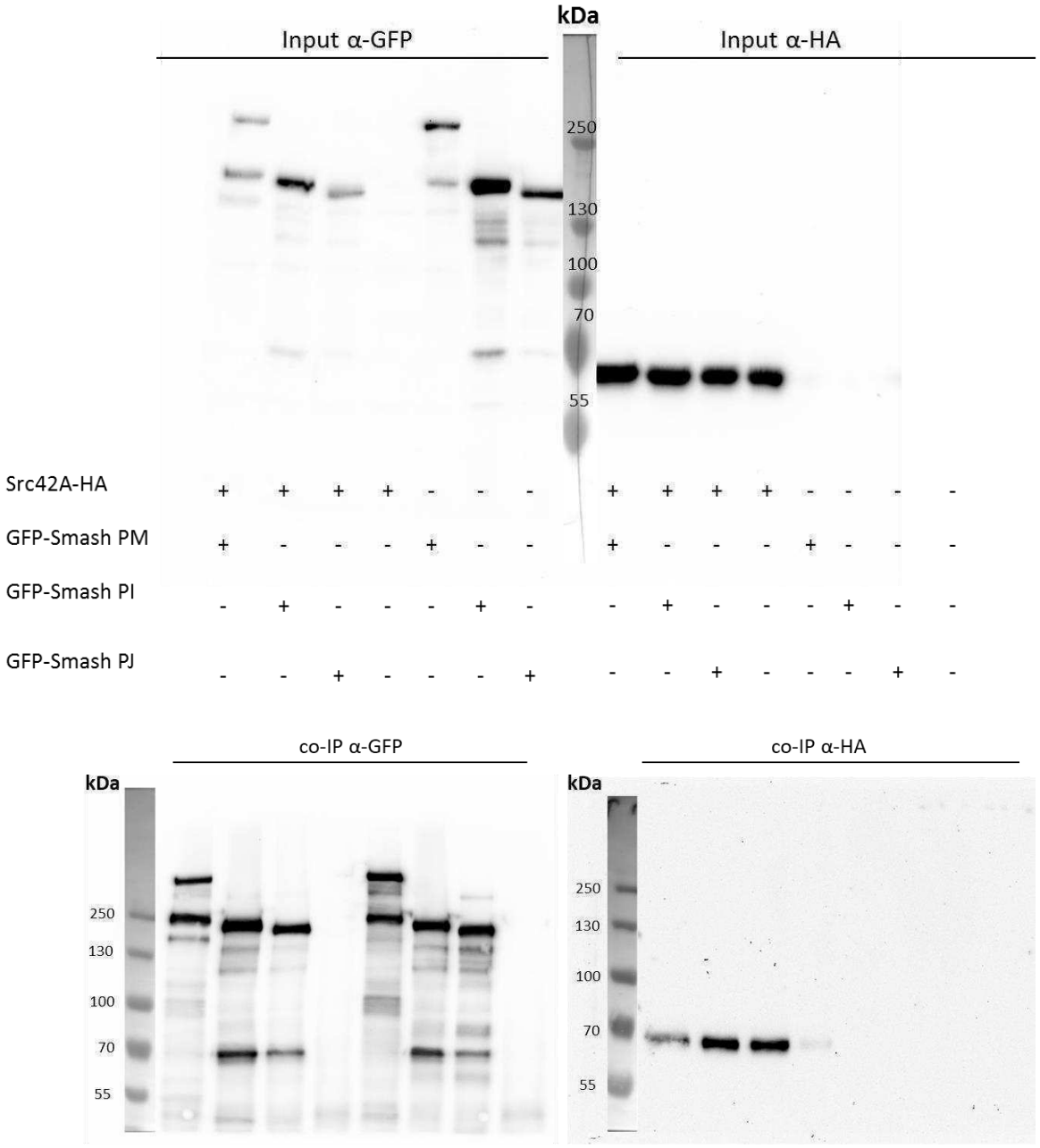
kDa
Input α-GFP
Input α-HA
250
130
100
70
55
Src42A-HA + + + + - - - + + + + - - - -
GFP-Smash PM + - - - + - - + - - - + - - -
GFP-Smash PI - + - - - + - - + - - - + - -
GFP-Smash PJ - - + - - - + - - + - - - + -
co-IP α-GFP
co-IP α-HA
kDa
250
130
100
70
55
Src42A-HA + + + + - - - - + + + + - - - -
GFP-Smash PM + - - - + - - - + - - - + - - -
GFP-Smash PI - + - - - + - - - + - - - + - -
GFP-Smash PJ - - + - - - + - - - + - - - + -

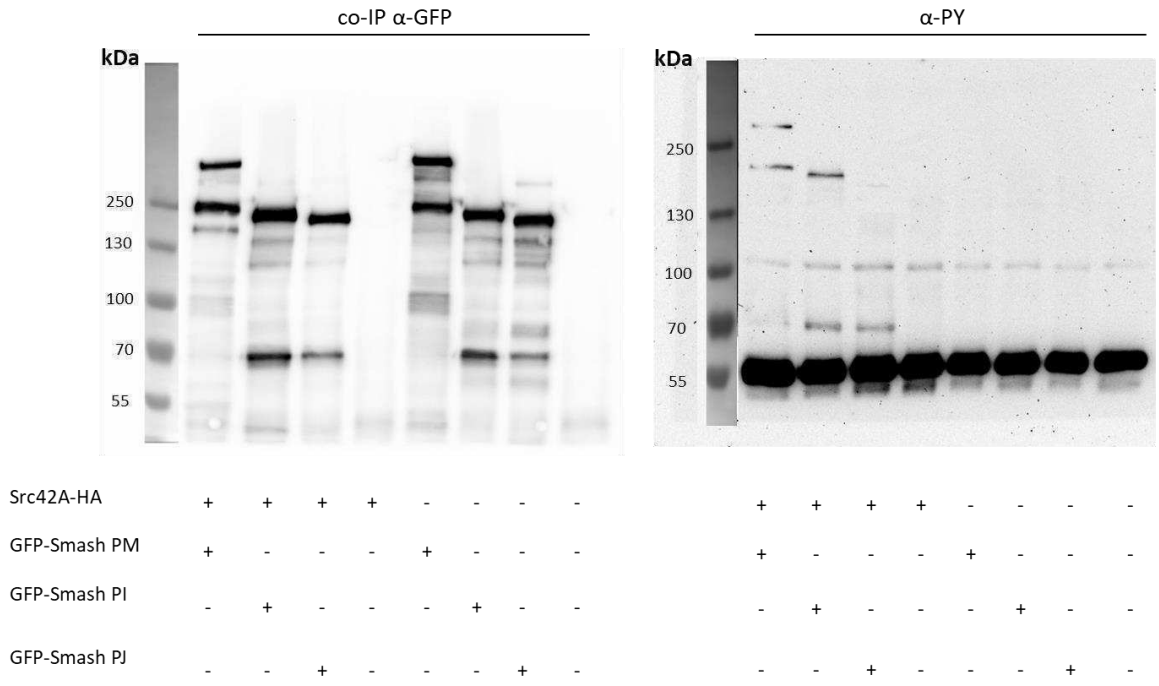

Figure 27: Src42A binds all isoforms of Smash. GFP-Smash was pulled down by co-IP using an anti-GFP antibody from transfected S2 cells and binding to Src42A-HA was confirmed using an anti-HA antibody. A clear signal corresponding to the size of Src42A was detected in all cases. Transfection was confirmed using an anti-HA antibody. Phosphorylation of GFP-Smash PM and GFP- Smash PI was confirmed by using an anti-Phosphotyrosine (anti-PY) antibody.

3.6.2 Smash contains several binding sites for Src42A

Referring to the rescue experiments, which were performed in this work (3.2), it was shown that phosphorylation of Smash by Src42A is not essential to rescue the semilethality of *smash*^{35} mutants. In further analyses the deletion constructs of GFP-Smash PI were used to investigate, which region of Smash is actually mediating the linking between Src42A and Smash. To this aim these versions of GFP-Smash PI were co-transfected with myc-tagged Src42A in S2 cells. The following table presents the expected size of the respective construct.

Table 3-1: Expected band sizes of transfected Smash and Src42A constructs based on their molecular weight.

construct	predicted size [kDa]
Src42A-myc	63,5
GFP-Smash PI	124,7
GFP-Smash PI ΔPBM	124,3
GFP-Smash PI ΔLIM	118,2
GFP-Smash PI C-term	44,7
GFP-Smash PI N-term	75,4
CD8-GFP	49,5

GFP-Smash constructs were pulled down by co-IP and binding of Src42A-myc was confirmed by western blot using an anti-myc antibody (Figure 28). A band corresponding to the size of Src42A-myc was detectable in all western blot lanes. Co-transfection of Src42A-myc with CD8-GFP for control resulted also in a signal with a similar intensity, which leads to doubt of the specificity of this binding assay. Should the observed signals for Src42A-myc nevertheless be specific, no specific binding domain or region of Smash could be identified to be responsible for the connection to Src42A. The fact that both the deletion construct of GFP-Smash PI just expressing the C-terminus as well as the alternate version just carrying the N-terminus seem to bind to Src42A, suggests that probably two or several binding sites exist (Figure 28).

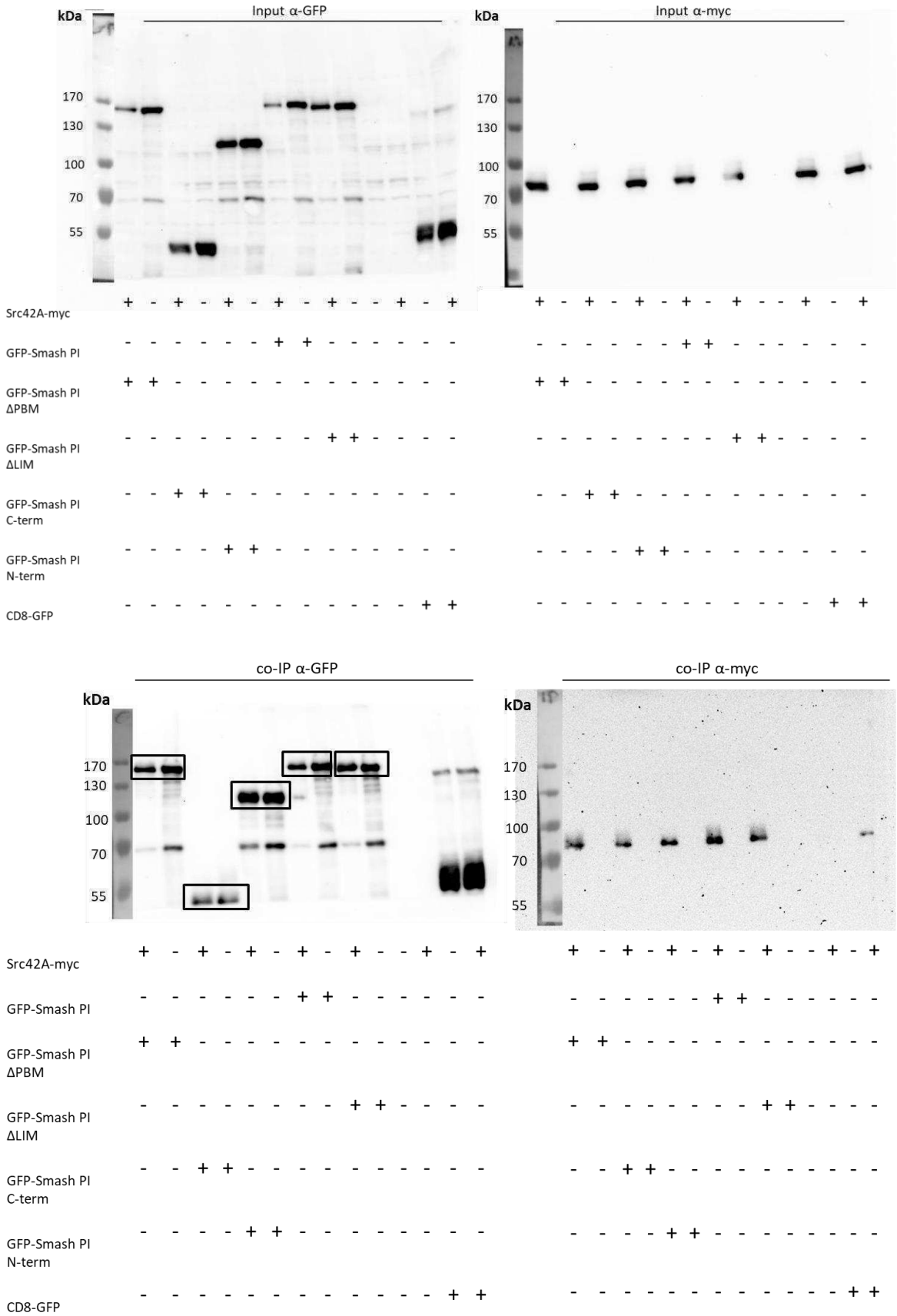

Figure 28: Src42A binds to all deletion constructs of Smash PI. GFP-Smash was pulled down by co-IP and binding to Src42A-myc was confirmed using an anti-myc antibody. A clear signal corresponding to the size of Src42A was detected in all cases. Control CD8-GFP also showed a band in an comparable intensity.

3.6.2.1 Phosphorylation by Src42A is not exclusively determined by the LIM-PBM module

In 3.6.1 it was shown that the smallest isoform Smash PJ, lacking the LIM-PBM module, is indeed binding to Src42A, but phosphorylation is strongly reduced (Beati et al. 2018). Further experiments were performed to examine whether Src42A is able to phosphorylate GFP-Smash deletion constructs. For this purpose the same membrane used for the binding assay in Figure 28 was stripped and a western blot using an anti-phosphotyrosine (PY) antibody was performed (Figure 29).

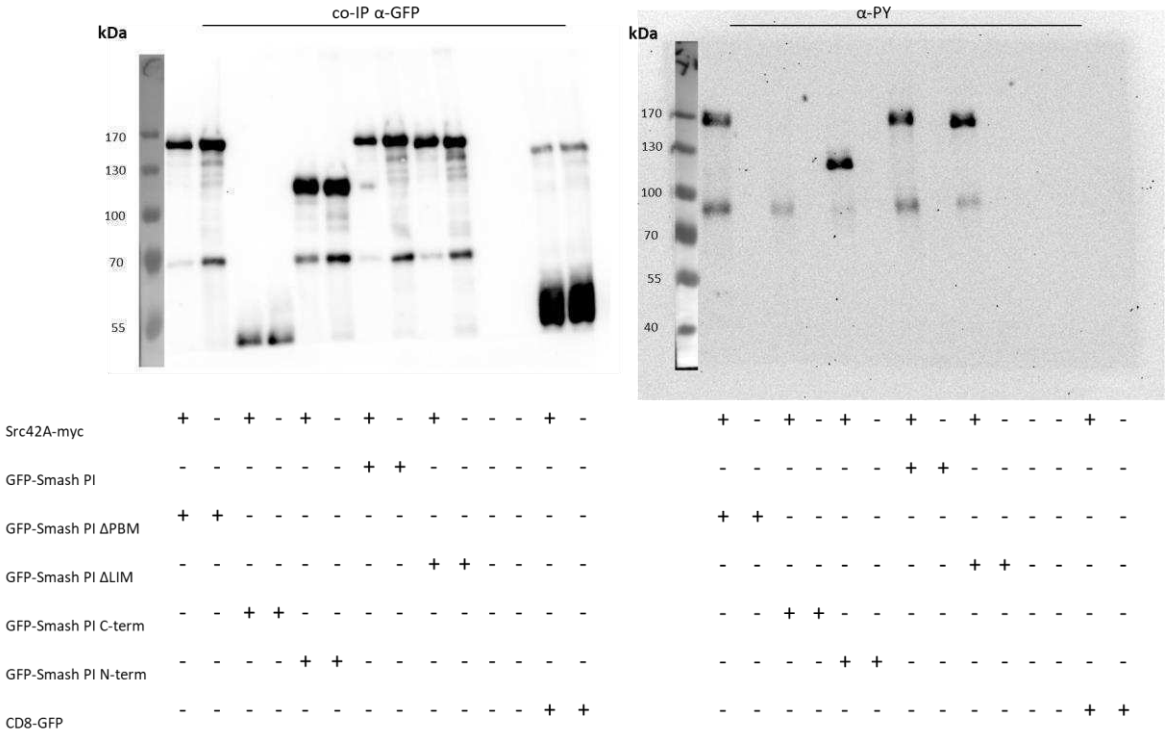

Figure 29: Only GFP-Smash PI C-term is not phosphorylated by Src42A. GFP-Smash was pulled down by co-IP and phosphorylation by Src42 was confirmed using an anti-phosphotyrosine (PY) antibody. A clear signal corresponding to the respective size of the GFP-Smash PI deletion construct was detected except for GFP-Smash PI C-term.

Interestingly, a clear signal corresponding to the size of the respective deletion construct was detected, except for GFP-Smash PI C-term. This deletion variant just expresses the C-terminal part of Smash, including the LIM-PBM module. In contrast, the alternate construct, which just expresses the N-terminus of Smash and thus also lacks the LIM-PBM module was also phosphorylated by Src42A, indicating that not the LIM-PBM module alone is responsible for mediating phosphorylation.

3.6.3 Subcellular dependency of Smash and Src42A

In the embryonic epidermis Src42A is localized along the entire plasma membrane, but accumulated in the apical region of the junctions. Here it forms a ternary complex with E-cadherin and Armadillo (Takahashi 2005).

In this apical area Src42A co-localizes with Smash (Figure 30A). In order to examine a possible influence on Src42A by Smash, subcellular distribution of Src42A in wild type situation was compared to its localization in *smash*$^{35m/z}$ mutant embryos via Immunofluoresence. The loss of maternal and zygotic *smash* did not cause any detectable mislocalization of Src42A (Figure 30A´). It was already confirmed that Src42A contributes to the process of rosette formation during germband extension, where it localizes in a planar polarized fashion in basolateral protrusions (Sun et al. 2017). Considering the possible role of Smash in mediating planar cell polarity, the distribution of Src42A in the apical area in wild type and *smash*$^{35m/z}$ mutant embryos was examined via antibody staining. No considerable planar polarization of Src42A in this region could be detected; also no significant change in its localization in *smash*$^{35m/z}$ mutant embryos was observed (Figure 30B).

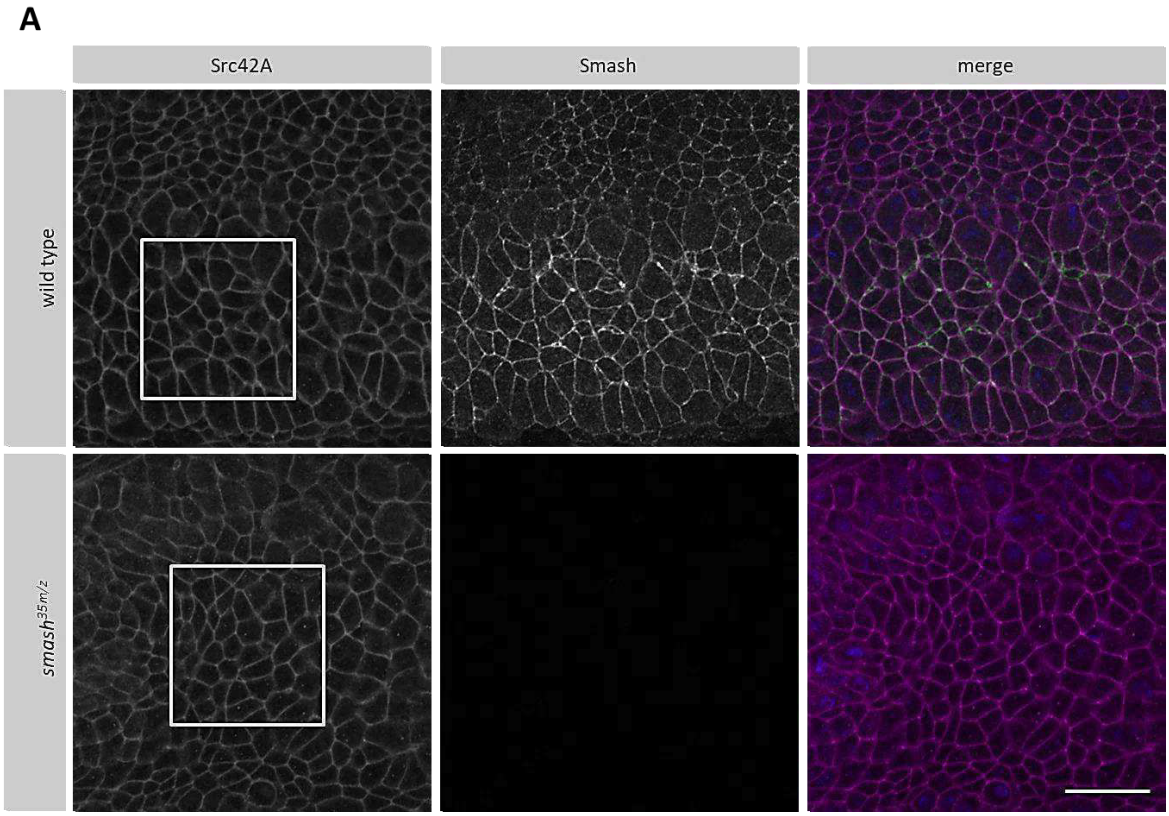

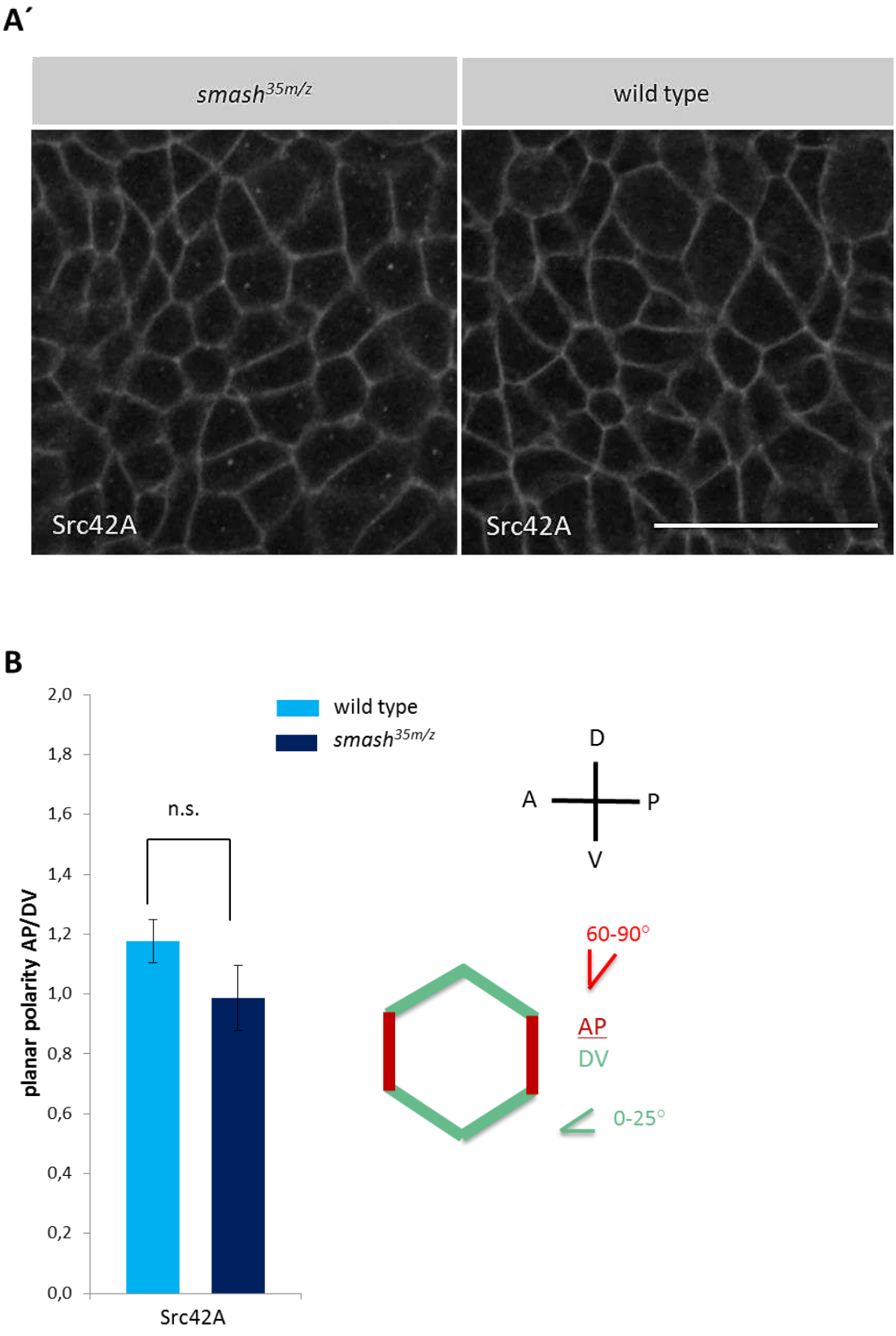

Figure 30: Src42A localization is not affected upon the loss of *smash*. (A) Immunostaining of wild type and *smash*$^{35m/z}$ stage 8 embryos. Smash and Src42A show a co-localization in the apical region of the ZA. (A´) Higher magnification of grey boxes in (A). Bars 20µm. (B) Quantification of planar cell polarity analysis ± SEM (ns: not significant). n= 200 cell contacts were analyzed, no significant mislocalization could be detected.

4 Discussion

In developing epithelia the dynamic connection between adjacent cells allows the tissue to grow and change its shape. In these morphogenetic processes the regulation of the zonula adherens and the contractile actomyosin network is of fundamental importance. Several studies document the involvement of several ZA-associated proteins like Rho family small GTPases, Rok, Myosin II, Baz or Shroom (Amano et al. 1996; Kaibuchi et al. 1999; Jaffe & Hall 2005; Hildebrand 2005; Nance & Zallen 2011). However, the exact mechanism of how epithelial integrity is maintained during processes of tissue remodeling is not completely understood. In this work, a new key factor in this network called Smash was identified to play an essential role in order to mediate cell bond tension and adhesion.

4.1 *smash* regulates morphogenesis and cell bond tension

Embryos mutant for both maternal and zygotic *smash* showed severe defects in morphogenesis. Furrows were formed uncoordinatedly, segmentation did not proceed properly or embryos were twisted completely. After identifying Smash as a binding partner of the polarity regulator Baz (Beati et al. 2018), the characterization of this loss-of-function phenotype provided the first indications of the major importance of this so far unknown gene. Besides this strong phenotype, it was already shown in Beati et al. (2018) that the overexpression of GFP-Smash PM in randomly induced clones in the follicular epithelium leads to apical constriction of these cells. Apical constriction presupposes a gain of tension in the cortex of the cells. Consequently, as the gain of function is accompanied by the gain of tension, the question was raised whether the loss-of-function phenotype is due to the loss of tension in the cells. In this study it was confirmed via laser ablation experiments that indeed cell bond tension was reduced in larval epidermal cells of animals lacking maternal and zygotic *smash*. On the cellular level, junctions showed a serpentine like phenotype, which also points to a loss of tension, since wild type junctions appear as straight, tight lines. Further laser ablation experiments in Smash overexpressing cells showing expected higher cell bond tension could substantiate these findings. Moreover, laser ablation experiments should be conducted not only in the larval epidermis but in

embryos to confirm that tension is also reduced here. In wild type situation the retraction velocities after ablation are higher at vertical edges than at horizontal edges during germband extension. This anisotropy of cortical tension at cell junctions is essential to drive tissue elongation (Rauzi et al. 2008; Fernandez-Gonzalez et al. 2009). It would also be interesting to investigate whether this planar polarized distribution of tension is affected in *smash*$^{35m/z}$ mutant embryos.

4.1.1 Structure-function analysis

Lethality tests showed that *smash* mutation is semilethal (Beati et al. 2018). This semilethality was completely rescued by the ectopic expression of full length GFP-Smash PM and PI, but not by GFP-Smash PJ, which lacks the LIM domain and PDZ binding motif. This result confirmed that semilethality is indeed caused by the loss of *smash* and not by a second site mutation, but also underlines the functional importance of the conserved LIM-PBM module. Deletion versions lacking one of these domains individually were also able to rescue semilethality, pointing to a strong interaction or redundancy of these domains. Another possible explanation would be a multiprotein complex, in which partial dysfunction of Smash is compensated by different members in a redundant fashion. Src42A is most likely one member in such a complex since Smash is a binding partner and a phosphorylation target of Src42A (Beati et al. 2018). However, a version of GFP-Smash PI mutated in six potential phosphorylation sites for Src42A rescued semilethality of *smash*^{35} mutants. This result demonstrates that phosphorylation of these residues is dispensable for function of Smash regarding to semilethality.

The vertebrate homologue of Smash, LMO7, has already been shown to be involved in actin-associated cytoskeleton remodeling (Ooshio et al. 2004). In order to address the question of functional homology, it would be interesting to test if a construct carrying the gene locus of LMO7 is able to rescue semilethality of *smash* mutants.

Smash plays a key role in mediating cell bond tension at the cortex of epithelial cells and therefore its recruitment to the ZA to junctions in the A/P axis appears to be essential. Concerning this spatially distinct subcellular localization of full length Smash, the differences in the localization of the deletion constructs were investigated. Consistent with the

assumption that Smash localization at cell-cell contacts is essential for functionality, a detachment from the junctions was observed for the fragment of Smash lacking the entire C-terminus, a construct which was not able to rescue semilethality. However, this observation was also made for deletion versions lacking either the LIM domain or the PDZ binding motif, which both rescued semilethality. This mislocalization was observed to a weaker extent here, since some GFP-Smash staining was still detectable at AJs, which would support the hypothesis that Smash localization at the ZA is crucial for functionality and thus for the ability to rescue semilethality. However, a construct expressing just the C-terminus of Smash was able to rescue semilethality, but also showed a detachment from AJs and a cytoplasmic distribution. This observation argues against the conclusion that cortical localization of Smash is indispensable for the ability to rescue semilethality. To investigate this in more detail, the GFP-Smash variants should be expressed in the *smash*^{35} mutant background to achieve a nearly physiological level of expression. In this context also the effect on known binding partners of Smash like Baz, Cno, Src42A or Rok should be examined. Due to missing domains, e.g. the LIM-PBM module, the linkage to these proteins could be disturbed, explaining the disability to rescue semilethality. In case of overexpression of GFP-Smash C-term, the interaction with these proteins may be still intact, explaining the ability to rescue semilethality through compensation, although Smash is detached from AJs here.

In further experiments the three isoforms and the generated deletion constructs should be investigated with respect to their ability to rescue not only semilethality but also the severe defects in embryonic morphogenesis. To that aim, an ubiquitous Gal4-driver, e.g. act5C::Gal4, should be recombined with the respective GFP-Smash isoform or deletion variant and crossed with a chromosome carrying a membrane marker in the *smash*$^{35\ m/z}$ mutant background. Live imaging of these embryos will provide more insight into the loss-of-function phenotype and the functional capacity of the different isoforms and constructs to rescue the observed severe morphogenetic defects. In this movies the localization of GFP-Smash isoforms and deletion constructs should be investigated with respect to their planar polarization in order to clarify, which domains are required for PCP and if those contribute to rescue the strong phenotype and semilethality.

4.1.2 Smash as regulator of the actomyosin network

The results of this study strongly indicate that Smash is involved in the Rok-Myosin II pathway. Myosin II is phosphorylated and thereby activated by Rok in order to move along actin filaments, so that the cell cortex is able to constrict. The inhibition of Rok results in a strong decrease of this tension in the cortex of the cell (Landsberg et al. 2009). Since cell bond tension and phosphorylation of Myo II is downregulated in embryos lacking *smash*, Smash may act as an adaptor protein to provide substrate specificity towards Sqh, the *Drosophila* Myosin light chain. Co-IP experiments underline this hypothesis, since a direct protein-protein interaction between Rok and Smash was confirmed. Investigations of the interaction of Smash and Sqh could not confirm a binding of these proteins with certainty. In some experiments a slight signal in the size of myc-Sqh after pulling down Smash-GFP could be detected. However, since this was not assuredly reproducible, future experiments should clarify, if the interaction of Smash and Sqh may be indirect via Rok. The co-IP experiments described in 3.5.4 have been conducted *in vitro* in transfected S2 cells. To test whether Smash may bind to Sqh *in vivo* or exclusively in the presence of Rok, co-IPs should be repeated with embryonic lysate or under conditions of S2 triple transfection including Smash, Rok and Sqh. Additionally, it would be interesting to examine, whether the interaction of Rok and Sqh is affected upon the loss of *smash*. Moreover, experiments with regard to the amount and localization of phosphorylated Myo II in Smash overexpressing cells could give more insight into the exact connection between these actomyosin network components.

Besides Myo II, Rok is also able to phosphorylate Baz and thereby contributes to the correct distribution of Myosin II and the AJ protein Arm/β-catenin (Simões et al. 2010). Interestingly, Smash interacts with both Baz and Rok, again suggesting that it may function as a cofactor providing substrate specificity of Rok towards Baz. It is tempting to speculate that Smash could interact with various kinases, including Rok and Src42A, to mediate interaction with their substrates. Since the largest isoform Smash-PM contains two coiled-coil domains, it seems likely that Smash forms dimers or multimers, linking Rok and Baz in order mediate Baz phosphorylation and thus AJ stability. The actin- and Rok-binding protein Shroom is required for junctional localization of Rok during axis elongation (De Matos Simões et al. 2014). Another study showed, that Shroom can act as a di-

rect activator of Rock in MDCK cells (Zalewski et al. 2016). Smash shares various similarities with Shroom, as in both cases the loss-of-function leads to semilethality, both display similar subcellular localization and the overexpression induces apical constriction of epithelial cells. In this work a direct interaction of Smash and Shroom on the protein level was confirmed. These functional parallels and the fact that Smash and Shroom are binding partners indicate that both proteins may act in a common molecular pathway regulating actomyosin activity. Future investigations of the interaction of Smash and Shroom *in vivo* should unravel the relation between these similar proteins and how they are embedded in the complex cytoskeleton network.

Another substrate of Rok is presented by Moesin, which is a member of the highly conserved Ezrin/Radixin/Moesin (ERM) proteins, providing a critical link between the plasma membrane and the cytoskeleton (Oshiro et al. 1998; Fukata et al. 1998; Pelaseyed & Bretscher 2018). ERM proteins belong to the FERM superfamily, which contain a N-terminal FERM domain (4.1 protein, ezrin, radixin, moesin) linking cytoplasmic proteins to the membrane (Chishti et al. 1998). In this study it was shown that Smash is a binding partner of Moe, probably in a larger complex together with Rok. In *in vitro* studies it has also been shown that in MDCK cells Moe binds to the Myosin binding subunit (MBS) of myosin phosphatase, which is a target of the small GTPase Rho, an upstream regulator of Rok. Rok also phosphorylates MBS and thereby inactivates myosin phosphatase. MBS shows phosphatase activity towards Moe, which is phosphorylated by Rok. This activity is inhibited when MBS is phosphorylated by Rok itself. Consequently, Myosin phosphatase and Rho-kinase seem to regulate the phosphorylation state of Moe downstream of Rho (Fukata et al. 1998). With Smash as binding partner of Moe a possible inhibitory function towards MBS by enhancing Rok activity is conceivable.

Smash shares some similarities with the LIM protein Ajuba, since both exhibit LIM domains and show a planar polarized localization during axis elongation at junctions in the A/P axis. Ajuba indirectly influences Myosin activity and tension through genetic interaction with Yorkie (Yki), a transcription factor regulated by the Hippo pathway (Rauskolb et al. 2014). The Hippo pathway is a conserved cascade regulating growth and consists of the core kinase kinases Warts (Wts) and Hippo (Hpo) and the adaptor proteins Salvador (Sav) and Mob as tumor suppressor (Mats). Yki is repressed by this complex and thereby

tissue growth is repressed. Activity of the Hippo pathway is regulated by various upstream regulators, which predominantly localize at AJs (Irvine & Harvey 2015), like Ajuba. Whether Smash is also involved in Hippo signaling to mediate actomyosin contractility and whether Ajuba and Smash interact in this context remains to be examined.

For Ajuba a tension dependent localization during germband extension has been described. Ajuba is recruited to junctions of increasing tension in a planar polarized fashion (Razzell et al. 2018). Since tension dependent behavior of epithelial cells correlates directly with Smash expression, Smash localization may also rely on factors regulating tension in these cells, which recruit Smash to the AJs at the A/P axis.

The vertebrate homologue of Smash, LMO7, has already been shown to regulate cytoskeleton dynamics via interaction with the actin binding scaffold protein Afadin (Ooshio et al. 2004). In Beati et al. (2018) a direct interaction of Smash and the *Drosophila* Afadin homologue Cno via its PDZ domain was confirmed, suggesting a strong evolutionary conservation of the Smash/LMO7 molecular function between *Drosophila* and vertebrates. Cno plays an important role in adhesion since it links the actomyosin network with the core cell adhesion molecules, the Cadherins. The process of apical constriction of mesodermal cells is disrupted upon the loss of Cno as a result of disconnection of the actomyosin cytoskeleton from AJs, uncoupling actomyosin constriction and cell shape change (Sawyer et al. 2009). The binding of Cno to Smash is mediated through its only PDZ domain and the C-terminal PDZ binding motif of Smash, implicating the interaction is exclusive unless Smash forms dimers, like assumed before. In this case, the role of Smash as a linker protein in a multiprotein complex regulating actomyosin associated events becomes more likely. A scheme of the possible interaction of probable members of this complex and how they may regulate each other is shown in Figure 31.

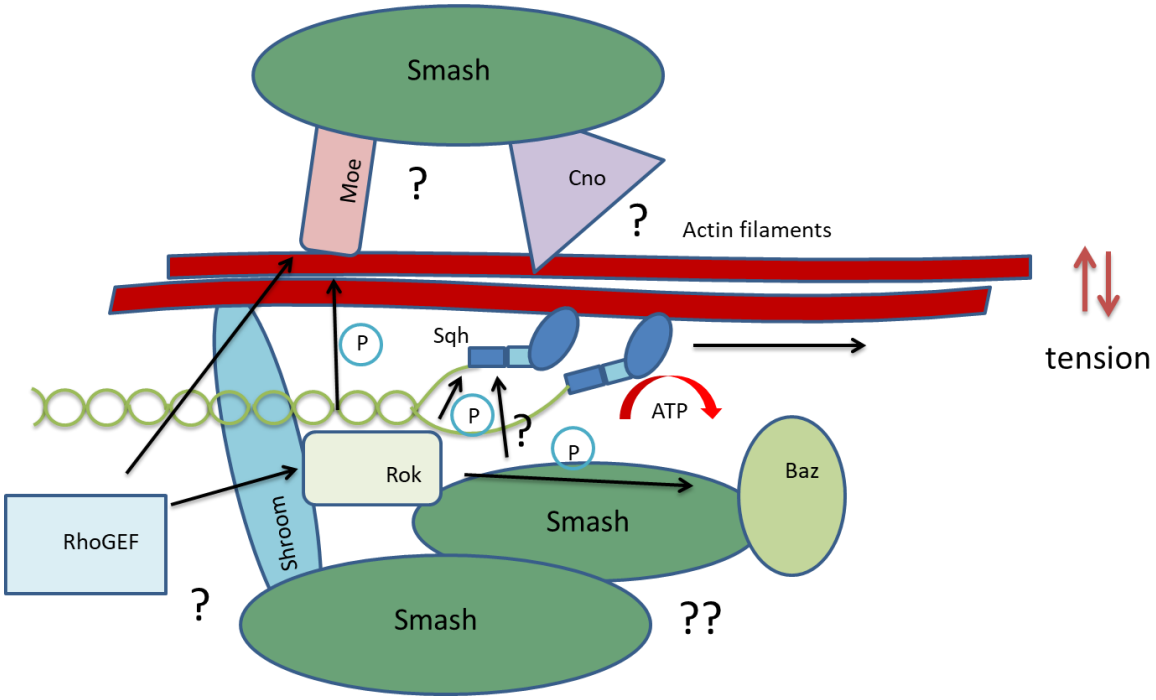

Figure 31: Scheme of how Smash may act in a multi protein complex. The binding of Smash- Baz, Smash-Cno, Smash-Rok, Smash-Shroom and Smah Moe was confirmed. How Smash regulates cell bond tension in this network is not clear, but it is likely that Smash provides substrate specificity towards phosphorylation targets of Rok.

4.1.2.1 Interaction of Smash and Src42A

In Beati et al. (2018) Smash was already confirmed as binding partner and phosphorylation target of the cell adhesion regulator Src42A. In this work this interaction was examined in more detail. Since phosphorylation of the smallest isoform Smash PJ, which lacks the PBM module, by Src42A is strongly reduced in contrast to the other isoforms, the question was raised whether the binding of these proteins is a precondition for phosphorylation. Smash PJ was shown to bind to Src42A, indicating phosphorylation does not influence the interaction of these proteins as binding partners, pointing to a function of this interaction which does not require phosphorylation. In rescue experiments described in 3.2, a version of Smash PI in which six potential phosphorylation sites were mutated (GFP-Smash PI YmultiF), was able to rescue semilethality of *smash*^{35} mutants, also indicating that phosphorylation of Smash by Src42A is dispensable for proper Smash function, at least in this rescue assay. The significance of phosphorylation of Smash by Src42A is therefore not yet clear. In further experiments the importance of this relationship should be investigated in more detail, for instance by studying the localization of Smash PI Ymul-

tiF. Moreover, the effect on Src42A distribution by overexpressing Smash PI YmultiF should be examined to clarify whether phosphorylation by Src42A directs Smash distribution. Another approach should be to investigate the interaction of Smash with known Src42A targets, to examine whether Smash may also act as a linker protein here.

Smash seems to contain several binding sites for Src42A, since Src42A was able to bind any deletion construct of Smash shown in 3.6.2. A version which just expresses the C-terminus as also the opposing version just containing the N-terminus were both able to bind to Src42A, indicating both termini exhibit sequences responsible for this interaction. Though, co-transfection of CD8-GFP and Src42A for control resulted also in a signal with a similar intensity, which leads to doubt of the specificity of this binding assay. These experiments should be repeated with differently tagged versions of Smash deletion constructs to confirm specificity of the binding. Interestingly, all deletion constructs of Smash were phosphorylated *in vitro*, except for the variant which contains the last 162 amino acids of the C-terminus, meaning not the LIM-PBM module alone is required for phosphorylation. However, since the phosphorylation of Smash by Src42A does not appear to be essential for proper function of Smash, the major importance of this interaction is still unclear.

The role of the Smash–Src42A interaction within the actomyosin network is not yet known. Due to the fact that phosphorylation of Smash is not required for survival of *smash*^{35} mutants, it appears likely that Smash and Src42A are both part of the proposed multiprotein complex, but that their interaction is not essential. With respect to their similarities, the potential redundancy of Smash and Shroom or Ajuba should be also investigated in this context.

In future experiments the role of Src42A with respect to Smash in this entire network should be investigated. To this purpose the genetic hierarchy of the actomyosin components mentioned above should be clarified.

4.1.2.2 Smash acts as a scaffold protein

Like described in the previous chapter, Smash is involved in processes mediating cell bond tension through regulation of the actomyosin network. In these processes Smash interacts with several components of this network but the molecular function of Smash was unclear so far. There is strong evidence that Smash either serves as an adaptor to

provide substrate specificity for various kinases or/and as scaffold protein, e.g. linking actin crosslinkers to the cytoskeleton. The following table provides an overview of the so far investigated binding partners of Smash with respect to their molecular function in the context of this work.

Table 4-1: Overview of Smash binding partners and their molecular function.

binding partner of Smash	**molecular function**
Rok	kinase
Baz	substrate of Rok
Sqh	substrate of Rok
Moe	substrate of Rok
Src42A	kinase
Cno	Actin binding
Shroom	substrate of Rok, Actin binding

With regard to Smash function as a cofactor for several kinases and their substrates, in future experiments other targets of Rok and Src42A should be examined. There is evidence that Src42A phosphorylates Arm/β-catenin to stabilize cell adhesion at AJs (Takahashi 2005). Here, a potential role for Smash as cofactor should be investigated. To test whether Smash regulates the kinase activity of Src42A and Rok, *in vitro* kinase assays with known substrates of the respective kinase should be conducted without and in the presence of Smash.

Among various substrates of Rok is the LIM domain kinase 1 (LMK1), a serine/threonine kinase containing two LIM domains and a PDZ domain (Ohashi et al. 2000). This structural composition of LMK1 increases the possibility of Smash as a binding partner through its PDZ binding motif. Interestingly, LMK1 is also phosphorylated by aPKC (Kang et al. 2007), which forms a complex with Baz and Par6 to establish apico-basal polarity (Kaplan et al. 2009). Whether Smash also binds to aPKC or eventually forms heterodimers with Baz to serve as scaffold protein to stabilize this complex, remains to be examined. Since Smash PM exhibits two coiled-coil domains, it is likely that Smash is also able to form homodimers, potentially linking several proteins to a complex. To characterize Smash function as

scaffold protein in more detail, Smash protein interaction with other ZA associated proteins, e.g. α-catenin or Armadillo has to be characterized. To that aim, Smash binding partners can be identified via co-IP experiments and mass spectrometry.

4.2 Subcellular localization of Smash is determined by multiple proteins at the ZA

Like many proteins associated with the actomyosin network, Smash shows a subcellular planar polarization in the apical region of epidermal cells at the ZA during germband extension. Smash is enriched at the junctions oriented in the A/P axis. Here, it co-localizes with its binding partners Rok and Cno and with one of the core components of the molecular motor to drive epithelial tension, Myosin II, Sqh in *Drosophila*. The polarity regulator Baz, the first identified binding partner of Smash, is also planar polarized during axis elongation, but accumulates at junctions in the D/V axis. Although Smash and Baz are binding partners and co-localize in general at the ZA, they show no identical localization. Such complementary distribution of proteins that directly interact with each other has been shown before, e.g. for Rok and Baz. Rok is, like Smash, enriched at cell-cell interfaces in the A/P axis, while Baz shows the opposing accumulation. Nevertheless Rok is able to phosphorylate Baz and thus destabilize its localization at A/P junctions (Simões et al. 2010). Like Rok, Smash may also restrict Baz from the A/P cell-cell contact sites. During dorsal closure, Smash localizes to the leading edge of the most dorsal cells of the epidermis, while Baz is completely excluded from there, indicating the binding between Smash and Baz is not constitutive. Consequently, Smash subcellular localization is determined not only by Baz, but by other binding partners like Rok, Cno or Src42A. To test whether localization of Smash is depending on Baz is difficult, since embryos lacking both maternal and zygotic *baz* show extreme defects in epithelial integrity and early embryonic development (Müller & Wieschaus 1996). As a consequence, it would not be possible to analyze Smash localization during germband extension. Embryos only mutant for zygotic *baz*, develop normally until late germband extension (Krahn et al. 2010). In this stage, epidermal cells start to loose Baz protein gradually. In those cells which already lost Baz, also no Smash is detectable. This could be a hint to the subcellular dependency of Smash and

Baz, but may also be a result of the failure to maintain epithelial integrity and thus mislocalization of proteins at the ZA.

Smash is also expressed in the somatic musculature. Here, it is enriched at the contact sites between somatic muscles and the epidermal tendon cells, which connect the muscles to the epidermis. At this so called myotendinous junction (MTJ), Smash co-localizes strongly with α-Actinin and β-PS-Intergrin. Tendon cells show a highly dynamic behavior as they modify microtubules and actin filaments, in order to resist mechanical forces (Subramanian et al. 2007). In response to external force, redistribution of actin crosslinkers and rearrangement of the actomyosin network takes place. After deformation of the plasma membrane, those crosslinkers and motorproteins like Myosin or the scaffold protein Filamin accumulate to this region (Valdivia et al. 2017). The development of MTJs mainly depends on the interaction of Integrins and extracellular matrix (ECM) molecules excreted by tendons and muscles (Geiger & Bershadsky 2002; Subramanian et al. 2007). The activation of Integrins is also a response to deformation or mechanical stimuli. Cell culture experiments showed that downstream of Integrin activation, various proteins are recruited (Valdivia et al. 2017). Interestingly among these proteins are the kinases Src and Rock, which are already shown to be closely linked to Smash in *Drosophila*. Integrin recruits Src, which in turn activates Rho signaling pathway, which through Rock induces the phosphorylation of the myosin regulatory light chain (Arthur et al. 2000; Arias-Salgado et al. 2003). In *Drosophila*, Smash may act here also as a cofactor connecting Src and Rok. It would be interesting to test if the phosphorylation of Smash by Src is essential in this context.

In *Drosophila*, Rok is indispensable in tendon cells to assemble stable MTJ and maintain cell shape. The loss of Rok in tendon cells results in misorientation of tendon cell extensions and diminished phosphorylation of Myosin (Vega-Macaya et al. 2016), similar to the loss-of-function phenotype of *smash* with respect to Myosin II. Additionally, the loss of Rok leads to abnormal Integrin localization, causing defective MTJs formation and muscle function. This pathway is not mainly dependent on Myosin II as key target of Rok (Vega-Macaya et al. 2016), suggesting that other proteins, potentially Smash, play an important role here.

How Smash is embedded in the Integrin pathway and if Smash functions in the same pathway at the MTJ as it does at AJs remains to be characterized. In this context the impact of *smash* loss-of-function on the somatic muscles, e.g. defects in larval movements should be examined.

The vertebrate homologue of Smash LMO7 has been described as a nucleocytoplasmic shuttling protein regulating the transcription of muscle relevant genes, for instance of the nuclear membrane protein Emerin. Mutations in *emerin* result in X-linked Emery–Dreifuss muscular dystrophy (X-EDMD), a hereditary neuromuscular degenerative disease with an associated dilated cardiomyopathy and cardiac conduction defect (Holaska et al. 2006; Ellis 2006). Whether a functional homology does exist here and Smash also plays a role in gene expression remains to be investigated. For Smash no endogenous nuclear localization could be detected. It might be the case that the nuclear Smash level is below the detection limit. Using drugs to inhibit nuclear export or coupling Smash to a nuclear export sequence to detect a potential increase at the cell cortex could provide information about a possible function for Smash in regulating gene expression.

4.2.1 Smash regulates planar cell polarity

In 3.4.1 it was described that planar cell polarity (PCP) is disrupted during germband extension upon the loss of *smash*. The tempo-spatial planar polarization of actomyosin network components is of fundamental importance during this event of axis elongation, since PCP allows the correctly directed body growth through certain cell neighbor change events.

PCP of Baz, Cno and Sqh was disturbed during axis elongation. Baz, which, like described above, is enriched at D/V junctions in wild type situation, accumulated at A/P junctions upon the loss of *smash*. This result indicates that Smash could restrict Baz from A/P cell interfaces in wild type condition. Cno and Sqh, which normally localize together with Smash predominantly at junctions in the A/P axis, lost their planar polarization as they were distributed evenly at the cell cortex, whereas Rok was unaffected.

As mentioned before, Rok is required for PCP of Sqh and Baz. Since Rok remained in its localization upon the loss of Smash, a possible role of Smash as a cofactor downstream of

Rok providing substrate specifity towards Sqh or Baz becomes more plausible. Alternatively, Smash and Moe, which was identified to bind to Smash, could serve as an inhibitor of Myosin phosphatase and thereby enhance Rok kinase activity. To consider this, further experiments regarding PCP of Moesin or the Rok activator RhoGEF in wild type and *smash* mutant embryos should be conducted to clarify the relation and hierarchy of these proteins. The loss of Rok results in a similar phenotype to that of *smash* with respect to Baz, as Baz loses its PCP. Baz in turn is required for planar localization of Sqh/Myosin II and Arm/β-catenin (Simões et al. 2010). In how far Smash is required for proper distribution of Arm/β-catenin, or directs Sqh to the A/P junctions together with Baz is not clear yet.

As described above, Smash interacts with the planar polarized cell adhesion regulator Src42A, which has been shown to contribute to the formation of basolateral protrusions during rosette formation. In this process the ventral-most and the dorsal-most cell of a future rosette migrate towards each other at the basolateral side, prior to the apical side (Sun et al. 2017). Smash is a phosphorylation target of Src42A and PCP and morphogenesis is disturbed embryos lacking *smash*, so it appears possible that Smash may also be involved in regulation of these directed cell movements. Since these neighbor change events like forming rosettes are highly connected to the turnover of junctions, a dynamic regulation of cell bond tension is needed. Here, Myosin II levels and mechanical tension are selectively increased at vertical interfaces and pulses of Myosin accumulation and dissociation occur within seconds (Bertet et al. 2004; Zallen & Wieschaus 2004; Rauzi et al. 2008; Rauzi et al. 2010; Kasza et al. 2014). In how far Smash is dynamically recruited to those junctions of increasing tension remains to be examined. Such a tension dependent localization has recently been described for the LIM domain protein Ajuba, which also plays an essential role in rosette formation during axis elongation. Embryos lacking Ajuba show severe defects in cell adhesion as rosettes exhibit gaps at the vertex resulting in an increase of rosettes due to failure of rosette resolution (Razzell et al. 2018). Smash shares structural similarities with Ajuba. Both exhibit LIM domains and show the same subcellular localization during germband extension as both are planar polarized and enriched at the A/P cell interfaces. To test whether these two proteins act in a redundant manner or if Ajuba is also part of the assumed protein complex Smash is involved in, further experiments should be conducted. In live imaging videos of embryos lacking *smash*, the loss-of-

function phenotype has to be characterized in more detail to clarify the cellular processes that lead to these severe defects. Special attention should be paid to eventual defects in cell movements like T1 transitions or rosette formations, like it was described for Ajuba or Src42A. In this context the interaction of Smash and the latter two proteins should be examined to clarify the molecular pathway of the protein complex Smash acts in and how PCP contributes to this mechanism.

5 Conclusion and Perspectives

In this work the LIM protein Smash, a ZA-associated protein involved in the regulation of PCP and actomyosin-dependent rearrangement of epithelial cells was examined.

This study establishes Smash as part of a molecular complex, coordinating these actomyosin forces, including the polarity regulators Baz and Cno and the regulator of cell–cell adhesion and morphogenesis Src42A. Moreover, Smash seems to be involved in Rho signaling including Rok, the regulatory subunit of nonmuscle myosin II, Sqh and the actin binding protein Shrm, which shares various similarities with Smash.

The loss-of-function of *smash* results in disruption of PCP and leads to severe defects in morphogenesis. These results demonstrate the great importance of the polarized distribution of cytoskeleton associated proteins for a proper function of the tension dependent regulation of the actomyosin network. Otherwise spatially directed morphogenetic processes fail and epithelial tissues are not able to grow in developing organisms.

In further experiments, additional proteins interacting with Smash remain to be identified. Furthermore, the exact mechanism and the hierarchy these components are subject, which have to be examined.

The vertebrate homologue of Smash, LMO7, has been shown to regulate actin dependent remodeling of the cytoskeleton (Ooshio et al. 2004). Additionally, LMO7 functions as a tumor suppressor for lung cancer in humans (Tanaka-Okamoto et al. 2009; Nakamura et al. 2011). In future studies, true functional homology of Smash and LMO7 should be investigated, for instance with respect to LMO7 role as tumor suppressor, indicating a clinical relevance in cancer research.

Abstract

Epithelial cells adhere to each other in a dynamic fashion, allowing the cells to change their shape and move along each other during morphogenesis. The regulation of adhesion occurs at the apical side through the belt-shaped adherens junctions at the zonula adherens (ZA). Junction formation depends on components of the polarity regulating Par–atypical PKC (Par-aPKC) complex in *Drosophila*. In this work the LIM protein Smallish (Smash), the orthologue of vertebrate LMO7 and binding partner of the Par-complex core component Baz was characterized.

Animals lacking Smash show reduced cell bond tension and loss of planar cell polarity leading to severe defects during embryonic morphogenesis of epithelial tissues and organs. These defects are characterized by uncoordinated formation of epithelial invaginations and furrows. Consequently, the loss of *smash* causes semilethality, whereby rescue experiments indicate that the C-terminus, containing the conserved LIM domain and PDZ binding motif, is essential for Smash function.

The data of this work established Smash as a key regulator of morphogenesis coordinating planar cell polarity and actomyosin contractility at the ZA. This regulation is achieved by interaction with a variety of regulatory proteins and kinases that localize at the ZA, including Baz, Src42A and the actin binding proteins Shrm and Cno. Smash seems to be involved in Rho signaling affecting the phosphorylation state of the regulatory subunit of nonmuscle myosin II, Sqh, through its associated kinase Rok.

The results of this work suggest that Smash regulates cell adhesion and cell bond tension dependent processes by acting as a scaffold protein in a multiprotein complex and serving as cofactor to provide substrate specificity between kinase and substrate.

Zusammenfassung

Die Verknüpfung von Epithelzellen zu einem integrierten Zellverband erfordert ein hohes Maß an Dynamik und Flexibilität, das eine Veränderung der Zellform und Zellmigration während der Morphogenese erlaubt. An der apikal lokalisierten zonula adherens erfolgt die Regulierung dieser Adhäsionskräfte. Die Entstehung und korrekte Organisation der zonula adherens wird durch den Par-Komplex gesteuert. Das *Drosophila melanogaster* Lin11, Isl-1, Mec-3 (LIM)- Protein Smallish (Smash), Ortholog des Proteins LMO7 in Vertebraten, wurde bereits als Bindungspartner des Par-Komplex Proteins Par3/Baz identifiziert. In dieser Arbeit wurde Smash detaillierter charakterisiert.

Smash ist an verschiedenen Prozessen beteiligt, die von der Zelladhäsion und der Regulierung der Spannung im Kortex der Zelle abhängen. Tiere, welche mutant für *smash* sind, weisen eine verringerte Spannung im Kortex der Zellen auf und verlieren ihre planare Zellpolarität, woraus schwere Defekte während der embryonalen Morphogenese von Epithelgeweben resultieren. Diese sind durch unkoordinierte Invaginationen und Furchenbildung gekennzeichnet. Dies führt zu einer Semilethalität der Tiere, wobei Rettungsexperimente gezeigt haben, dass der C-Terminus, welcher die LIM-Domäne und das PDZ-Bindungsmotiv enthält, essentiell für die Funktion von Smash ist.

Smash bindet neben Baz mehrere Proteine, die Teil des Rho GTPase Signaltransduktionswegs und als essentielle Regulatoren des Actomyosin-Netzwerks bekannt sind. Smash interagiert mit den Actin-bindenden Proteinen Canoe (Cno), Shroom (Shrm) und Moesin (Moe) und ist ein Bindungspartner und Substrat der Kinase Src42A, ein essentieller Regulator der epithelialen Morphogenese. Weiterhin bindet Smash die Rho-Kinase Rok und ist wichtig für dessen Funktion in der Phosphorylierung und Aktivierung des Motorproteins Myosin II, Spaghetti Squash (Sqh) in *Drosophila*. Diese Ergebnisse legen nahe, dass Smash in einem Proteinkomplex als Gerüstprotein und Kofaktor fungiert, welches Substratspezifität zwischen Kinase und Substrat sicherstellen kann.

Zusammenfassend wird in dieser Arbeit das LIM Protein Smash als wichtiger Regulator von Spannungsmechanismen des Actomyosin-Netzwerks und planarer Zellpolarität beschrieben.

References

Adam JC, Pringle JR & Peifer M (2000) Evidence for functional differentiation among *Drosophila* septins in cytokinesis and cellularization. *Mol. Biol. Cell* 11, 3123–3135.

Amano M, Ito M, Kimura K, Fukata Y, Chihara K, Nakano T, Matsuura Y & Kaibuchi K (1996) Phosphorylation and Activation of Myosin by Rho-associated Kinase (Rho-kinase). *J. Biol. Chem.* 271, 20246–20249.

Arias-Salgado EG, Lizano S, Sarkar S, Brugge JS, Ginsberg MH & Shattil SJ (2003) Src kinase activation by direct interaction with the integrin cytoplasmic domain. *Proc. Natl. Acad. Sci.* 100, 13298–13302.

Arthur WT, Petch LA & Burridge K (2000) Integrin engagement suppresses RhoA activity via a c-Src-dependent mechanism. *Curr. Biol.* 10, 719–722.

Ashburner M (1989) Drosophila: a laboratory manual. *Trends Genet.* 6, 340.

Axelrod JD (2001) Unipolar membrane association of Dishevelled mediates Frizzled planar cell polarity signaling. *Genes Dev.* 15, 1182–1187.

Barrett K, Leptin M & Settleman J (1997) The Rho GTPase and a putative RhoGEF mediate a signaling pathway for the cell shape changes in Drosophila gastrulation. *Cell* 91, 905–915.

Bastock R (2003) Strabismus is asymmetrically localised and binds to Prickle and Dishevelled during Drosophila planar polarity patterning. *Development* 130, 3007–3014.

Beati H (2013) *Functional analysis of the Drosophila gene smallish (CG43427)*.

Beati H, Peek I, Hordowska P, Honemann-Capito M, Glashauser J, Renschler FA, Kakanj P, Ramrath A, Leptin M, Luschnig S, Wiesner S & Wodarz A (2018) The adherens junction-associated LIM domain protein Smallish regulates epithelial morphogenesis. *J. Cell Biol.* 217, 1079–1095.

Behrens J, Vakaet L, Friis R, Winterhager E, Van Roy F, Mareel MM & Birchmeier W (1993) Loss of epithelial differentiation and gain of invasiveness correlates with tyrosine phosphorylation of the E-cadherin/β-catenin complex in cells transformed with a temperature-sensitive v-SRC gene. *J. Cell Biol.* 120, 757–766.

Benton R & St Johnston D (2003) Drosophila PAR-1 and 14-3-3 inhibit Bazooka/PAR-3 to establish complementary cortical domains in polarized cells. *Cell* 115, 691–704.

Bertet C, Sulak L & Lecuit T (2004) Myosin-dependent junction remodelling controls planar cell intercalation and axis elongation. *Nature* 429, 667.

Betschinger J, Mechtler K & Knoblich JA (2003) The Par complex directs asymmetric cell division by phosphorylating the cytoskeletal protein Lgl. *Nature* 422, 326–330.

Bischof J, Maeda RK, Hediger M, Karch F & Basler K (2007) An optimized transgenesis system for Drosophila using germ-line-specific phiC31 integrases. *Proc. Natl. Acad. Sci. U. S. A.* 104, 3312–3317.

Blankenship JT, Backovic ST, Sanny JSSP, Weitz O & Zallen JA (2006) Multicellular

Rosette Formation Links Planar Cell Polarity to Tissue Morphogenesis. *Dev. Cell* 11, 459–470.

Boggon TJ & Eck MJ (2004) Structure and regulation of Src family kinases. *Oncogene* 23, 7918–7927.

Bolinger C, Zasadil L, Rizaldy R & Hildebrand JD (2010) Specific isoforms of drosophila shroom define spatial requirements for the induction of apical constriction. *Dev. Dyn.* 239, 2078–2093.

Boyer B, Roche S, Denoyelle M & Thiery JP (1997) Src and Ras are involved in separate pathways in epithelial cell scattering. *EMBO J.* 16, 5904–5913.

Brand AH & Perrimon N (1993) Targeted gene expression as a means of altering cell fates and generating dominant phenotypes. *Development* 118, 401–15.

Brodsky MH & Steller H (1996) Positional information along the dorsal-ventral axis of the Drosophila eye: Graded expression of the four-jointed gene. *Dev. Biol.* 173, 428–446.

Bromann PA, Korkaya H & Courtneidge SA (2004) The interplay between Src family kinases and receptor tyrosine kinases. *Oncogene* 23, 7957–7968.

Brown MT & Cooper JA (1996) Regulation, substrates and functions of src. *Biochim. Biophys. Acta - Rev. Cancer* 1287, 121–149.

Cenciarelli C, Chiaur DS, Guardavaccaro D, Parks W, Vidal M & Pagano M (1999) Identification of a family of human F-box proteins. *Curr. Biol.* 9, 1177–1179.

Chen W, Antic D, Matis M, Logan CY, Povelones M, Anderson GA, Nusse R & Axelrod JD (2008) Asymmetric Homotypic Interactions of the Atypical Cadherin Flamingo Mediate Intercellular Polarity Signaling. *Cell* 133, 1093–1105.

Chishti A, Kim A & Hoover KB (1998) The FERM domain : a unique module involved in. *Tibs* 0004, 281–282.

Chou T & Perrimon N (1996) The autosomal FLP-DFS technique for generating Germline Mosaics in Drosophila melanogaster. *Genetics* 144, 1673–1679.

Chou TB & Perrimon N (1992) Use of a yeast site-specific recombinase to produce female germline chimeras in drosophila. *Genetics* 131, 643–653.

Clark HF, Brentrup D, Schneitz K, Bieber A, Goodman C & Noll M (1995) Dachsous encodes a member of the cadherin superfamily that controls imaginal disc morphogenesis in Drosophila. *Genes Dev.* 9, 1530–1542.

Cooper JA, Gould KL, Cartwright CA & Hunter T (1986) Tyr527 is phosphorylated in pp60c-src:Implications for regulation. *Science* 231, 1431–1434.

Dedeic Z, Cetera M, Cohen TV & Holaska JM (2011) Emerin inhibits Lmo7 binding to the Pax3 and MyoD promoters and expression of myoblast proliferation genes. *J. Cell Sci.* 124, 1691–1702.

Devenport D (2014) The cell biology of planar cell polarity. *J. Cell Biol.* 207, 171–179.

Ellis JA (2006) Emery-Dreifuss muscular dystrophy at the nuclear envelope: 10 Years on. *Cell. Mol. Life Sci.* 63, 2702–2709.

Feiguin F, Hannus M, Mlodzik M & Eaton S (2001) The Ankyrin Repeat Protein Diego

Mediates Frizzled-Dependent Planar Polarization. *Dev. Cell* 1, 93–101.

Fernandez-Gonzalez R, Simoes S de M, Röper JC, Eaton S & Zallen JA (2009) Myosin II Dynamics Are Regulated by Tension in Intercalating Cells. *Dev. Cell* 17, 736–743.

Field CM & Alberts BM (1995) Anillin, a contractile ring protein that cycles from the nucleus to the cell cortex. *J. Cell Biol.* 131, 165–178.

Förster D & Luschnig S (2012) Src42A-dependent polarized cell shape changes mediate epithelial tube elongation in Drosophila. *Nat. Cell Biol.* 14, 526–534.

Fukata, Kimura K, Oshiro N, Saya H, Matsuura Y & Kaibuchi K (1998) Association of the myosin-binding subunit of myosin phosphatase and moesin: Dual regulation of moesin phosphorylation by Rho-associated kinase and myosin phosphatase. *J. Cell Biol.* 141, 409–418.

Gates J & Peifer M (2005) Can 1000 reviews be wrong? Actin, α-catenin, and adherens junctions. *Cell* 123, 769–772.

Geiger B & Bershadsky A (2002) Exploring the neighborhood: Adhesion-coupled cell mechanosensors. *Cell* 110, 139–142.

Getz TM, Dangelmaier CA, Jin J, Daniel JL & Kunapuli SP (2010) Differential phosphorylation of myosin light chain (Thr)18 and (Ser)19 and functional implications in platelets. *J. Thromb. Haemost.* 8, 2283–2293.

Giot L (2003) A Protein Interaction Map of Drosophila melanogaster. *Science* 302, 1727–1736.

Guillot C & Lecuit T (2013) Mechanics of epithelial tissue homeostasis and morphogenesis. *Science* 340, 1185–9.

Haigo SL, Hildebrand JD, Harland RM & Wallingford JB (2003) Shroom Induces Apical Constriction and Is Required for Hingepoint Formation during Neural Tube Closure. *Curr. Biol.* 13, 2125–2137.

Harris TJC & Peifer M (2007) aPKC Controls Microtubule Organization to Balance Adherens Junction Symmetry and Planar Polarity during Development. *Dev. Cell* 12, 727–738.

Harris TJC & Peifer M (2005) The positioning and segregation of apical cues during epithelial polarity establishment in Drosophila. *J. Cell Biol.* 170, 813–823.

Harris TJC & Tepass U (2010) Adherens junctions: From molecules to morphogenesis. *Nat. Rev. Mol. Cell Biol.* 11, 502–514.

Hartenstein V & Wodarz A (2013) Initial neurogenesis in Drosophila. *Wiley Interdiscip. Rev. Dev. Biol.* 2, 701–721.

Hartman MA & Spudich JA (2012) The myosin superfamily at a glance. *J. Cell Sci.* 125, 1627–1632.

Hildebrand JD (2005) Shroom regulates epithelial cell shape via the apical positioning of an actomyosin network. *J. Cell Sci.* 118, 5191–5203.

Hildebrand JD & Soriano P (1999) Shroom, a PDZ domain-containing actin-binding protein, is required for neural tube morphogenesis in mice. *Cell* 99, 485–97.

Holaska JM, Rais-Bahrami S & Wilson KL (2006) Lmo7 is an emerin-binding protein that regulates the transcription of emerin and many other muscle-relevant genes. *Hum. Mol. Genet.* 15, 3459–3472.

Howard J (1997) Molecular motors: Structural adaptations to cellular functions. *Nature* 389, 561–567.

Huang J, Zhou W, Dong W, Watson AM & Hong Y (2009) From the Cover: Directed, efficient, and versatile modifications of the Drosophila genome by genomic engineering. *Proc. Natl. Acad. Sci. U. S. A.* 106, 8284–9.

Hunter C & Wieschaus E (2000) Regulated expression of nullo is required for the formation of distinct apical and basal adherens junctions in the Drosophila blastoderm. *J. Cell Biol.* 150, 391–401.

Hurov JB, Watkins JL & Piwnica-Worms H (2004) Atypical PKC Phosphorylates PAR-1 Kinases to Regulate Localization and Activity. *Curr. Biol.* 14, 736–741.

Ia KK, Mills RD, Hossain MI, Chan K-C, Jarasrassamee B, Jorissen RN & Cheng H-C (2010) Structural elements and allosteric mechanisms governing regulation and catalysis of CSK-family kinases and their inhibition of Src-family kinases. *Growth Factors* 28, 329–350.

Irvine KD & Harvey KF (2015) Control of organ growth by patterning and hippo signaling in drosophila. *Cold Spring Harb. Perspect. Biol.* 7, 1–16.

Jaffe AB & Hall A (2005) Rho GTPases: biochemistry and biology. *Annu. Rev. Cell Dev. Biol.* 21, 247–69.

Johnson K & Wodarz A (2003) A genetic hierarchy controlling cell polarity. *Nat. Cell Biol.* 5, 12–14.

Julian L & Olson MF (2014) Rho-associated coiled-coil containing kinases (ROCK). *Small GTPases* 5, e29846.

Kadrmas JL & Beckerle MC (2004) The LIM domain: From the cytoskeleton to the nucleus. *Nat. Rev. Mol. Cell Biol.* 5, 920–931.

Kaibuchi K, Kuroda S & Amano M (1999) Regulation of the cytoskeleton and cell adhesion by the Rho family GTPases in mammalian cells. *Annu. Rev. Biochem.* 68, 459–86.

Kainu T, Juo SH, Desper R, Schaffer AA, Gillanders E, Rozenblum E, Freas-Lutz D, Weaver D, Stephan D, Bailey-Wilson J, Kallioniemi OP, Tirkkonen M, Syrjäkoski K, Kuukasjärvi T, Koivisto P, Karhu R, Holli K, Arason A, Johannesdottir G, Bergthorsson JT, Johannsdottir H, Egilsson V, Barkardottir RB, Johannsson O, Haraldsson K, Sandberg T, Holmberg E, Grönberg H, Olsson H, Borg A, Vehmanen P, Eerola H, Heikkila P, Pyrhönen S & Nevanlinna H (2000) Somatic deletions in hereditary breast cancers implicate 13q21 as a putative novel breast cancer susceptibility locus. *Proc. Natl. Acad. Sci. U. S. A.* 97, 9603–8.

Kakanj P, Moussian B, Grönke S, Bustos V, Eming SA, Partridge L & Leptin M (2016) Insulin and TOR signal in parallel through FOXO and S6K to promote epithelial wound healing. *Nat. Commun.* 7, 12972.

Kang J-H, Jiang Y, Toita R, Oishi J, Kawamura K, Han A, Mori T, Niidome T, Ishida M,

Tatematsu K, Tanizawa K & Katayama Y (2007) Phosphorylation of Rho-associated kinase (Rho-kinase/ROCK/ROK) substrates by protein kinases A and C. *Biochimie* 89, 39–47.

Kang S, Xu H, Duan X, Liu JJ, He Z, Yu F, Zhou S, Meng XQ, Cao M & Kennedy GC (2000) PCD1, a novel gene containing PDZ and LIM domains, is overexpressed in several human cancers. *Cancer Res.* 60, 5296–5302.

Kaplan NA, Liu X & Tolwinski NS (2009) Epithelial polarity: Interactions between junctions and apical-basal machinery. *Genetics* 183, 897–904.

Karess RE, Chang X jia, Edwards KA, Kulkarni S, Aguilera I & Kiehart DP (1991) The regulatory light chain of nonmuscle myosin is encoded by spaghetti-squash, a gene required for cytokinesis in Drosophila. *Cell* 65, 1177–1189.

Kasza KE, Farrell DL & Zallen JA (2014) Spatiotemporal control of epithelial remodeling by regulated myosin phosphorylation. *Proc. Natl. Acad. Sci.* 111, 11732–11737.

Khurana T, Khurana B & Noegel AA (2002) LIM proteins: association with the actin cytoskeleton. *Protoplasma* 219, 1–12.

Knust E & Bossinger O (2002) Composition and formation of intercellular junctions in epithelial cells. *Science* 298, 1955–1959.

Knust E & Leptin M (1996) Adherens junctions in the Drosophila embryo: The role of E-cadherin in their establishment and morphogenetic function. *BioEssays* 18, 609–612.

Krahn MP, Bückers J, Kastrup L & Wodarz A (2010) Formation of a Bazooka–Stardust complex is essential for plasma membrane polarity in epithelia. *J. Cell Biol.* 190, 751–760.

Krahn MP, Klopfenstein DR, Fischer N & Wodarz A (2010) Membrane Targeting of Bazooka/PAR-3 Is Mediated by Direct Binding to Phosphoinositide Lipids. *Curr. Biol.* 20, 636–642.

Landsberg KP, Farhadifar R, Ranft J, Umetsu D, Widmann TJ, Bittig T, Said A, Jülicher F & Dahmann C (2009) Increased Cell Bond Tension Governs Cell Sorting at the Drosophila Anteroposterior Compartment Boundary. *Curr. Biol.* 19, 1950–1955.

Lang CF & Munro E (2017) The PAR proteins: from molecular circuits to dynamic self-stabilizing cell polarity. *Development* 144, 3405–3416.

Lecuit T (2005) Adhesion remodeling underlying tissue morphogenesis. *Trends Cell Biol.* 15, 34–42.

Lee HJ & Zheng JJ (2010) PDZ domains and their binding partners: Structure, specificity, and modification. *Cell Commun. Signal.* 8, 1–18.

Levinson AD, Oppermann H, Levintow L, Varmus HE & Bishop JM (1978) Evidence that the transforming gene of avian sarcoma virus encodes a protein kinase associated with a phosphoprotein. *Cell* 15, 561–572.

Luttrell DK & Luttrell LM (2004) Not so strange bedfellows: G-protein-coupled receptors and Src family kinases. *Oncogene* 23, 7969–7978.

Lye CM & Sanson B (2011) Tension and Epithelial Morphogenesis in Drosophila Early Embryos. *Curr. Top. Dev. Biol.* 95, 145–187.

Martin AC & Goldstein B (2014) Apical constriction: themes and variations on a cellular

mechanism driving morphogenesis. *Development* 141, 1987–1998.

Martin AC, Kaschube M & Wieschaus EF (2009) Pulsed contractions of an actin–myosin network drive apical constriction. *Nature* 457, 495–499.

Matakatsu H (2004) Interactions between Fat and Dachsous and the regulation of planar cell polarity in the Drosophila wing. *Development* 131, 3785–3794.

De Matos Simões S, Mainieri A & Zallen JA (2014) Rho GTPase and Shroom direct planar polarized actomyosin contractility during convergent extension. *J. Cell Biol.* 204, 575–589.

Mazumdar A & Mazumdar M (2002) How one becomes many: Blastoderm cellularization in Drosophila melanogaster. *BioEssays* 24, 1012–1022.

McGarrigle D & Huang XY (2007) GPCRs signaling directly through Src-family kinases. *Sci. STKE* 2007, 1–4.

Merks AM, Swinarski M, Meyer AM, Müller NV, Özcan I, Donat S, Burger A, Gilbert S, Mosimann C, Abdelilah-Seyfried S & Panáková D (2018) Planar cell polarity signalling coordinates heart tube remodelling through tissue-scale polarisation of actomyosin activity. *Nat. Commun.* 9, 2161.

Mével-Ninio M, Fouilloux E, Guénal I & Vincent A (1996) The three dominant female-sterile mutations of the Drosophila ovo gene are point mutations that create new translation-initiator AUG codons. *Development* 122, 4131–4138.

Mizuno T, Amano M, Kaibuchi K & Nishida Y (1999) Identification and characterization of Drosophila homolog of Rho-kinase. *Gene* 238, 437–444.

Mlodzik MS and M, Simons M & Mlodzik MS and M (2010) Planar Cell Polarity Signaling: From Fly Development to Human Disease. *Annu. Rev. Genet.* 42, 1–29.

Morais-de-Sá E, Mirouse V & St Johnston D (2010) aPKC Phosphorylation of Bazooka Defines the Apical/Lateral Border in Drosophila Epithelial Cells. *Cell* 141, 509–523.

Müller A & Bossinger O (2003) Molecular networks controlling epithelial cell polarity in development. *Mech. Dev.* 120, 1231–1256.

Müller HAJ & Wieschaus E (1996) armadillo, bazooka, and stardust are critical for early stages in formation of the zonula adherens and maintenance of the polarized blastoderm epithelium in Drosophila. *J. Cell Biol.* 134, 149–163.

Munjal A & Lecuit T (2014) Actomyosin networks and tissue morphogenesis. *Development* 141, 1789–1793.

Nakamura H, Hori K, Tanaka-Okamoto M, Higashiyama M, Itoh Y, Inoue M, Morinaka S & Miyoshi J (2011) Decreased expression of LMO7 and its clinicopathological significance in human lung adenocarcinoma. *Exp. Ther. Med.* 2, 1053–1057.

Nance J & Zallen JA (2011) Elaborating polarity: PAR proteins and the cytoskeleton. *Development* 138, 799–809.

Nelson KS, Khan Z, Molnár I, Mihály J, Kaschube M & Beitel GJ (2012) Drosophila Src regulates anisotropic apical surface growth to control epithelial tube size. *Nat. Cell Biol.* 14, 518–525.

Ohashi K, Nagata K, Maekawa M, Ishizaki T, Narumiya S & Mizuno K (2000) Rho-

associated kinase ROCK activates LIM-kinase 1 by phosphorylation at threonine 508 within the activation loop. *J. Biol. Chem.* 275, 3577–3582.

Ohno S (2001) Intercellular junctions and cellular polarity: The PAR-aPKC complex, a conserved core cassette playing fundamental roles in cell polarity. *Curr. Opin. Cell Biol.* 13, 641–648.

Ooshio T, Irie K, Morimoto K, Fukuhara A, Imai T & Takai Y (2004) Involvement of LMO7 in the Association of Two Cell-Cell Adhesion Molecules, Nectin and E-cadherin, through Afadin and alpha-Actinin in Epithelial Cells. *J. Biol. Chem.* 279, 31365–31373.

Oshiro N, Fukata Y & Kaibuchi K (1998) Phosphorylation of Moesin by Rho-associated Kinase (Rho-kinase) Plays a Crucial Role in the Formation of Microvilli-like Structures. *J. Biol. Chem.* 273, 34663–34666.

Ott EB, Van Den Akker NMS, Sakalis PA, Gittenberger-de Groot AC, Te Velthuis AJW & Bagowski CP (2008) The lim domain only protein 7 is important in zebrafish heart development. *Dev. Dyn.* 237, 3940–3952.

Parsons SJ & Parsons JT (2004) Src family kinases, key regulators of signal transduction. *Oncogene* 23, 7906–7909.

Patwardhan P & Resh MD (2010) Myristoylation and Membrane Binding Regulate c-Src Stability and Kinase Activity. *Mol. Cell. Biol.* 30, 4094–4107.

Pelaseyed T & Bretscher A (2018) Regulation of actin-based apical structures on epithelial cells. *J. Cell Sci.* 131, jcs221853.

Pilot F & Lecuit T (2005) Compartmentalized morphogenesis in epithelia: From cell to tissue shape. *Dev. Dyn.* 232, 685–694.

Ramrath A (2002) Isolierung und Charakterisierung von Bindungspartnern des PDZ-Domänen-Proteins BAZOOKA aus Drosophila melanogaster.

Ranscht B (1994) Cadherins and catenins: interactions and functions in embryonic development. *Curr. Opin. Cell Biol.* 6, 740–6.

Rauskolb C, Sun S, Sun G, Pan Y & Irvine KD (2014) Cytoskeletal Tension Inhibits Hippo Signaling through an Ajuba-Warts Complex. *Cell* 158, 143–156.

Rauzi M, Lenne P-F & Lecuit T (2010) Planar polarized actomyosin contractile flows control epithelial junction remodelling. *Nature* 468, 1110.

Rauzi M, Verant P, Lecuit T & Lenne P-F (2008) Nature and anisotropy of cortical forces orienting Drosophila tissue morphogenesis. *Nat. Cell Biol.* 10, 1401.

Razzell W, Bustillo ME & Zallen JA (2018) The force-sensitive protein Ajuba regulates cell adhesion during epithelial morphogenesis. *J. Cell Biol.* 217, 3715–3730.

Reynolds AB & Roczniak-Ferguson A (2004) Emerging roles for p120-catenin in cell adhesion and cancer. *Oncogene* 23, 7947–7956.

Roskoski R (2005) Src kinase regulation by phosphorylation and dephosphorylation. *Biochem. Biophys. Res. Commun.* 331, 1–14.

Roskoski R (2004) Src protein-tyrosine kinase structure and regulation. *Biochem. Biophys. Res. Commun.* 324, 1155–1164.

Rozenblum E, Vahteristo P, Sandberg T, Bergthorsson JT, Syrjakoski K, Weaver D,

Haraldsson K, Johannsdottir HK, Vehmanen P, Nigam S, Golberger N, Robbins C, Pak E, Dutra A, Gillander E, Stephan DA, Bailey-Wilson J, Juo SHH, Kainu T, Arason A, Barkardottir RB, Nevanlinna H, Borg A & Kallioniemi OP (2002) A genomic map of a 6-Mb region at 13q21-q22 implicated in cancer development: Identification and characterization of candidate genes. *Hum. Genet.* 110, 111–121.

Sawyer JK, Harris NJ, Slep KC, Gaul U & Peifer M (2009) The Drosophila afadin homologue Canoe regulates linkage of the actin cytoskeleton to adherens junctions during apical constriction. *J. Cell Biol.* 186, 57–73.

Schindelin J, Arganda-Carreras I, Frise E, Kaynig V, Longair M, Pietzsch T, Preibisch S, Rueden C, Saalfeld S, Schmid B, Tinevez JY, White DJ, Hartenstein V, Eliceiri K, Tomancak P & Cardona A (2012) Fiji: An open-source platform for biological-image analysis. *Nat. Methods* 9, 676–682.

Schneider CA, Rasband WS & Eliceiri KW (2012) NIH Image to ImageJ: 25 years of image analysis. *Nat. Methods* 9, 671–675.

Schneider I (1972) Cell lines derived from late embryonic stages of Drosophila melanogaster. *J. Embryol. exp. Morph.* 27, 353–365.

Schwartz DC & Cantor CR (1984) Separation of yeast chromosome-sized DNAs by pulsed field gradient gel electrophoresis. *Cell* 37, 67–75.

Shahab J, Tiwari MD, Honemann-Capito M, Krahn MP & Wodarz A (2015) Bazooka/PAR3 is dispensable for polarity in Drosophila follicular epithelial cells. *Biol. Open* 4, 528–541.

Shindo M, Wada H, Kaido M, Tateno M, Aigaki T, Tsuda L & Hayashi S (2008) Dual function of Src in the maintenance of adherens junctions during tracheal epithelial morphogenesis. *Development* 135, 1355–1364.

Simões SDM, Blankenship JT, Weitz O, Farrell DL, Tamada M, Fernandez-Gonzalez R & Zallen J a. (2010) Rho-kinase directs bazooka/Par-3 planar polarity during drosophila axis elongation. *Dev. Cell* 19, 377–388.

Simon MA, Xu A, Ishikawa HO & Irvine KD (2010) Modulation of Fat:Dachsous Binding by the Cadherin Domain Kinase Four-Jointed. *Curr. Biol.* 20, 811–817.

Simpson L & Wieschaus E (1990) Zygotic Activity of the Nullo-Locus Is Required To Stabilize the Actin Myosin Network During Cellularization in Drosophila. *Development* 110, 851–863.

S**tehelin D, Fujita DJ, Padgett T, Varmus HE & Bishop JM** (1977) Detection and enumeration of transformation-defective strains of avian sarcoma virus with molecular hybridization. *Virology* 76, 675–684.

von Stein W (2005) Direct association of Bazooka/PAR-3 with the lipid phosphatase PTEN reveals a link between the PAR/aPKC complex and phosphoinositide signaling. *Development* 132, 1675–1686.

Strutt DI (2001) Asymmetric localization of frizzled and the establishment of cell polarity in the Drosophila wing. *Mol. Cell* 7, 367–375.

Su WH, Mruk DD, Wong EWP, Lui WY & Cheng CY (2013) Polarity protein complex scribble/lgl/dlg and epithelial cell barriers. *Adv. Exp. Med. Biol.* 763, 149–170.

Subramanian A, Wayburn B, Bunch T & Volk T (2007) Thrombospondin-mediated

adhesion is essential for the formation of the myotendinous junction in Drosophila. *Development* 134, 1269–1278.

Sun Z, Amourda C, Shagirov M, Hara Y, Saunders TE & Toyama Y (2017) Basolateral protrusion and apical contraction cooperatively drive Drosophila germ-band extension. *Nat. Cell Biol.* 19, 375–383.

Suzuki A & Ohno S (2006) The PAR-aPKC system: lessons in polarity. *J. Cell Sci.* 119, 979–987.

Tada M & Heisenberg C-P (2012) Convergent extension: using collective cell migration and cell intercalation to shape embryos. *Development* 139, 3897–3904.

Takahashi F, Endo S, Kojima T & Saigo K (1996) Regulation of cell-cell contacts in developing Drosophila eyes by Dsrc41, a new, close relative of vertebrate c-src. *Genes Dev.* 10, 1645–1656.

Takahashi M (2005) Requirements of genetic interactions between Src42A, armadillo and shotgun, a gene encoding E-cadherin, for normal development in Drosophila. *Development* 132, 2547–2559.

Takeichi M (2014) Dynamic contacts: rearranging adherens junctions to drive epithelial remodelling. *Nat. Rev. Mol. Cell Biol.* 15, 397–410.

Tanaka-Okamoto M, Hori K, Ishizaki H, Hosoi A, Itoh Y, Wei M, Wanibuchi H, Mizoguchi A, Nakamura H & Miyoshi J (2009) Increased susceptibility to spontaneous lung cancer in mice lacking LIM-domain only 7. *Cancer Sci.* 100, 608–616.

Tanentzapf G & Tepass U (2003) Interactions between the crumbs, lethal giant larvae and bazooka pathways in epithelial polarization. *Nat. Cell Biol.* 5, 46–52.

Tepass U & Knust E (1993) Crumbs and stardust act in a genetic pathway that controls the organization of epithelia in Drosophila melanogaster. *Dev. Biol.* 159, 311–326.

Tepass U, Tanentzapf G, Ward R & Fehon R (2001) Epithelial Cell Polarity and Cell Junctions in Drosophila. *Annu. Rev. Genet.* 35, 747–784.

Tepass U, Theres C & Knust E (1990) crumbs encodes an EGF-like protein expressed on apical membranes of Drosophila epithelial cells and required for organization of epithelia. *Cell* 61, 787–799.

Tice D a, Biscardi JS, Nickles a L & Parsons SJ (1999) Mechanism of biological synergy between cellular Src and epidermal growth factor receptor. *Proc. Natl. Acad. Sci.* 96, 1415–1420.

Toyoshima YY, Kron SJ, McNally EM, Niebling KR, Toyoshima C & Spudich JA (1987) Myosin subfragment-1 is sufficient to move actin filaments in vitro. *Nature* 328, 536–9.

Tree DRP, Shulman JM, Rousset R, Scott MP, Gubb D & Axelrod JD (2002) Prickle mediates feedback amplification to generate asymmetric planar cell polarity signaling. *Cell* 109, 371–81.

Tsukita S, Furuse M & Itoh M (2001) Multifunctional strands in tight junctions. *Nat. Rev. Mol. Cell Biol.* 2, 285–293.

Tsukita S, Yonemura S & Tsukita S (1997) ERM (ezrin/radixin/moesin) family: from

cytoskeleton to signal transduction. *Curr. Opin. Cell Biol.* 9, 70–75.

Umetsu D & Kuranaga E (2017) Planar polarized contractile actomyosin networks in dynamic tissue morphogenesis. *Curr. Opin. Genet. Dev.* 45, 90–96.

Usui T, Shima Y, Shimada Y, Hirano S, Burgess RW, Schwarz TL, Takeichi M & Uemura T (1999) Flamingo, a seven-pass transmembrane cadherin, regulates planar cell polarity under the control of Frizzled. *Cell* 98, 585–595.

Valdivia M, Vega-Macaya F & Olguín P (2017) Mechanical Control of Myotendinous Junction Formation and Tendon Differentiation during Development. *Front. Cell Dev. Biol.* 5, 1–8.

Varmus H, Hirai H, Morgan D, Kaplan J & Bishop JM (1989) Function, location, and regulation of the src protein-tyrosine kinase. *Princess Takamatsu Symp.* 20, 63—70.

Vega-Macaya F, Manieu C, Valdivia M, Mlodzik M & Olguín P (2016) Establishment of the muscle-tendon junction during thorax morphogenesis in drosophila requires the Rho-kinase. *Genetics* 204, 1139–1149.

te Velthuis AJW & Bagowski CP (2007) PDZ and LIM Domain-Encoding Genes: Molecular Interactions and their Role in Development. *Sci. World J.* 7, 1470–1492.

Venken KJT, Carlson JW, Schulze KL, Pan H, He Y, Spokony R, Wan KH, Koriabine M, de Jong PJ, White KP, Bellen HJ & Hoskins RA (2009) Versatile P[acman] BAC libraries for transgenesis studies in Drosophila melanogaster. *Nat. Methods* 6, 431–434.

Verdier V, Guang-Chao-Chen & Settleman J (2006) Rho-kinase regulates tissue morphogenesis via non-muscle myosin and LIM-kinase during Drosophila development. *BMC Dev. Biol.* 6, 1–10.

Vicente-Manzanares M, Ma X, Adelstein RS & Horwitz AR (2009) Non-muscle myosin II takes centre stage in cell adhesion and migration. *Nat. Rev. Mol. Cell Biol.* 10, 778–790.

Vladar EK, Antic D & Axelrod JD (2009) Planar cell polarity signaling: the developing cell's compass. *Cold Spring Harb. Perspect. Biol.* 1, 1–19.

Wang Y (2006) The Role of Frizzled3 and Frizzled6 in Neural Tube Closure and in the Planar Polarity of Inner-Ear Sensory Hair Cells. *J. Neurosci.* 26, 2147–2156.

Wang Y & Nathans J (2007) Tissue/planar cell polarity in vertebrates: new insights and new questions. *Development* 134, 647–658.

Watanabe T, Hosoya H & Yonemura S (2007) Regulation of Myosin II Dynamics by Phosphorylation and Dephosphorylation of Its Light Chain in Epithelial Cells E. Holzbaur, ed. *Mol. Biol. Cell* 18, 605–616.

Willott E, Balda MS, Fanning a S, Jameson B, Van Itallie C & Anderson JM (1993) The tight junction protein ZO-1 is homologous to the Drosophila discs-large tumor suppressor protein of septate junctions. *Proc. Natl. Acad. Sci. U. S. A.* 90, 7834–7838.

Wodarz A, Ramrath A, Grimm A & Knust E (2000) Drosophila atypical protein kinase C associates with Bazooka and controls polarity of epithelia and neuroblasts. *J. Cell Biol.* 150, 1361–74.

Wodarz A, Ramrath A, Kuchinke U & Knust E (1999) Bazooka provides an apical cue for

inscuteable localization in Drosophila neuroblasts. *Nature* 402, 544–547.

Wong LL & Adler PN (1993) Tissue polarity genes of Drosophila regulate the subcellular location for prehair initiation in pupal wing cells. *J. Cell Biol.* 123, 209–221.

Yamanaka T & Ohno S (2008) Role of Lgl/Dlg/Scribble in the regulation of epithelial junction, polarity and growth. *Front. Biosci.* 13, 6693–6707.

Yang CH, Axelrod JD & Simon MA (2002) Regulation of Frizzled by Fat-like cadherins during planar polarity signaling in the Drosophila compound eye. *Cell* 108, 675–688.

Young PE, Richman AM, Ketchum AS & Kiehart DP (1993) Morphogenesis in Drosophila requires nonmuscle myosin heavy chain function. *Genes Dev.* 7, 29–41.

Zalewski JK, Mo JH, Heber S, Heroux A, Gardner RG, Hildebrand JD & VanDemark AP (2016) Structure of the Shroom-Rho kinase complex reveals a binding interface with monomeric shroom that regulates cell morphology and stimulates kinase activity. *J. Biol. Chem.* 291, 25364–25374.

Zallen JA (2007) Planar Polarity and Tissue Morphogenesis. *Cell* 129, 1051–1063.

Zallen JA & Blankenship JT (2008) Multicellular dynamics during epithelial elongation. *Semin. Cell Dev. Biol.* 19, 263–270.

Zallen JA & Wieschaus E (2004) Patterned gene expression directs bipolar planar polarity in Drosophila. *Dev. Cell* 6, 343–355.

List of abbreviations

%	Prozent
°C	Grad Celsius
AJ	adherens junction
ATP	adenonsine triphosphate
bp	base pair
ca	circa
DSHB	Developmental Studies Hybridoma Bank
EDTA	Ethylenediaminetetraacetic acid
e.g.	for example
g	gram
GFP	green fluorescent protein
h	hour
HRP	Horseradish peroxidase
IF	Immunofluorescence
KAc	potassium acetate
kb	kilo base
kDa	kiloDalton
LIM	Lin11, Isl-1, Mec-3
M	Molar
MeOH	Methanol
mg	milligram
min	minutes
mL	milliliter
n	nano
NaCl	sodium chloride
NaOH	sodium hydroxide
NHS	Normal horse serum

ns	Not significant
PAGE	Polyacrylamide gel electrophoresis
PBM	PDZ-binding motif
PBS	Phosphate buffered saline
PBSTw	Phosphate buffered saline with Tween-20
PBSTx	Phosphate buffered saline with Triton X-100
PCP	planar cell polarity
PCR	polymerase chain reaction
PDZ	Postsynaptic density 95/Discs large/Zonula occludens 1
pH	*potentia Hydrogenii*
rev	reverse
RNA	Ribonucleic acid
RNAse	Ribunuclease
rpm	Rounds per minute
RT	Room temperature (21 °C)
s	Second
Sb	Stubble
SDS	Sodium dodecyl sulfate
SJ	septate junction
TBS	Tris-buffered saline
TBST	Tris-buffered saline with Tween-20
TEMED	Tetramethylethylenediamine
TJ	tight junction
TM	Third multiple
TNT	Tris-NaCl-Triton
Tris	Tris(hydroxymethyl)aminomethane
Twi	Twist
U	Unit
UV	Ultraviolet
V	Volt
WB	western blot

WT	wild type
ZA	zonula adherens
µg	microgram
µl	microliter
µm	micrometer

Appendix

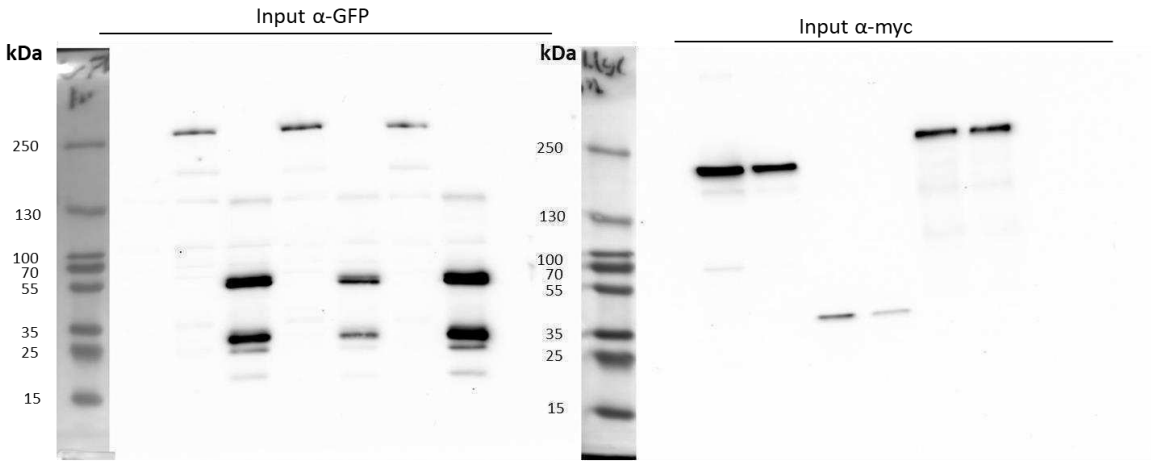
Input α-GFP
kDa
250
130
100
70
55
35
25
15
Input α-myc
kDa
250
130
100
70
55
35
25
15
GFP-Smash PM - + - + - + - - + - + - + - +
Rok-myc - + + - - - - - + + - - - -
Sqh-myc - - - + + - - - - - + + - -
Shroom-myc - - - - - + + - - - - + +
CD8-GFP - - + - + - + - - + - + - +

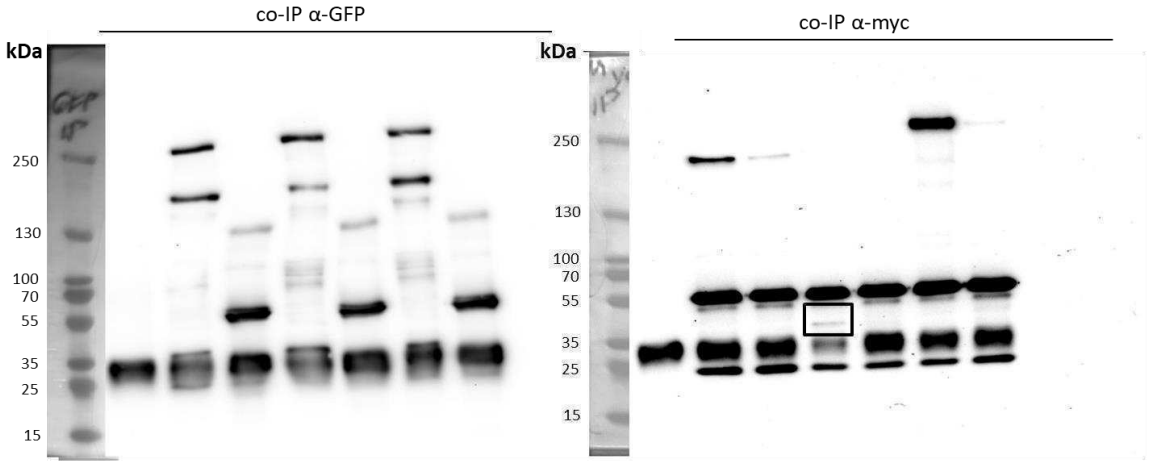
co-IP α-GFP
kDa
250
130
100
70
55
35
25
15
co-IP α-myc
kDa
250
130
100
70
55
35
25
15
GFP-Smash PM - + - + - + - - + - + - + - +
Rok-myc - + + - - - - - + + - - - -
Sqh-myc - - - + + - - - - - + + - -
Shroom-myc - - - - - + + - - - - + +
CD8-GFP - - + - + - + - - + - + - +

Figure S 1: Smash may bind to Sqh. S2 cells were co-transfected with GFP-Smash PI and the respective myc-tagged protein. GFP- was pulled down and potential binding was confirmed using an anti-myc antibody. A clear signal could be detected in case of Rok, Shroom and Moesin. In some experiments, e.g. in this blot, a slight signal in the corresponding size of Sqh-myc could be detected. This result was not reproducible in all repeats.

Acknowledgements/Danksagung

First of all I want to thank Prof. Andreas Wodarz for giving me the opportunity to join his department and for his supervision and advice. Thank you for giving me the chance to develop myself and my own ideas in these years.

Moreover, I want to thank Prof. Siegfried Roth and Prof. Carien Niessen for being part of my thesis committee and for helpful comments and discussions.

Special thanks go to Dr. Parisa Kakanj for conducting the Laser Ablation. Thank you for the fruitful discussions and for your enthusiasm. I also want to thank Steffen Köhler for performing the scanning electron microscopy.

I am grateful to all current and former lab members of the Molecular Cell Biology for their support. Olaf and Christian, thank you for solving any computer problem. Ferdi, I really appreciate your help with any fly work and thank you for keeping up the Ostwestfalen-connection. I want to thank Jolanta and Monique for being great colleagues and for your help in the lab. Klaus, thank you for your help with the statistics. Manu, Soya, Bharath and Hong thank you for your input and for fun times. I also want to thank Fabienne for being such an interested and dedicated student.

I am more than grateful to Julia, Katja, Theresa, Stephi and Maggy (you are kind of a lab member, too ;)) not only for being colleagues, but for being great friends. Thank you so much for standing me singing, talking, listening, celebrating and laughing.

Der größte Dank gilt meiner Familie und meinen Freunden, die mich schon mein ganzes Leben begleiten. Danke an alle, die von Büren bis Bochum und Köln immer an meiner Seite waren. Eure Freundschaft über Kilometer und Kontinente ist unbezahlbar. Nina und Elli, mit euch bin ich gegen jeden drohenden Sharknado gerüstet!
Meinen Großeltern danke ich besonders für Ihre Unterstützung. Oma & Opa, danke für euren unverbesserlichen Optimismus bis zum Schluss. Oma, danke, dass du mich zum Lachen bringst.
Danke an meine Eltern und meine Brüder für das Öffnen aller Türen, den Glauben an mich, fürs Laminat verlegen und dafür, dass ich immer weiß, wo Zuhause ist.

Erklärung

Erklärung (entsprechend §4 Abs. 1 Nr. 9 der Promotionsordnung vom 02. Februar 2006, mit Änderungen vom 10. Mai 2012):

Ich versichere, dass ich die von mir vorgelegte Dissertation selbständig angefertigt, die benutzten Quellen und Hilfsmittel vollständig angegeben und die Stellen der Arbeit − einschließlich Tabellen, Karten und Abbildungen −, die anderen Werken im Wortlaut oder dem Sinn nach entnommen sind, in jedem Einzelfall als Entlehnung kenntlich gemacht habe; dass diese Dissertation noch keiner anderen Fakultät oder Universität zur Prüfung vorgelegen hat; dass sie − abgesehen von unten angegebenen Teilpublikationen − noch nicht veröffentlicht worden ist, sowie, dass ich eine solche Veröffentlichung vor Abschluss des Promotionsverfahrens nicht vornehmen werde. Die Bestimmungen der Promotionsordnung sind mir bekannt. Die von mir vorgelegte Dissertation ist von Prof. Dr. Andreas Wodarz und Prof. Dr. Siegfried Roth betreut worden.

Irina Peek

Teilpublikationen:

Beati H*, Peek I*, Hordowska P, Honemann-Capito M, Glashauser J, Renschler FA, Kakanj P, Ramrath A, Leptin M, Luschnig S, Wiesner S & Wodarz A (2018) The adherens junction-associated LIM domain protein Smallish regulates epithelial morphogenesis. *J. Cell Biol.* 217, 1079–1095.

*equal contribution